Eco-evolutionary dynamics in predator-prey systems

Masato Yamamichi

DOCTOR OF PHILOSOPHY

Department of Evolutionary Studies of Biosystems
School of Advanced Sciences
The Graduate University for Advanced Studies

2011

Contents

Acknowledgements

Firstly, I would like to show my gratitude to my supervisors, Prof. Akira Sasaki, Prof. Hideki Innan, and Prof. Mariko Hiraiwa-Hasegawa. Without their kind help, this thesis would not have been possible. I would also like to thank my collaborators, Prof. Takehito Yoshida and Dr. Masaki Hoso, a committee member, Prof. Masakazu Shimada, and members of Sasaki-Ohtsuki lab, Innan lab, and Department of Evolutionary Studies of Biosystems. They have continuously encouraged my research and their comments have improved my studies and presentations. Prof. Nelson G. Hairston Jr., Prof. Stephen P. Ellner, and members of the chemostat meeting, the Hairston lab, the Ellner lab, and Department of Ecology and Evolutionary Biology gave a great opportunity to do research at Cornell University. Lecturers and members of summer schools in Switzerland (eawag) and Okinawa (OIST), the community ecology seminar, CTS seminar, and the Darwin seminar gave me a great opportunity to broaden my knowledge about ecology and evolution. Finally, I would like to thank my parents and family for their support for all the years. This work was supported by Japan Society for the Promotion of Science (JSPS) research fellowship for young scientists (DC1: 21-7611), Japan Student Services Organization (JASSO), and the Graduate University for Advanced Studies (Sokendai).

Summary

Recent studies have revealed that ecological and evolutionary dynamics have close interactions. Not only ecological dynamics affect adaptive evolution, evolution can occur as rapidly as ecological dynamics (i.e., rapid evolution) and can also affect ecology including population dynamics, community structures, and even ecosystem functions. Ecological settings cause adaptive evolution, and then trait evolution modifies its surrounding environments and thereby changes selection pressure: such feedbacks between ecology and evolution are called as eco-evolutionary dynamics. Recently it was cautioned that predicting future biological dynamics would be difficult ignoring eco-evolutionary feedbacks. Understanding eco-evolutionary dynamics is crucial not only for the consilience of basic ecology and evolutionary biology but also for applied ecology: conservation and management of the wildlife. Here I theoretically investigated eco-evolutionary dynamics in one of the most common interspecific interactions, predator-prey systems. Because predation is tightly related to organisms' fitness, eco-evolutionary dynamics is widespread in predator-prey systems and important to predict future dynamics.

In chapter 2, I focused on eco-evolutionary dynamics of phenotypic plasticity and population dynamics. Understanding causes and consequences of population cycles has been an important research focus as cycles can cause extinction of populations and one third of population dynamics in the wild shows periodic dynamics (cycles). Plankton predator-prey systems in chemostats (continuously flowing microcosms) are ideal experimental systems to investigate the effects of rapid evolution and phenotypic plasticity (induced defense) of prey species on population dynamics in detail. Based on the chemostat models, I confirmed that phenotypic plasticity is better at stabilizing population dynamics whereas a plastic genotype has higher fitness in fluctuating environments than in stable environments. Combining these two characteristics that have been studied separately in population and evolutionary ecology, I found a dilemma of plasticity: the plastic genotype is better in fluctuating environments, but it stabilizes the fluctuation and thereby decreases its fitness by itself. By decreasing the plastic genotype, the system again begins to oscillate. The dilemma results in a novel phenomenon in which phenotypic plasticity evolve rapidly causing intermittent cycles. I proposed to call this as 'eco-evolutionary bursting.'

In chapter 3, I focused on ecological speciation via functional pleiotropy, in which evolution of the speciation gene contributes not only to reproductive isolation, but also to anti-predatory adaptation. Classically it was believed that single-gene speciation is almost impossible, because the first mutant is strongly selected against. However, there are some empirical evidences of single-gene speciation in snails. Recent studies proposed a 'right-handed' predator hypothesis, in which specialized predation of snakes on dextral (clockwise coiling) snails can elevate relative survival rate of sinistral (counter-clockwise coiling) snails and thereby promote fixation of a sinistral mutant allele. I theoretically revealed that functional pleiotropy and the maternal effect (i.e., delayed inheritance, in which an individual's phenotype is determined by its mother's genotype) of the speciation gene can promote single-gene speciation. In small populations, indeed, I found that a recessive mutant has higher fixation probabilities without pleiotropy, whereas a dominant mutant has higher one with pleiotropy. In large populations, the dominant and recessive mutant alleles have the same fixation probability without pleiotropy. This theoretical prediction would be testable by examining allele dominance of the speciation gene in snails living within or outside the snake range.

As future perspectives of studies on eco-evolutionary dynamics, I propose four important topics: (1) space and time, (2) combining theoretical and empirical approaches, (3) genomics and eco-evolutionary studies, and (4) eco-evolutionary conservation and management. This thesis did not consider macroscale dynamics of space (e.g., metacommunity) or time (e.g., macro evolution), but it would be interesting to consider eco-evolutionary dynamics in these scales. Second, here I focused on theoretical modeling to understand dynamics, but combining theoretical and empirical approaches with a sophisticated statistical framework is crucial to understand real biological systems. Especially, in this post-genomic era, it will be possible to understand eco-evolutionary dynamics from the genomic scale to the ecological scale. Therefore, future researches are needed to directly connect evolution in the genomic level to ecological dynamics. Finally, conservation and management studies should incorporate perspectives from eco-evolutionary dynamics, as evolution can drastically alter ecological dynamics of nearly extinct populations (e.g., evolutionary rescue) or heavily exploited populations (e.g., fisheries-induced evolution). With eco-evolutionary dynamics, it will be possible to conserve and manage wild populations better.

List of Publications

Peer-reviewed papers

1. Blake Matthews, Anita Narwani, Stephen Hausch, Etsuko Nonaka, Hannes Peter, **Masato Yamamichi**, Karen E. Sullam, Kali C. Bird, Mridul K. Thomas, Torrance C. Hanley, Caroline B. Turner (2011) Toward an integration of evolutionary biology and ecosystem science. *Ecology Letters* **14**(7): 690-701

2. **Masato Yamamichi**, Takehito Yoshida, Akira Sasaki (2011) Comparing the effects of rapid evolution and phenotypic plasticity on predator-prey dynamics. *The American Naturalist* **178**(3): 287-304

3. **Masato Yamamichi**, Jun Gojobori, Hideki Innan (2012) An autosomal analysis gives no genetic evidence for complex speciation of humans and chimpanzees. *Molecular Biology and Evolution* **29**(1): 145-156

4. **Masato Yamamichi**, Hideki Innan (2012) Estimating the migration rate from genetic variation data. *Heredity* **108**(4): 362-363

5. Ayumi Tezuka, Satoshi Kasagi, Cock van Oosterhout, Mark McMullan, Watal M. Iwasaki, **Masato Yamamichi**, Hideki Innan, Shoji Kawamura, Masakado Kawata (submitted) Divergent selection on opsin gene variation in guppy (*Poecilia reticulata*) populations of Trinidad and Tobago.

6. **Masato Yamamichi**, Akira Sasaki (in preparation) Single-gene speciation with functional pleiotropy: effects of allele dominance, population size, and maternal effect.

List of Publications (continued)

Peer-reviewed papers in Japanese

7. 山道真人・角谷拓 (2009) マルコフ連鎖モンテカルロ（MCMC）法を用いたシミュレーションモデルのパラメータ推定：ベイジアンキャリブレーション入門. 日本生態学会誌 **59**(2): 207-216

8. 山道真人 (in revision) 系統地理学における統計的推定の手法と今後の展望. 種生物学研究第 **37** 号「DNA から生き物の過去がよみがえる（仮）」（池田啓・小泉逸郎編）, 文一総合出版, 東京

9. 山道真人・長谷川眞理子 (in revision) 『保全生態学研究』の掲載論文に見られる研究対象の偏り.

Non-reviewed papers in Japanese

10. 山道真人・印南秀樹 (2008) 始めよう！エコゲノミクス (1) 局所適応と形質の分化. 日本生態学会誌 **58**(3): 241-247

11. 山道真人・印南秀樹 (2009a) 始めよう！エコゲノミクス (2) ゲノムワイド関連マッピング. 日本生態学会誌 **59**(1): 105-113

12. 山道真人・印南秀樹 (2009b) 始めよう！エコゲノミクス (3) 集団内変異データが語る過去:解析手法と理論的背景（その 1）. 日本生態学会誌 **59**(3): 339-349

13. 山道真人・印南秀樹 (2010a) 始めよう！エコゲノミクス (4) 集団内変異データが語る過去:解析手法と理論的背景（その 2）. 日本生態学会誌 **60**(1): 137-148

14. 山道真人・印南秀樹 (2010b) 始めよう！エコゲノミクス (5) 自然選択の検出（その 1）. 日本生態学会誌 **60**(2): 293-302

15. 山道真人・印南秀樹 (2011) 始めよう！エコゲノミクス (6) 自然選択の検出（その 2）. 日本生態学会誌 **61**(2): 237-249

16. 山道真人 (2011) 迅速な進化と表現型可塑性が個体群動態に及ぼす影響. 数理解析研究所講究録 **1751**: 140-147

17. 山道真人・印南秀樹 (2012) 始めよう！エコゲノミクス (7) 今後のエコゲノミクス研究の展望. 日本生態学会誌 **62**(1): 95-109

Chapter 1. Introduction

But it is difficult to tell, and immaterial for us, whether habits generally change first and structure afterwards; or whether slight modifications of structure lead to changed habits; both probably often change simultaneously. (Darwin 1859)

1.1 Eco-evolutionary dynamics

Ecology is defined as "the scientific study of the interactions between organisms and their environment" (Begon et al. 2006). Evolution is "the unifying theory of the biological sciences" and "it aims to discover the history of life and the causes of the diversity and characteristics of organisms" (Futuyma 2005). Although there has been a traditional connection between ecology and evolution, it is rather recent that researchers get to understand the close relationship between ecological and evolutionary dynamics (Johnson and Stinchcombe 2007, Schoener 2011). For example, Lawrence B. Slobodkin drew a distinction between 'ecological time' (~ 10 generations) and 'evolutionary time' (on the order of half a million years) in his influential book (Slobodkin 1961). According to his definition, ecological time is a period over which populations could maintain approximate steady state, and evolutionary time is sufficient for evolutionary change to disrupt ecological steady states. In the same way, G. Evelyn Hutchinson titled his famous book "*The Ecological Theater and The Evolutionary Play*" (Hutchinson 1965), describing ecological systems as analogous to theaters, in which species or individuals (i.e., the actors) have roles determined by their evolutionary history, and the acts are played out in an unscripted fashion that is contingent on the environmental setting (i.e., the local theater).

Recent studies have indicated that (1) evolution can occur on the same timescale as ecology (i.e., rapid/ongoing/contemporary evolution) (Thompson 1998, Hendry and Kinnison 1999, Hairston et al. 2005). Here I define evolution as an allele frequency change over generations and it is adaptive when alleles have different fitness. In the Wright-Fisher model of haploid organisms assuming discrete generation and constant population size (Fisher 1930, Wright 1931), the speed of allele frequency change due to natural selection is given by

$$\Delta p = \frac{sp(1-p)}{\bar{w}}, \tag{1.1}$$

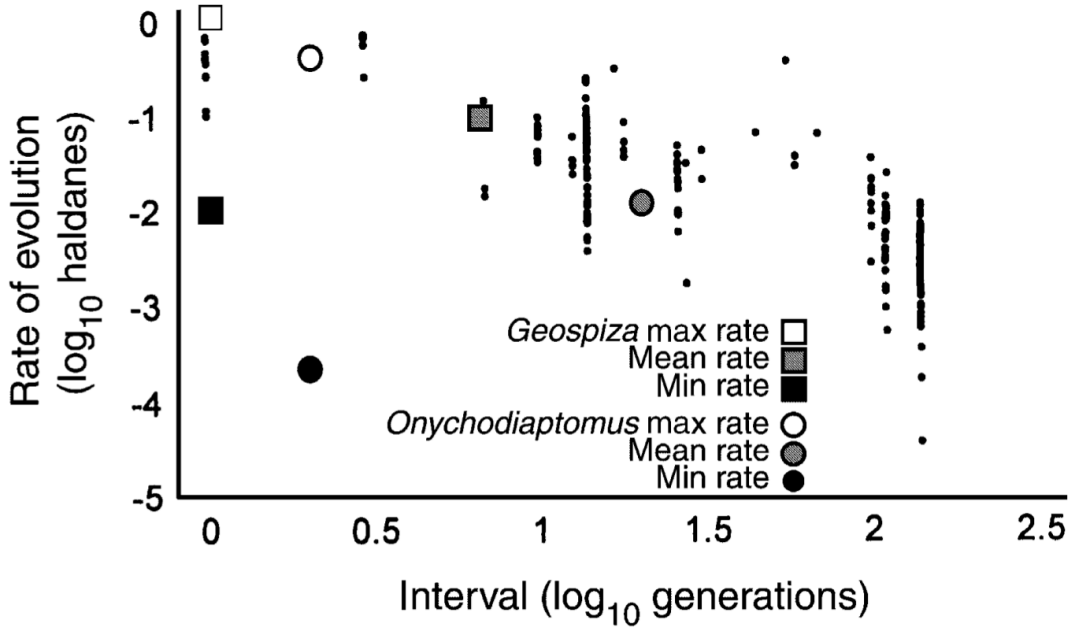

Figure 1.1: Relation between rate of phenotypic evolution and number of generations over which measurements were made. Original figure (small dots) is from Hendry and Kinnison (1999) with new calculations added for Darwin's finch (*Geospiza fortis*) and the freshwater copepod (*Onychodiaptomus sanguineus*), showing the slowest, the most rapid, and the average rates of evolution (per generation) over the 30- and 10-year, respectively, periods of study (Hairston et al. 2005).

where p is a favored allele frequency, s is a positive selection coefficient, and $\overline{w}$ is a mean fitness. In the trait level, adaptive evolution process is generally described by the Price equation:

$$\Delta\overline{z} = \frac{Cov(w,z)}{\overline{w}} + \frac{E(w\Delta z)}{\overline{w}}, \qquad (1.2)$$

where the first term, a covariance of trait (z) and fitness (w), is a change in mean phenotype due to selection and the second term is due to transmission bias (e.g., mutation and genetic drift) (Price 1970). Therefore, if the selection coefficient and genetic variance were sufficiently large, adaptive evolution can occur rapidly.

(2) Rapid evolution is pervasive in the wild. Hendry and Kinnison (1999) compared rates of evolution (measured by haldane, which is the per generation change relative to character variance: Gingerich 1993) and generations over which measurements were made by a meta-analysis. They proposed that studies covering only

a few generations typically show faster evolution than those covering more generations (small dots in fig. 1). This may be because selection coefficients are fluctuating around zero. The clear negative correlation may be partly due to a publication bias (Hairston et al. 2005), but still the graph shows that evolution can be rapid before averaging over longer periods (Hoekstra et al. 2001). This speed is partly because of rapid environmental changes by humans such as habitat destruction, introduction of exotic species, and climate change (Palumbi 2002). Classic examples include industrial melanism of peppered moth in Great Britain (Kettlewell 1958).

(3) Rapid evolution can affect population dynamics (Yoshida et al. 2003), community structures (Johnson et al. 2009), and even ecosystem functions (Bassar et al. 2010, Loreau 2010), and in tern, changed environments impose different selection pressure on organisms (so-called 'eco-evolutionary dynamics': Pelletier et al. 2009). This modern ideas about eco-evolutionary dynamics call for a more nuanced analogy than Hutchinson's 'ecological theater and the evolutionary play.' For instance, we can consider that the roles of actors (i.e., species' or individuals' phenotypes) in local theaters (i.e., ecosystems) change over generations in response to direct pressures from actors' peers and audiences (i.e., the agents of selection). Actors' roles can evolve because of reciprocal interactions (i.e., eco-evolutionary feedbacks) between actors and their peers (i.e., the community) or between actors and the structural components of the theater (e.g., the abiotic environment of ecosystems). In addition, actors can influence the development and renovation of the theater (i.e., ecosystem modification and engineering) and this, in turn, can increase the number of actors in the play (i.e., via niche construction) and affect the outcome of future plays (Matthews et al. 2011).

In addition to fundamental importance of the consilience of ecology and evolution, understanding eco-evolutionary dynamics is crucial for predicting ecological dynamics (Ellner et al. 2011) and therefore conserving and managing rapidly adapting wild populations (Kinnison and Hairston 2007).

1.2 Predator-prey systems

Predation is defined as "a biological interaction where a predator feeds on its prey" (Begon et al. 2006). Predator-prey interaction is one of the most common interspecific interactions and resultant ecological dynamics are studied intensively (Barbosa and Castellanos 2005). Classical topics of ecology on predation include the HSS hypothesis

(Hairston et al. 1960), keystone predation (Paine 1966), trophic cascades (Terborgh and Estes 2010), and paradox of enrichment (Rosenzweig 1971).

Recent studies have found many examples of eco-evolutionary dynamics in predator-prey systems (Abrams 2000, Hairston et al. 2005). This is because fitness of prey would be zero if it were eaten, thus anti-predator adaptation is crucial for prey. For predator, eating prey efficiency is also significant for its fitness. In this Ph.D. thesis, I try to understand eco-evolutionary dynamics in predator-prey systems theoretically. Specifically, I focus on phenotypic plasticity and population dynamics in chapter 2 and on ecological speciation due to predation in chapter 3.

1.2.1 Population dynamics

In ecology, one of the most popular questions is 'to oscillate or not to oscillate?' Causes and consequences of predator-prey cycles have been the focus of many ecological studies. Population cycles are important because it is tightly related to persistence of populations: increasing amplitude of oscillation with smaller minimum abundance can result in deterministic or stochastic extinction of populations. In addition, population cycles are pervasive: by a meta-analysis of the *Global Population Dynamics Database* (http://www3.imperial.ac.uk/cpb/research/patternsandprocesses/gpdd), it was shown that one-third of population dynamics showed periodic dynamics (cycles) and part of this is due to predator-prey interaction (Kendall et al. 1998).

Theoretical modeling has been used to investigate predator-prey population dynamics. The classic Lotka-Volterra model (Lotka 1925, Volterra 1926) is

$$\begin{aligned} \frac{dx}{dt} &= x(a - by), \\ \frac{dy}{dt} &= y(cx - d), \end{aligned} \tag{1.3}$$

where x and y are prey and predator, a is a growth rate of prey, b is a predation rate of prey, c is a growth rate of predator, and d is a mortality rate of predator. Equilibria of this system are $(x, y) = (0, 0)$ and $(d/c, a/b)$. Because the trace of the Jacobian matrix is 0 in the second equilibrium, this system is neutrally stable. Therefore amplitude of cycles depends on initial conditions. The Rosenzweig-MacArthur model is more complex by adding biological details (Rosenzweig and MacArthur 1963):

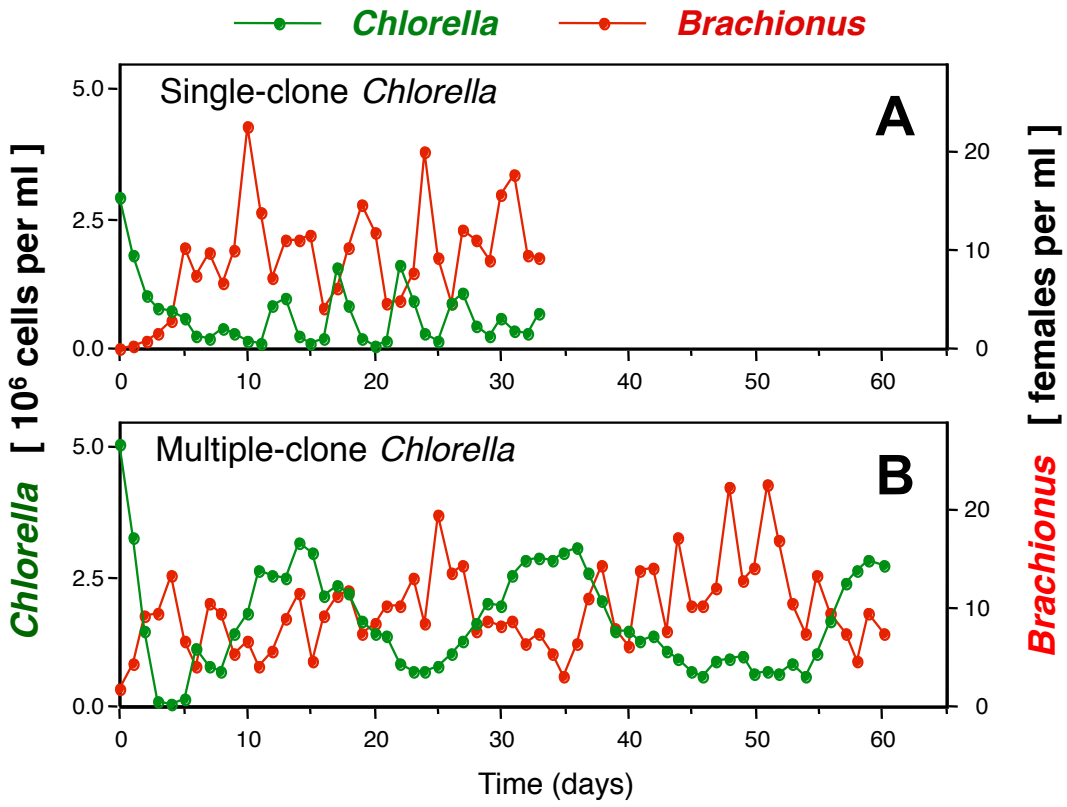

Figure 1.2: Experimental results of chemostats with predator (rotifer: *Brachionus calyciflorus*) and prey (green algae: *Chlorella vulgaris*) (Yoshida et al. 2003). A. Single-clone of *Chlorella* causes ordinary predator-prey cycles (1/4 phase lag). B. Multiple-clone of *Chlorella* causes evolutionary cycles (anti-phase cycles) with longer period length.

$$\begin{aligned} \frac{dx}{dt} &= x\left[a\left(1-\frac{x}{K}\right)-\frac{sy}{1+shx}\right], \\ \frac{dy}{dt} &= y\left(c\frac{sx}{1+shx}-d\right), \end{aligned} \tag{1.4}$$

where K is a carrying capacity of prey, h is a handling time of predator to eat prey, s is a searching efficiency of predator to eat prey, and c is a conversion rate of predator. The system shows stable limit cycles with predator and prey as shown in figure 2A.

Microcosm experiments have been performed to understand such oscillations (e.g., Gause 1934, Utida 1957, Huffaker 1958, Fussmann et al. 2000). By using

chemostat (continuously flowing microcosm) experiments as well as theoretical modeling, it was shown that eco-evolutionary dynamics in predator-prey systems cause strange cycles: evolutionary or cryptic cycles (Abrams and Matsuda 1997, Yoshida et al. 2003, Yoshida et al. 2007). In evolutionary cycles, temporally varying predation pressure cause balancing selection: when predator is abundant, more defended genotype is selected for whereas less defended genotype is favored when predator is scarce due to trade-off between the defensive trait and growth rate (Yoshida et al. 2004, Meyer et al. 2006, Becks et al. 2010). Because algae reproduce asexually in chemostats, adaptation occurs by frequency change of genotypes. This adaptation process affects population cycles: ordinary predator-prey cycles show 1/4 phase-lag between them (fig. 2A) whereas evolutionary cycles show 1/2 phase-lag (anti-phase cycles) with longer period length (fig. 2B). This is a typical example of eco-evolutionary dynamics.

Rapid adaptation can be observed in the wild, but it is difficult to tell whether it is adaptation due to evolution (genetic change) or phenotypic plasticity (without genetic change). To predict population dynamics with rapid adaptation, therefore, it is important to know the effects of evolution and plasticity on predator-prey dynamics precisely. We investigate this problem in chapter 2.

1.2.2 Ecological speciation

Speciation is a source of biodiversity and has been a major research topic of evolutionary biology (Coyne and Orr 2004). Eco-evolutionary feedbacks between predator and prey can sometimes result in speciation of predator or prey. Resource competition has been thought as a primary factor driving phenotypic divergence, but predation can cause adaptive divergence of prey (Abrams et al. 1993). For example, Nosil and Crespi (2006) showed experimentally that divergent selection from visual predators could promote speciation in stick insects (Nosil and Crespi 2006). This kind of speciation is called as ‘ecological speciation’. More precisely, ecological speciation is defined as “the process by which barriers to gene flow evolve between populations as a result of ecologically-based divergent selection” (Rundle and Nosil 2005). Also, sequential ecological speciation is called as ‘adaptive radiation’ (Schluter 2000). Another study also showed that the speed of ecological speciation can be on ecological timescale (Hendry et al. 2007). Therefore, predator-prey interactions can result in rapid evolution of reproductive isolation as a byproduct of feeding or anti-predatory

adaptation.

Theoretical studies on ecological speciation have been concentrating on Adaptive Dynamics (Doebeli 2011) or Monte Carlo simulations to show the specific condition for speciation to occur (Gavrilets 2003). Numerical simulations can include complicated genetic basis of the trait contributing reproductive isolation whereas it is difficult to obtain general conclusions. Adaptive Dynamics is an analytical and general approach, but it neglects genetic detail (but see Sasaki and Dieckmann 2011). Therefore we analytically as well as numerically consider the special case of speciation with genetic detail in chapter 3.

1.3 Chapter contents

In chapter 2, I focused on plankton predator-prey systems in microcosms to understand the effects of rapid evolution and phenotypic plasticity of prey species on population dynamics. I theoretically confirmed that plasticity is better at stabilizing population dynamics (as Vos et al. 2004a) whereas a plastic genotype has higher fitness in fluctuating environments than stable environments (as Svanbäck et al. 2009). The first topic has been studied in population ecology (ecological effect of plasticity) and the second one has been in evolutionary ecology (condition for evolution of plasticity). Combining these two characteristics, I found a dilemma of plasticity: the plastic genotype is better at fluctuating environments, but it stabilizes the fluctuation and thereby decreases its fitness by itself. The dilemma results in rapid evolution of phenotypic plasticity in intermittent cycles. We proposed to call this phenomenon as "eco-evolutionary bursting" because the intermittent cycles are similar to bursting in neurobiology.

In chapter 3, I focused on single-gene speciation of snails promoted by right-handed snakes. Bateson (1909), Dobzhansky (1937), and Muller (1942) proposed that single-gene speciation is almost impossible, but there are some evidences of such speciation in snails (Ueshima and Asami 2003). Hoso et al. (2010) proposed a 'right-handed' predator hypothesis, in which specialized predation of snakes on dextral snails can promote fixation of sinistral mutant alleles. I theoretically revealed that right-handed predation can promote speciation of snails. In small populations, indeed, I found that a recessive mutant has higher fixation probabilities without predation, whereas a dominant mutant has higher one with predation.

Chapter 2. Eco-evolutionary dynamics of phenotypic plasticity

Masato Yamamichi, Takehito Yoshida, Akira Sasaki

2.1 Abstract

Ecologists have increasingly focused on how rapid adaptive trait changes can affect population dynamics. Rapid adaptation can result from either rapid evolution or phenotypic plasticity, but their effects on population dynamics are seldom compared directly. Here we examine theoretically the effects of rapid evolution and phenotypic plasticity of antipredatory defense on predator-prey dynamics. Our analyses reveal that phenotypic plasticity tends to stabilize population dynamics more strongly than rapid evolution. It is therefore important to know the mechanism by which phenotypic variation is generated for predicting the dynamics of rapidly adapting populations. We next examine an advantage of a phenotypically plastic prey genotype over the polymorphism of specialist prey genotypes. Numerical analyses reveal that the plastic genotype, if there is a small cost for maintaining it, cannot coexist with the pairs of specialist counterparts unless the system has a limit cycle. Furthermore, for the plastic genotype to replace specialist genotypes, a forced environmental fluctuation is critical in a broad parameter range. When these results are combined, the plastic genotype enjoys an advantage with population oscillations, but plasticity tends to lose its advantage by stabilizing the oscillations. This dilemma leads to an interesting intermittent limit cycle with the changing frequency of phenotypic plasticity.

2.2 Introduction

Adaptive trait change is a central topic of evolutionary biology. A vast number of studies have shown how individual organisms change traits in response to ecological factors. In contrast, little is known about how adaptive trait changes result in changes of population and community dynamics. Most classical studies in population and community ecology assume an organism's traits to be fixed. However, the significance of the effect of "rapid" adaptive trait change on population dynamics has increasingly been recognized (Lima 1998, Thompson 1998, Bolker et al. 2003, Werner and Peacor 2003, Agrawal et al. 2007, Peckarsky et al. 2008).

Both rapid contemporary evolution and phenotypic plasticity, the two

mechanisms that cause rapid and adaptive phenotypic change (Shimada et al. 2010), have the potential to affect population dynamics. However, their effects on population and community dynamics are seldom compared directly. Here we briefly summarize the characteristics and ecological effects of mechanisms that can cause rapid adaptation and then introduce our study design.

Despite the longstanding and unwarranted belief that evolution occurs so slowly that it does not affect ecological phenomena, rapid evolution (also referred to as contemporary or ongoing evolution) is rather common in the wild (Thompson 1998, Kinnison and Hendry 2001, Carroll et al. 2007, Pelletier et al. 2009). Here we define rapid evolution as "a genetic change occurring rapidly enough to have a measurable impact on simultaneous ecological change" (Hairston et al. 2005). An increasing number of ecological studies have demonstrated the effects of rapid evolution on the population dynamics of a single species (Sinervo et al. 2000), predator-prey dynamics (Abrams 2000, Yoshida et al. 2003, Yoshida et al. 2007), host-parasite dynamics (Duffy and Sivars-Becker 2007), community structures (Johnson and Stinchcombe 2007), and even ecosystems (Fussmann et al. 2007, Post and Palkovacs 2009, Matthews et al. 2011). Feedbacks between ecological and evolutionary dynamics are referred to as eco-evolutionary dynamics (Pelletier et al. 2009).

We here view evolution as the change in the frequency of several genotypes that result from standing genetic variation (Barrett and Schluter 2008). Thus, intraspecific genetic diversity is a prerequisite for rapid evolution. The effect of standing genetic diversity on ecological dynamics is also a topic of active research (Whitham et al. 2006, Kokko and López-Sepulcre 2007, Hughes et al. 2008).

Phenotypic plasticity, by which a single genotype produces different phenotypes in response to environmental cues, also affects population dynamics (Verschoor et al. 2004b, Vos et al. 2004a, Kishida et al. 2010), trophic cascades (Werner and Peacor 2003, Vos et al. 2004b, Ohgushi 2005, van der Stap et al. 2007), and ecosystem functioning (Schmitz et al. 2008; for review, see Tollrian and Harvell 1999; Agrawal 2001; Miner et al. 2005).

A frequently asked and important question about the effects of rapid adaptation on ecological dynamics is whether rapid phenotypic changes stabilize population dynamics. Many studies have tried to determine whether rapid adaptations cause population oscillations or result in a stable equilibrium. It has been shown that for

theoretical predator-prey systems, rapid adaptation of prey species (Ives and Dobson 1987, Ramos-Jiliberto 2003, Vos et al. 2004a, Kopp and Gabriel 2006, Kondoh 2007), predator species (Kondoh 2003, Křivan 2003), or both predator and prey species (Yamauchi and Yamamura 2005, Křivan 2007, Mougi and Nishimura 2008, Mougi and Kishida 2009) stabilizes population dynamics (see review in Abrams 2000, Kishida et al. 2010). Still, few studies have compared effects from the different mechanisms that drive rapid adaptation. Thus, we seek to compare the effects of rapid evolution and phenotypic plasticity on population and community dynamics.

Both rapid evolution and plasticity are adaptive changes that increase an individual's fitness, and the changes are rapid enough to affect ecological dynamics (Hairston et al. 2005, Miner et al. 2005). The three main different characteristics between them are operating timescale, recovery speed of minor traits, and phenotypic range. First, as for operating timescale, plastic response is essentially fast but not inherited (although it can be transgenerational; Agrawal et al. 1999). Evolution is transgenerational by definition, so its resultant effects will persist longer. Thus, evolution may generate a longer "time lag" in adapting to new environmental conditions. Second, because evolution is affected by former states, it needs more time for the traits that are rare in the population (minor traits) to recover. When a genotype abundance becomes temporally low, then adaptation must wait for the minor genotype to recover. Especially, once the minor genotype becomes extinct, evolution has to wait for a new mutation. Plasticity, on the other hand, can change the phenotype to fit the current environments regardless of the former state. Thus, slower recovery speed of minor traits can also cause time lag in evolution. Finally, as for phenotypic range, the plasticity range is restricted by reaction norm characteristics. Rapid evolution relies on the genetic diversity of a population exposed to selection pressures. Thus, extant genetic variation in a population determines phenotypic range (Barrett and Schluter 2008). It might seem intuitive that genetic diversity offers a broader phenotypic range than reaction norms within an individual organism. However, by examining 18 species of plants, invertebrates, and vertebrates, Bolnick et al. (2003) observed that intraindividual phenotypic range was broader than interindividual phenotypic range (Bolnick et al. 2003). Thus, it remains unclear as to whether the phenotypic range of rapid evolution is broader than that of plasticity.

Here we focus on the differences of operating timescale and minor traits

recovery speed for phenotypic changes caused by rapid evolution and phenotypic plasticity and assess effects on population and community dynamics. To compare these effects, we use mathematical models of predator-prey systems and examine the consequences of phenotypic changes in prey (inducible defense) rather than in predators, because predator-prey interactions are asymmetrical and are often characterized by greater responses of prey to predators than vice versa (Abrams 2000). Specifically, we focus on two aspects of stability: ecological and evolutionary stability.

We examine ecological stability (demographic stability) in a population given either mechanism of rapid adaptation (rapid evolution or phenotypic plasticity). Here we define ecologically stable states as the predator-prey coexistence in stable equilibria. When the system shows limit cycle oscillations or deterministic extinction of predator, we call them ecologically unstable states. Although we do not treat extreme population oscillations as extinction here, when the amplitude of limit cycle increases, the minimum abundances may become very close to zero to cause extinction by demographic stochasticity in the real world. Note that we concentrate on the sustainability of trophic levels in the food chain, regardless of prey species identity. Coexistence of competitors is not the focus of ecological stability here (Křivan 2003). Either phenotypic plasticity (e.g., Verschoor et al. 2004b; Vos et al. 2004a) or rapid evolution owing to standing genetic variation (e.g., Doebeli and de Jong 1999, Johnson and Agrawal 2003, Agashe 2009) can stabilize population. However, making such a generalization based on previous studies is difficult, because plasticity and evolution have also been shown to destabilize population dynamics (Edelstein-Keshet and Rausher 1989, Abrams and Matsuda 1997, Underwood 1999, Kopp and Gabriel 2006). Is there any difference between the stabilizing effect of genetic diversity and that of plasticity? If so, which mechanism is better at stabilizing population dynamics? Our models use identical pairs of palatable and defended phenotypes, but the plastic genotype can produce two phenotypes, depending on environmental cues, whereas the nonplastic genotypes cannot (fig. 1*B*, 1*C*).

In terms of evolutionary stability, we ask which state is evolutionarily stable (or not) over a longer period of time (Mougi and Kishida 2009) if either a plastic or nonplastic genotype is better at stabilizing population dynamics (ecological stability). That is, when plastic genotypes compete with nonplastic genotypes (fig. 1*D*), which one outcompetes the other in stable or fluctuating environments? It has been hypothesized

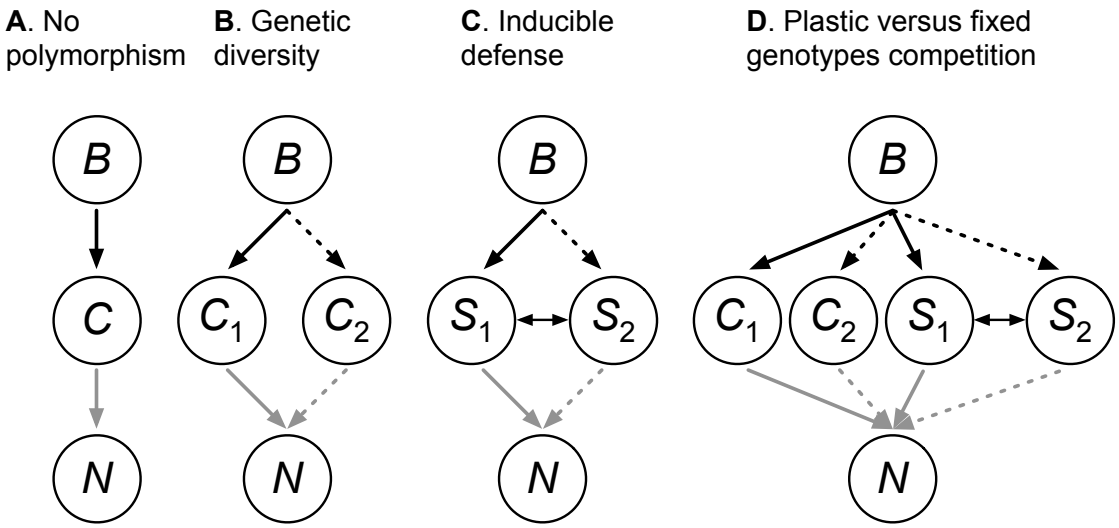

Figure 2.1: Model description. *A*, 1 predator –1 prey chemostat model. *B*, 1 predator–2 prey chemostat model. Prey have fixed (nonplastic) phenotypes. Solid arrows indicate large searching efficiency, and dashed arrows indicate small searching efficiency (parameters s_{1i} and s_{2i} in eqq. [3]). *C*, 1 predator–1 plastic prey chemostat model. The plastic prey changes its phenotype according to predator density. *D*, 1 predator–3 prey chemostat model. Palatable and defended phenotypes are identical between nonplastic and plastic genotypes.

that genetic variation for a fixed phenotype is favored in stable environments, whereas phenotypic plasticity is favored in unstable environments (Scheiner 1993, de Jong 1995, Stomp et al. 2008, Svanbäck et al. 2009). Thus, we compare the outcome of a competition model (fig. 1*D*) in stable and fluctuating environments.

Although rapid evolution and phenotypic plasticity occur often in the wild (Tollrian and Harvell 1999, Agrawal 2001, Post and Palkovacs 2009 and references therein), it is in general difficult to compare their effects on population dynamics directly. A rotifer–green algae chemostat system provides an excellent experimental venue for studying these effects. *Scenedesmus* green algae form colonies plastically when exposed to chemical cues (kairomones) released by predators (Hessen and van Donk 1993). Because these colonies are too big to be eaten by gape-limited predators (e.g., rotifers), the prey species avoid predation. However, this defense has potentially serious costs. If the colony grows too large, it can sink to a depth where sunlight cannot penetrate and thus stop growing (Lürling and van Donk 2000). When predators are

abundant, induced prey defense reduces the per capita growth rate of predators. When predators are scarce, prey species relax their defenses, resulting in an increase in the per capita growth rate of predators. This plasticity-based feedback can stabilize population oscillations (Verschoor et al. 2004b; Vos et al. 2004a). Although *Scenedesmus* is plastic, its congener *Desmodesmus* is not, being always either unicellular (palatable) or colonial (defended). This type of polymorphism may cause the rapid evolution observed in *Chlorella* and *Chlamydomonas* chemostat systems (Yoshida et al. 2003, Jones et al. 2009, Becks et al. 2010). To compare potential differences in the effects of rapid evolution and plasticity on *Scenedesmus* and *Desmodesmus*, with which the model-based hypotheses are experimentally testable, we construct mathematical models based on a rotifer–green algae chemostat system.

2.3 Models

We consider four variations of models to examine the effects of genetic diversity and plasticity on predator-prey population dynamics. These models describe the dynamics of nutrient, prey, and predator. The first model assumes no adaptation, the second model assumes evolution of prey, the third assumes plasticity of prey, and the fourth is a mixture of the second and the third models (fig. 1). Local stability of equilibria and limit cycles is analyzed both analytically and numerically to produce bifurcation and phase diagrams in parameter space. We focus specifically on the two parameters in the phase diagrams: chemostat dilution rate (δ) and prey nutrient searching efficiency (s_1), which relates to predator searching efficiency in acquiring prey (s_2). We use the ratio of stable equilibrium to oscillatory and deterministic extinction dynamics calculated from their relative area in the two-dimensional (2-D) phase diagram as an indicator of ecological stability.

2.3.1 *Model I: Basic Model*

Our basic chemostat model (fig. 1*A*; after Fussmann et al. 2000) is composed of limiting nutrient *N*, phytoplankton prey *C* (e.g., green algae *Chlorella vulgaris*), and zooplankton predator *B* (e.g., rotifer *Brachionus calyciflorus*) and assumes a Holling type II functional response for nutrient/prey uptake (Kot 2001). We do not include predator age structure, unlike Fussmann et al. (2000). Nutrient, prey, and predator concentration changes with time, respectively, are calculated as

$$\frac{dN}{dt} = \delta\left(N_I - N\right) - \frac{1}{\varepsilon_1}\left(\frac{s_1 NC}{1 + h_1 s_1 N}\right), \tag{2.1a}$$

$$\frac{dC}{dt} = C\left[\frac{s_1 N}{1 + h_1 s_1 N} - \frac{1}{\varepsilon_2}\left(\frac{s_2 B}{1 + h_2 s_2 C}\right) - \delta\right], \tag{2.1b}$$

$$\frac{dB}{dt} = B\left[\frac{s_2 C}{1 + h_2 s_2 C} - \left(m + \delta\right)\right], \tag{2.1c}$$

where δ is dilution rate, N_I is inflow nutrient concentration, s_1 is prey searching efficiency for nutrient, h_1 is prey handling time for nutrient, s_2 is predator searching efficiency for prey, h_2 is predator handling time for prey, m is predator death rate, ε_1 is prey assimilation efficiency, and ε_2 is predator assimilation efficiency. In our model, organism state variables (C and B) are expressed in units of total limiting nutrient rather than number of individuals. Certain parameters are fixed using measured values from previous studies (Halbach and Halbach-Keup 1974, Tischner and Lorenzen 1979, Aoki and Hino 1996, Fussmann et al. 2000; see table 1).

Although measuring the trade-off function and cost of defensive trait is still challenging, there are several experiments that show the defense cost of green algae is associated with algal searching efficiency in acquiring nutrient (Yoshida et al. 2004), growth rate (Meyer et al. 2006), and sinking rate (Lürling and van Donk 2000). Here we assume that both searching efficiency parameters, s_1 and s_2, are positively correlated (i.e., there is a trade-off between defense and growth in prey) as representative of previous studies on green algae (Jones and Ellner 2004, 2007). Considering the empirical data (table 1) of Fussmann et al. (2000), we assume the trade-off relationship as

$$\frac{s_1}{s_{10}} = \left(\frac{s_2}{s_{20}}\right)^{\alpha} \tag{2.2}$$

where s_{10} and s_{20} are empirical constants and α is a positive constant. This function is formulated so that it always crosses the observed point (s_{10}, s_{20}) and the origin. We can make the function convex or concave by changing α. If $\alpha < 1$, investment in defense (lower s2) is increasingly more costly in terms of resource uptake rate (accelerating cost). If $\alpha > 1$, the initial investment in defense is very costly, but further investments become increasingly less costly. If $\alpha = 1$, the trade-off is linear. The effect of α on

Table 2.1: Parameter sets estimated from a rotifer–green algal system

Parameter	Description	Value	Reference
N_I	Limiting nutrient conc. (supplied medium)	80 μmol N/l	Set
δ	Chemostat dilution rate	variable /day	Set
h_1	Algal handling time	0.303 day	Fussmann et al. (2000)
h_2	Rotifer handling time	0.444 day	Fussmann et al. (2000)
m	Rotifer mortality	0.055 /day	Fussmann et al. (2000)
s_{10}	Algal searching efficiency	0.767 day	Tischner & Lorenzen (1979), Fussmann et al. (2000)
s_{20}	Rotifer searching efficiency	0.15 day	Halbach & Halbach-Keup (1974), Fussmann et al. (2000)
ε_1	Algal assimilation efficiency	1.0	Fussmann et al. (2000)
ε_2	Rotifer assimilation efficiency	0.25	Aoki & Hino (1996)
b	Shape of defense functions	2.0	Vos et al. (2004a, b)

Note: Set = adjust parameters set by an experimenter.

population stability is discussed in "Results." A local stability analysis of model I is presented in appendix A.

2.3.2 *Model II: Genetic Diversity Model*

Several mathematical modeling methods describe eco-evolutionary dynamics, including biclonal models (Abrams and Matsuda 1997, Jones and Ellner 2007), multiclonal models (Jones et al. 2009), adaptive dynamics models (Geritz et al. 1998), and one-locus and quantitative genetics models (Abrams 2001; Fussmann et al. 2007). We here adopt a biclonal model (fig. 1*B*), the simplest among the "genetic diversity" models, the closest to describing the *Desmodesmus*-rotifer system, and the easiest to compare with phenotypic plasticity model (phenotypic plasticity models usually involve two phenotypes, and organisms change their states according to environmental cues; e.g., Vos et al. 2004a). Our model is the same as that of Jones and Ellner (2007), except for the assumptions on trade-offs between prey palatability and resource uptake rates. Similar models have been used by Abrams and Matsuda (1997), Jones and Ellner (2004), and Yoshida et al. (2007). In our model II, there are two prey genotypes:

palatable, easily eaten, but rapidly growing; and defended but slow growing (Yoshida et al. 2004; Meyer et al. 2006). Concentration changes for nutrient N, palatable and unpalatable preys C_1 and C_2, and predator B are given by

$$\frac{dN}{dt} = \delta\left(N_I - N\right) - \frac{1}{\varepsilon_1}\left(\sum_{i=1}^{2} \frac{s_{1i} N C_i}{1 + h_1 s_{1i} N}\right), \tag{2.3a}$$

$$\frac{dC_i}{dt} = C_i\left[\frac{s_{1i} N}{1 + h_1 s_{1i} N} - \frac{1}{\varepsilon_2}\left(\frac{s_{2i} B}{1 + h_2 \sum_{j=1}^{2} s_{2j} C_j}\right) - \delta\right], \ (i = 1, 2), \tag{2.3b}$$

$$\frac{dB}{dt} = B\left[\frac{\sum_{i=1}^{2} s_{2i} C_i}{1 + h_2 \sum_{i=1}^{2} s_{2i} C_i} - \left(m + \delta\right)\right], \tag{2.3c}$$

where s_{1i} is palatable/defended prey searching efficiency for nutrient and s_{2i} is predator efficiency in searching for palatable/defended prey. Because mounting a defense to a predator involves a cost, increasing the defense level (decreasing s_{2i}) leads to a reduced ability to compete for scarce nutrients (decreasing s_{1i}), following the trade-off function of equation (2). A local stability analysis of model II is presented in appendix 2.6.2.

2.3.3 *Model III: Plasticity Model*

We develop a model with plastic prey S (e.g., inducible defense in *Scenedesmus obliquus*) following previous studies (Vos et al. 2004a, Vos et al. 2004b, Serizawa et al. 2008, Mougi and Kishida 2009) but with a slightly changed plastic function (fig. 1*C*). The model of Vos et al. (2004a) had a carrying capacity K but no nutrient dynamics to describe microcosm systems. Because we want to compare phenotypic plasticity with rapid genetic changes, we adopt the chemostat model to allow for direct comparisons with model II (as in van der Stap et al. 2009). We also propose a new plastic response function for our model (hereafter model IIIA) as opposed to the model of Vos et al. (2004a; hereafter model IIIB). This is because plasticity of *Scenedesmus* is intergenerational phenomenon, whereas former models are for intragenerational plasticity. In model IIIA the concentrations change as

$$\frac{dN}{dt} = \delta\left(N_I - N\right) - \frac{1}{\varepsilon_1}\left(\sum_{i=1}^{2} \frac{s_{1i} N S_i}{1 + h_1 s_{1i} N}\right), \tag{2.4a}$$

$$\frac{dS_i}{dt} = Q_i(B)\left(\sum_{j=1}^{2}\frac{s_{1j}NS_j}{1+h_1 s_{1j}N}\right) - \frac{1}{\varepsilon_2}\left(\frac{s_{2i}S_iB}{1+h_2\sum_{j=1}^{2}s_{2j}S_j}\right) - \delta S_i, \quad (i = 1, 2), \text{(2.4b)}$$

$$\frac{dB}{dt} = B\left[\frac{\sum_{i=1}^{2}s_{2i}S_i}{1+h_2\sum_{i=1}^{2}s_{2i}S_i} - (m+\delta)\right]. \text{(2.4c)}$$

Note that the only difference between model II and model IIIA is the prey reproduction term. The plastic genotype can have two phenotypes that are exactly the same as those of the two nonplastic genotypes. The phenotype of newly produced plastic prey is determined according to the factor $Q_i(B)$. The plastic response function $Q_i(B)$ is defined as

$$Q_1(B) = \frac{1}{1+(B/g)^b}, \text{(2.5a)}$$

$$Q_2(B) = \frac{(B/g)^b}{1+(B/g)^b}, \text{(2.5b)}$$

where g is a predator threshold density where defense induction reaches half its maxima and b is a plasticity sensitivity parameter (Verschoor et al. 2004a, Vos et al. 2004a). Terms $Q_1(B)$ and $Q_2(B)$ are decreasing/increasing functions of predator density. If predator density is large relative to the threshold parameter (g), $Q_1(B)$ becomes smaller and $Q_2(B)$ becomes larger. A large proportion of newly produced prey then is unpalatable (S2) or vice versa. We at first set the value of b on the basis of previous studies (Vos et al. 2004a, 2004b; table 1), but later we relax this assumption and vary the values of b and g to examine their effects on the results. The effects of these parameter values are discussed in "Results." In reality, the difference between palatable and defended types of *Scenedesmus* depends on the number of cells in a colony. Palatable type are unicellular or bicellular per colony, whereas defended types are 4, 8, or even 16 cells per colony (Hessen and van Donk 1993). Because we describe organism state variables (S and B) in units of total limiting nutrient rather than cell count, conversion efficiency between palatable and defended phenotypes of plastic prey can be set to 1.

As discussed previously, we examine another plasticity model (model IIIB) described in previous studies (Vos et al. 2004a, 2004b; Serizawa et al. 2008; Mougi and

Kishida 2009):

$$\frac{dS_1}{dt} = \frac{s_{11} N S_1}{1 + h_1 s_{11} N} - \frac{1}{\varepsilon_2}\left(\frac{s_{21} S_1 B}{1 + h_2 \sum_{j=1}^{2} s_{2j} S_j} \right) - \delta S_1 - fQ_2(B) S_1 + fQ_1(B) S_2, \quad (2.6a)$$

$$\frac{dS_2}{dt} = \frac{s_{12} N S_2}{1 + h_1 s_{12} N} - \frac{1}{\varepsilon_2}\left(\frac{s_{22} S_2 B}{1 + h_2 \sum_{j=1}^{2} s_{2j} S_j} \right) - \delta S_2 + fQ_2(B) S_1 - fQ_1(B) S_2. \quad (2.6b)$$

The primary difference between model IIIA (eqq. [4]) and model IIIB (eqq. [6]) is in the timing of when a prey species decides whether or not to form a colony. Our model (model IIIA) assumes that all members of a population make decisions regarding reproduction (e.g., cell segmentations in *Scenedesmus*) based on the current predator abundance. We propose that this more suitably describes the *Scenedesmus* colony formation process. Alternatively, model IIIB assumes that a portion of individuals in a population change their phenotype plastically according to predator abundance, reacting with no direct relationship to reproduction (intragenerational plasticity). This assumption is appropriate for describing morphological defense that is not linked to reproduction (e.g., tadpoles; Kishida et al. 2010) or behavioral plasticity (e.g., escaping behavior). In model IIIB, the ratio of a population that exhibits a plastic response within a certain time period is defined as f. Thus, model IIIB has one more degree of freedom than model IIIA. This situation is still suitable to test the effect of plasticity response speed on population dynamics. For both models IIIA and IIIB, local stability analysis is too complex, and only simulation analyses are performed.

2.3.4 *Model IV: Combined Effect Model*

Situations in which plastic genotypes (reproduction-associated inducible defense: model IIIA) and specialist (nonplastic) genotypes (i.e., those either palatable or defended) compete for nutrients are considered (fig. 1*D*). We add plasticity maintenance costs (after DeWitt et al. 1998) to equations (4), so

$$\frac{dN}{dt} = \delta(N_I - N) - \frac{1}{\varepsilon_1}\left[\sum_{i=1}^{2} \frac{s_{1i} N (S_i + C_i)}{1 + h_1 s_{1i} N} \right], \quad (2.7a)$$

$$\frac{dC_i}{dt} = C_i \left\{ \frac{s_{1i} N}{1 + h_1 s_{1i} N} - \frac{1}{\varepsilon_2}\left[\frac{s_{2i} B}{1 + h_2 \sum_{j=1}^{2} s_{2j} (C_j + S_j)} \right] - \delta \right\}, \quad (i = 1, 2), \quad (2.7b)$$

$$\frac{dS_i}{dt} = Q_i(B)\left(\sum_{j=1}^{2}\frac{s_{1j}NS_j}{1+h_1 s_{1j}N}\right) - \frac{1}{\varepsilon_2}\left[\frac{s_{2i}S_iB}{1+h_2\sum_{j=1}^{2}s_{2j}(C_j+S_j)}\right] - (\gamma+\delta)S_i, (i = 1, 2), \quad (2.7c)$$

$$\frac{dB}{dt} = B\left[\frac{\sum_{i=1}^{2}s_{2i}(C_i+S_i)}{1+h_2\sum_{i=1}^{2}s_{2i}(C_i+S_i)} - (m+\delta)\right], \quad (2.7d)$$

where the cost of plasticity, γ, is the death rate of the plastic genotype ($\gamma = 0.01$ is assumed thereafter). Because the plastic prey always needs to be sensitive to predator density, we assume that there is some sort of the maintenance cost of plasticity (e.g., production of a receptor protein; DeWitt et al. 1998). Without the maintenance cost, a plastic genotype can coexist with nonplastic genotypes in a stable equilibrium (region $SC_{12}E$ in fig. S9*A* [supplemental figs. S1–S14 are in 2.6.4]). In this situation, predator density remains stable, and the plastic genotype does not change the ratio of palatable and defended phenotypes through time and reproduces both phenotypes in a fixed ratio (fig. S9*A*). Under this condition, the plastic genotype does not exhibit plasticity, and we cannot determine the advantages of plasticity. Thus, we add the maintenance cost, and a very small maintenance cost is sufficient to prevent such neutrally stable coexistence at stable equilibria.

2.4 Results

2.4.1 *Comparison with Previous Studies*

Using models I, II, and III, we confirmed results observed in previous studies (e.g., Vos et al. 2004a; Jones and Ellner 2007). Both model II (genetically polymorphic prey) and model III (phenotypically plastic prey) have a broader parameter region than model I (monomorphic prey) that leads to stable predator-prey coexistence equilibrium points (table 2), supporting the idea that rapid adaptive trait changes stabilize population dynamics (Johnson and Agrawal 2003; Vos et al. 2004a).

For model I, increasing the chemostat dilution rate δ change population dynamics from limit cycle to equilibrium, predator extinction, or both predator and prey extinction (figs. 2*A*, 2*B*, 3*A*). Increasing the defense investment of prey (decreasing prey palatability s_2 and, by the trade-off, nutrient intake rate s_1) change population dynamics in a similar way (fig. 3*A*). This pattern is consistently observed in the local stability analysis (fig. S1*A*) and the numerical simulation (fig. 3*A*).

Table 2.2: Relative area of deterministic extinction (either predator or both predator and prey), stable equilibria, and limit cycles of 2D phase diagrams (as fig. 3).

	Extinction	Equilibrium	Oscillation	Stability
I $\alpha = 1$	0.25	0.28	0.46	0.39
II $\alpha = 1$ (right)	0.06	0.39	0.56	0.64
II $\alpha = 1$ (left)	0.06	0.38	0.57	0.61
IIIA $\alpha = 1$	0.06	0.45	0.49	0.83
IIIA $b = 0.1$	0.08	0.35	0.57	0.55
IIIA $b = 10$	0.06	0.47	0.47	0.90
IIIA $g = 2$	0.06	0.48	0.47	0.92
IIIA $g = 10$	0.06	0.34	0.60	0.52
IIIB $f = 0.1$	0.06	0.40	0.54	0.67
IIIB $f = 1$	0.06	0.42	0.53	0.72
I $\alpha = 0.5$	0.38	0.26	0.36	0.36
II $\alpha = 0.5$	0.02	0.36	0.62	0.57
IIIA $\alpha = 0.5$	0.02	0.59	0.39	1.41
I $\alpha = 2$	0.18	0.24	0.58	0.31
II $\alpha = 2$ (right)	0.07	0.25	0.68	0.34
II $\alpha = 2$ (left)	0.07	0.19	0.74	0.23
IIIA $\alpha = 2$	0.07	0.31	0.62	0.46

Note: Here we use the ratio of stable equilibria/(extinction + limit cycles) as an index of ecological stability. Because of bi-stability, model II has two bifurcations. Left/right: the simulation started from the left/right end of the phase diagram (s_{12} = 0.01/0.99) and used the last density of predator and prey as the first density of subsequent simulation runs. When $\alpha = 0.5$, there seems virtually no bi-stability.

For model II, many attractors are found in the parameter space of dilution rate and defended prey palatability (figs. 2*C*, 3*B*), including (1) stable equilibria with predator and two prey genotypes (region C_{12} E of figs. 3*B*, S1*B*), (2) stable equilibria with predator and palatable prey (region C_1 E), (3) stable equilibria with predator and defended prey (region C_2 E), (4) stable equilibria with palatable prey only (region PEx),

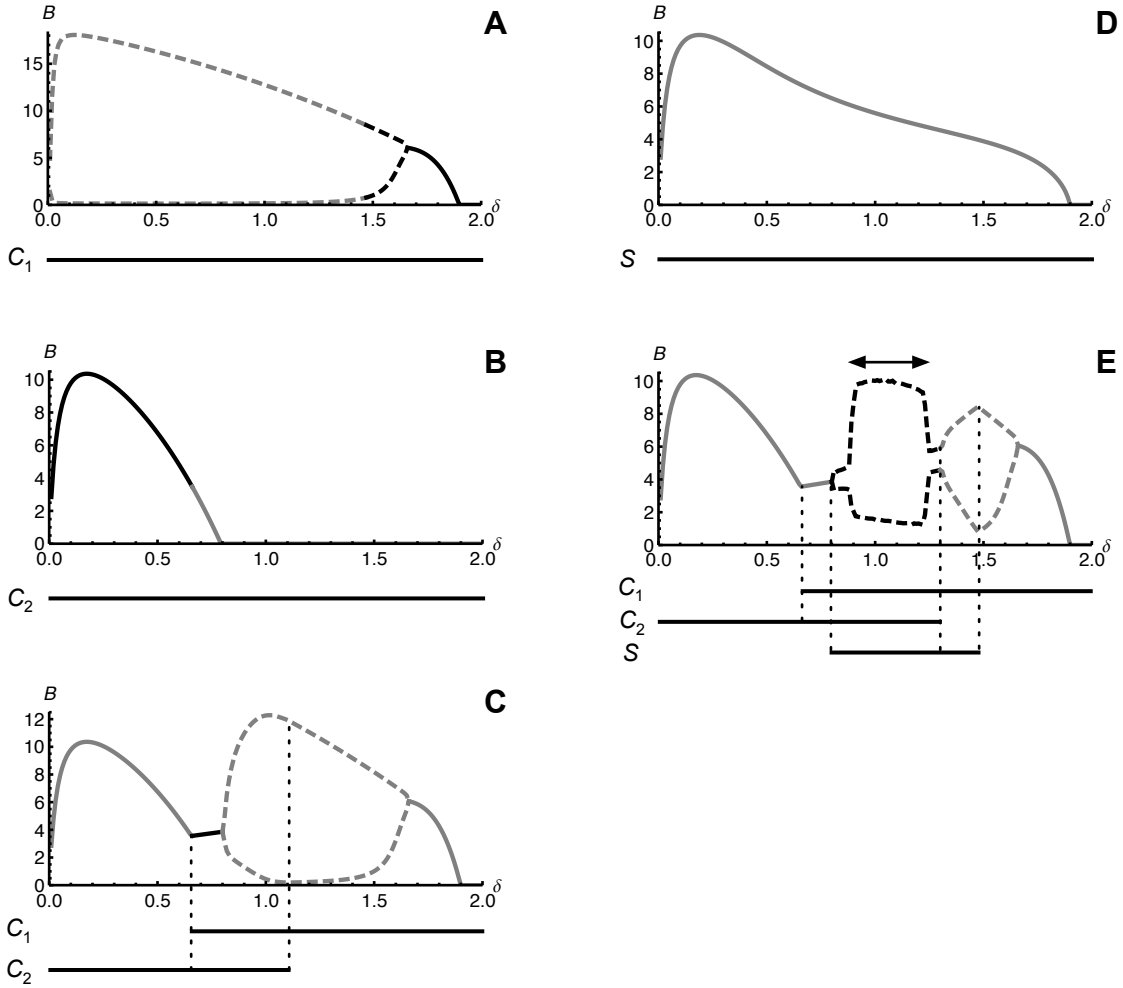

Figure 2.2: Bifurcation diagrams of models I, II, IIIA, and IV. Here the *X*-axis is dilution rate (δ), and the *Y*-axis is predator maximum and minimum abundance. Black lines represent evolutionarily stable regions; gray lines are evolutionarily unstable regions. Solid lines represent stable equilibria; dotted lines are maxima and minima of limit cycles. Horizontal lines below diagrams are parameter regions where focal prey can exist. A, Model I with palatable prey ($s_1 = 1.0$). *B*, Model I with defended prey ($s_1 = 0.1$). *C*, Model II with palatable and defended prey ($s_{11} = 1.0$, $s_{12} = 0.1$). *D*, Model IIIA with the same parameters as *C* ($b = 2$, $g = 5$). *E*, Model IV with palatable, defended, and plastic prey.

(5) limit cycles with predator and two prey genotypes (region C_{12} O), (6) limit cycles with predator and palatable prey (region C_1 O), and (7) limit cycles with predator and defended prey (region C_2 O). At the boundaries in figure 3*B*, an equilibrium point changed its stability. For example, moving from region C_1 E into region C_{12} E by

decreasing the dilution rate, defended prey are able to invade and produce a stable community composed of both palatable and defended prey and a predator. The pattern is consistent between the local stability analysis (fig. S1*B*) and the numerical simulation (fig. 3*B*).

In the region of limit cycles in which both genotypes coexist, evolutionary cycles are observed. Figure 4*A* shows a typical evolutionary cycle time series: defended prey numbers increase when predators are abundant, whereas palatable prey numbers increase when predators are scarce. When we combine the numbers of the two prey genotypes, the oscillation phase-lag change from an ordinary quarter-period of monomorphic prey to a half-period (fig. 4*A*; Jones and Ellner 2007). Note that these phase lags are approximate values, though they are exact at bifurcation points.

In model II, the continuous rapid evolution (evolutionary cycles) or the stable coexistence of two prey do not always occur, but the presence of two genotypes promote ecological stability: when dilution rate is low, palatable genotypes exhibit a limit cycle if present alone (fig. 2*A*), but when both genotypes are present, defended genotypes dominate and stabilize the system (fig. 2*C*). When dilution rate is high, the defended genotype cause predator extinction (fig. 2*B*), but in the presence of genetic diversity, palatable genotypes dominate and prevent predator extinction (fig. 2*C*).

Bistabilities of attractors are found around regions C_1 E, C_1 O, C_{12} E, and C_{12} O (cf. figs. S3, S4). These bistabilities include (1) stable equilibria with three species (palatable prey, defended prey, and predator) versus limit cycles with two species (palatable prey and predator), (2) limit cycles with three species (evolutionary cycle) versus limit cycles with two species, (3) stable equilibria with three species versus limit cycles with three species (nonevolutionary cycle), and (4) limit cycles of small amplitude with three species (evolutionary cycle) versus limit cycles of large amplitude with three species (nonevolutionary cycle). Note that a previous study did not detect the existence of region C_1 O and the bistabilities (Jones and Ellner 2007). This is probably due to differences in the choice of bifurcation parameters and trade-off assumptions. Actually, when $\alpha < 1$, bistable regions disappear, whereas when $\alpha > 1$, they broaden out (figs. S3, S4).

For model III, there are limit cycle regions, stable equilibrium regions, and predator extinction regions, depending on the dilution rate and the defended prey palatability (figs. 2*D*, 3*C*). Increasing the dilution rate change the dynamics from

predator-prey oscillation to stable coexistence, and further increase led to predator extinction, as was observed previously (van der Stap et al. 2009).

We obtain new insights by comparing the results from models I, II, III, and IV. One relates to the relative stabilizing effect of rapid evolution to that of phenotypic plasticity, and the other relates to the effect of environmental changes on competition between plastic and nonplastic genotypes.

2.4.2 *Stabilizing Effects of Prey Polymorphisms*

We summarize the relative areas of extinction, stable equilibria, and limit cycles in the 2-D phase diagram and the index of ecological stability (see "Models") in table 2. For example, we can see that model IIIA has a larger stability index than model I, and this is mainly due to a smaller fraction of extinction (see fig. 3*A*, 3*C*).

Comparing results from models II and III, we can answer our earlier question of whether rapid evolution or phenotypic plasticity is more efficient to stabilize population dynamics. When we compare model II with IIIA (induction of defended prey at cell division), it is clear that model IIIA has a broader stable equilibrium range and a narrower limit cycle range than model II (table 2), especially when defended prey has a phenotype distinct from that of palatable prey (fig. 3*B*, 3*C*, in the left region of the phase diagrams). The same tendency of phenotypic plasticity to more readily stabilize the system than rapid evolution is observed in model IIIB (induced switching between defended and palatable prey) if the switching speed (f) is fast enough (eqq. [6]; table 2; fig. S8).

Plasticity can, however, destabilize dynamics, whereas fixed genotypes promote stability (fig. 4*B*, 4*C*) in some parameter combinations (e.g., $\delta = 1.2$ and $s_{12} = 0.5$). Palatable prey species become extinct and the system reaches a stable equilibrium in model II (fig. 4*B*), whereas plasticity results in a large-amplitude limit cycle (fig. 4*C*). Despite these cases, the equilibrium region of model IIIA is broader in general than that of model II, indicating that plasticity promotes ecological stability.

Parameter sensitivity is also examined by simulations. Trade-off function parameter (a) largely affects the bistability area of model II but does not change the general tendency of the relative stabilizing effect in the models (table 2; cf. figs. S2–S5). Increasing the threshold parameter g of plastic function (eqq. [5]) destabilizes dynamics (table 2; fig. S6), whereas decreasing the sensitivity parameter b has the same effect

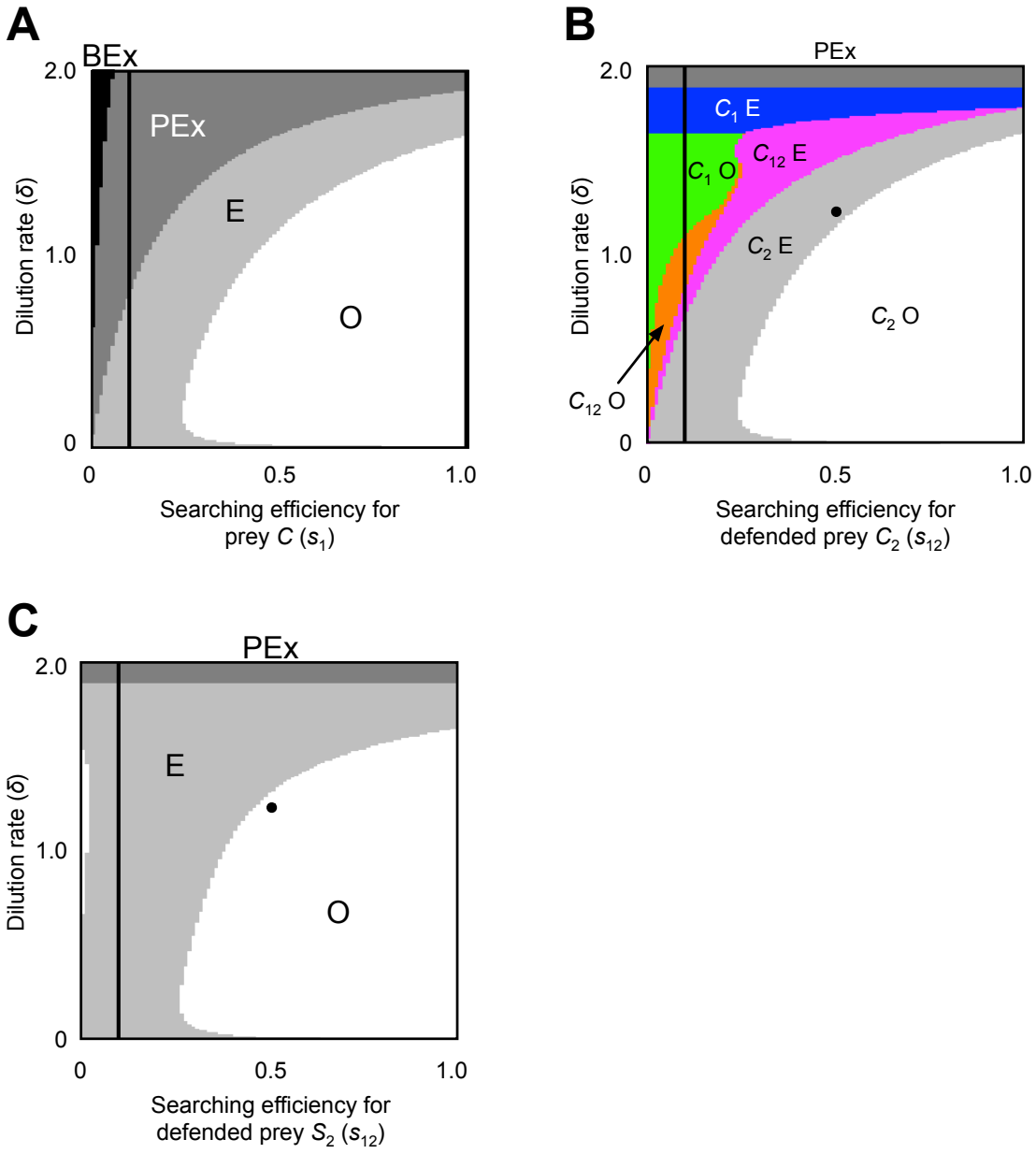

Figure 2.3: *A*, Phase diagram of model I. Prey nutrient searching efficiency (s_1) is shown on the *X*-axis and chemostat dilution rate (δ) on the *Y*-axis. Region BEx (both extinction; *black*): both predator and prey are extinct. Region PEx (predator extinction; *dark gray*): predator is extinct and prey exists in a stable equilibrium. Region E (equilibrium; *pale gray*): predator and prey coexist in a stable equi- librium. Region O (oscillation; *white*): predator and prey coexist in a limit cycle. The black lines represent the parameter regions of the bifurcation diagrams in figure 2*A* and 2*B*. *B*, Phase diagram of model II. The searching efficiency for palatable prey (s_{11}) is fixed to 1, and that for defended prey (s_{12}) is shown on the *X*-axis; dilution rate (δ) is shown on the *Y*-axis.

Region PEx: predator is extinct, and palatable prey exists in a stable equilibrium. Region C_1E (C_1 equilibrium; *blue*): palatable prey and predator coexist in a stable equilibrium. Region C_1 O (C_1 oscillation; *green*): palatable prey and predator coexist in a limit cycle. Region C_{12} O (C_1 and C_2 oscillation; *orange*): palatable prey, defended prey, and predator coexist in a limit cycle. Region C_{12} E (C_1 and C_2 equilibrium; *magenta*): palatable prey, defended prey, and predator coexist in a stable equilibrium. Region C_2 E (C_2 equilibrium; *pale gray*): defended prey and predator coexist in a stable equilibrium. Region C_2 O (C_2 oscillation; *white*): defended prey and predator coexist in a limit cycle. The black line represents the parameter region of the bifurcation diagram in figure 2*C*. The bistable regions are not shown in this figure for simplicity (see figs. S3, S4). The black point represents the parameter setting in figure 4*B*. *C*, Phase diagram of model IIIA ($b = 2$, $g = 5$). The axes are the same as for *B*. The legend is the same as for *A*. The black line represents the parameter region of the bifurcation diagram (fig. 2*D*). The black point represents the parameter setting in figure 4*C* where plastic prey destabilize while nonplastic prey stabilize population dynamics by the extinction of the palatable genotype.

(table 2; fig. S7). Because increasing the threshold parameter and decreasing the sensitivity parameter result in ineffective plastic response, we can conclude that plasticity is more stable than evolution as long as plasticity is effective. For subsequent evolutionary stability analysis, we fundamentally use the parameter set $\alpha = 1$ (trade-off is linear), $b = 2$, and $g = 5$ (plasticity is effective), but this assumption is relaxed later.

2.4.3 *Competition between Plastic and Nonplastic Genotypes*

We examine competition between two nonplastic genotypes (either a purely palatable or defended strategy) and one plastic genotype. The plastic genotype produces phenotypes identical to the two pure strategists, but phenotype ratio depends on predator density (model IV). When competing in a stable nutrient supply environment, plastic genotypes cannot outcompete nonplastic genotypes (figs. 2*E*, 5*A*). Plastic genotypes can survive in limit cycle regions but cannot eliminate the single-strategy genotypes. This indicates that ecological stability produced by plasticity (figs. 2*D*, 3*C*) is evolutionarily unstable, because a system can be invaded by nonplastic genotypes, resulting in destabilized dynamics. The black line in figure 2 represents an evolutionarily stable community.

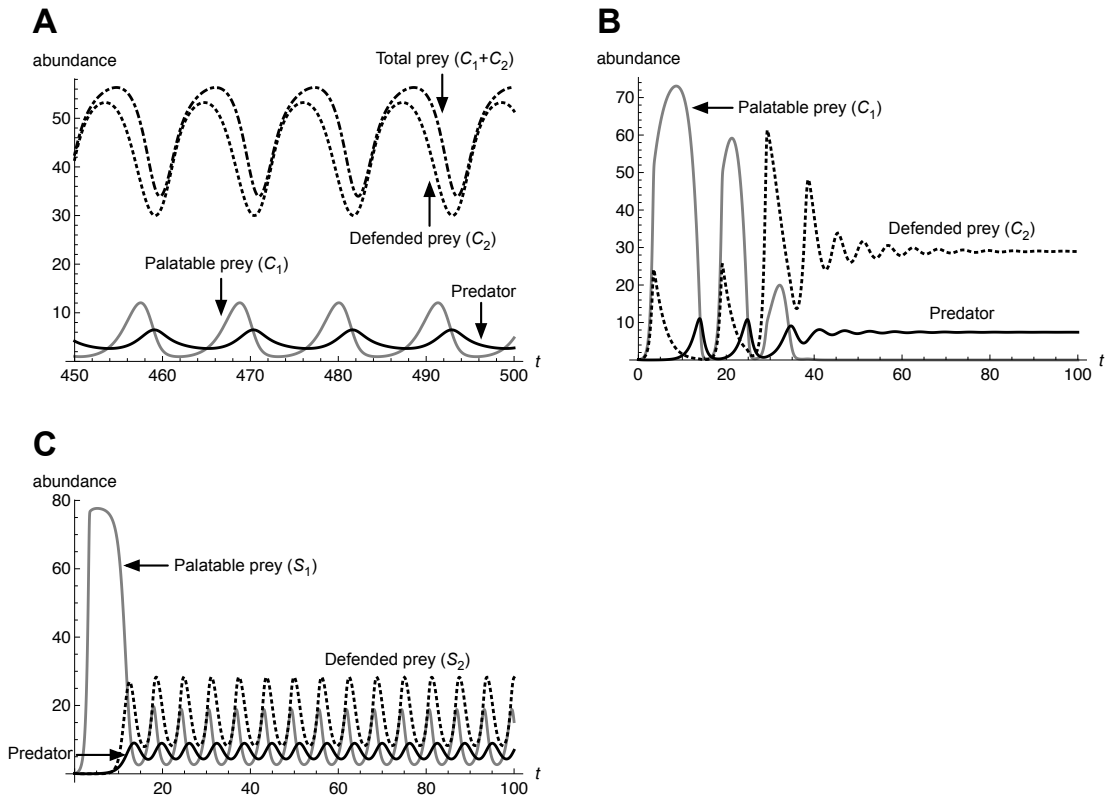

Figure 2.4: *A*, An example of the evolutionary cycle (s_{12} = 0.136, δ = 1.0). *B*, Dynamics of stabilization by nonplastic prey. *C*, Dynamics of destabilization by plastic prey (s_{12} = 0.5, δ = 1.2). *Solid line* = predator, *dotted line* = defended prey, *gray line* = palatable prey, and *dashed-dotted line* = sum of prey abundance.

Communities consisting of only plastic genotypes are always evolutionarily unstable (fig. 2*D*). When both nonplastic genotypes invade and coexist with a plastic genotype, limit cycle amplitudes are smaller than those of the genetic diversity model (fig. 2*C*, 2*E*). These results indicate that a plastic genotype fails to eliminate nonplastic genotypes, but a plastic genotype can take part in an evolutionarily stable community, and its presence can reduce demographic instability.

In the purple region of figure 5*A*, the plastic genotype coexists with only the palatable genotype; the defended genotype cannot persist. In the limit cycle, the plastic genotype increases immediately after reduction of predator density (fig. 6*A*). This burst of plastic genotype is due to its quick response advantage over nonplastic types in a predator-free environment. The plastic genotype is then gradually replaced by the palatable genotype, because unlike the plastic genotype, the palatable genotype does not

need to create defended types and incur maintenance costs (in terms of the increased mortality by the amount γ). Once the palatable phenotype increases to a certain level, predator numbers increase, and defended types produced by the plastic genotype again replace the palatable specialists. Clearly it is changing predator density, or an internal limit cycle, that enabled a more costly plastic genotype to survive.

What is interesting is that when three prey genotypes coexist at intermediate dilution rate values (yellow region, fig. 5*A*), there are discontinuities in limit cycle amplitude (fig. 2*E*). For larger amplitudes (arrows, fig. 2*E*), prey and predator densities follow short period cycles, and the relative abundance of nonplastic and the plastic genotypes show cycles with a longer period (fig. 6*B*–6*D*). These cycles are difficult to interpret when looking only at total prey density (fig. 6*B*). When we look at prey and predator densities, the system suddenly starts exhibiting cycles at a certain time point, but after a period of big waves it calms down. If we distinguish plastic from nonplastic genotypes, we can see that there is a clear relationship between plastic genotype abundance and stability (fig. 6*C*, 6*D*). Before the initial burst, fixed-genotype organisms (both palatable and defended) coexist with predators in a state of quasi-equilibrium but then begin to oscillate. Plastic genotypes increase when the amplitude of the limit cycle becomes large because they are able to take advantage of the changing environment. Once the number of plastic genotypes increases, the system is stabilized. In a stable environment, the plastic genotype is no better than the specialists because of its higher cost: thus, both of the specialist genotypes increase again, which lead to population cycling. These sorts of intermittent cycles are very similar to "bursting cycles" described in the physiological literature (discrete neuron firing patterns; Coombes and Bressloff 2005), and we refer to it as "eco-evolutionary bursting."

2.4.4 *Competition in a Fluctuating Environment*

Up to this point, nutrient supply rate has been constant. We introduce fluctuations in nutrient supply rate to examine the effect of exogenous oscillation on competition between plastic and specialist genotypes. Previous studies have suggested that a plastic genotype is advantageous when environmental variables fluctuate (Scheiner 1993, Stomp et al. 2008, Svanbäck et al. 2009), so we assume a situation in which limiting nutrient concentration N_I oscillates as a sinusoidal function:

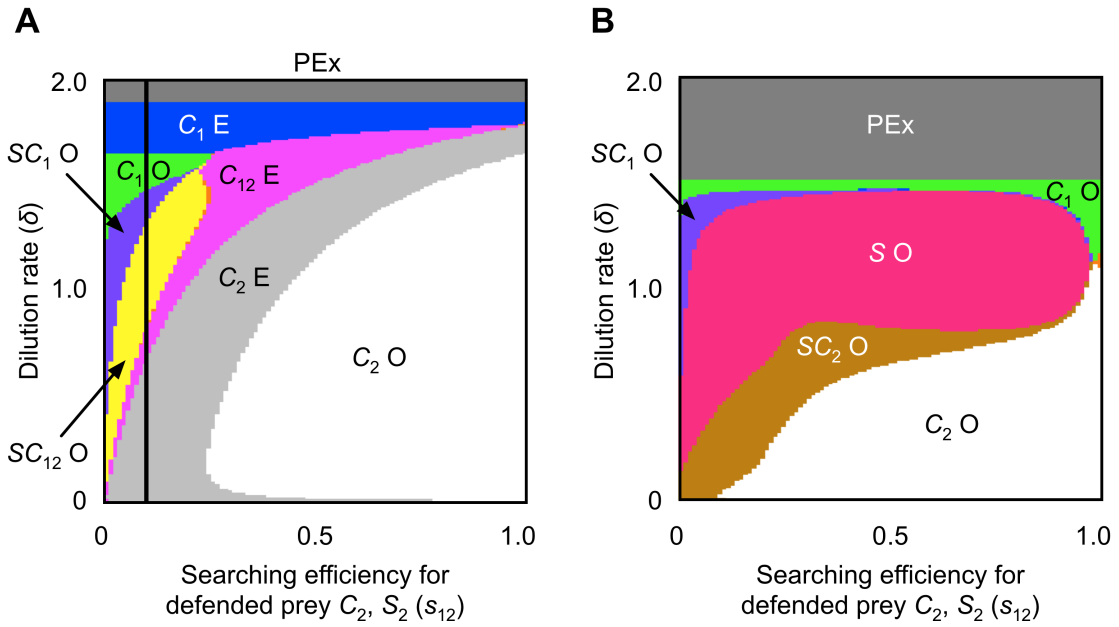

Figure 2.5: *A*, Phase diagram of model IV in a stable environment; plastic prey can persist only in yellow and purple regions with specialist prey. Region SC_1 O (*S* and C_1 oscillation; *purple*): palatable and plastic prey coexist in oscillation. Region SC_{12} O (*S*, C_1, and C_2 oscillation; *yellow*): palatable, defended, and plastic prey coexist in oscillation. The other legend is the same as for figure 3*B*. The black line represents the parameter region of the bifurcation diagram in figure 2*E*. *B*, Phase diagram of model IV with fluctuation of limiting nutrient inflow, N_I, as equation (8) ($\sigma = 0.99$ and $T = 100$). Region *S* O (*S* oscillation; *red*): plastic genotype outcompetes with specialist prey in oscillation. Region SC_2 O (*S* and C_2 oscillation; ocher): defended and plastic genotypes coexist in oscillation. The other legend is the same as in *A*.

$$N_I(t) = N_I\left[1 + \sigma \sin\left(\frac{2\pi t}{T}\right)\right]. \qquad (2.8)$$

When nutrient supply is fluctuating externally (eq. [8]), the plastic genotype outcompetes the fixed genotypes when amplitude is large ($\sigma = 0.99$) and period length intermediate ($T = 100$; fig. 5*B*). This phenomenon occurs when dilution rate is intermediate. When dilution rate is high, a palatable genotype enjoys the most advantage, and when dilution rate is low, a defended genotype is most advantageous (fig. 5*B*). Thus, producing both phenotypes (exhibiting plasticity) is advantageous in parameter spaces between the two regions. Although the general tendency holds true,

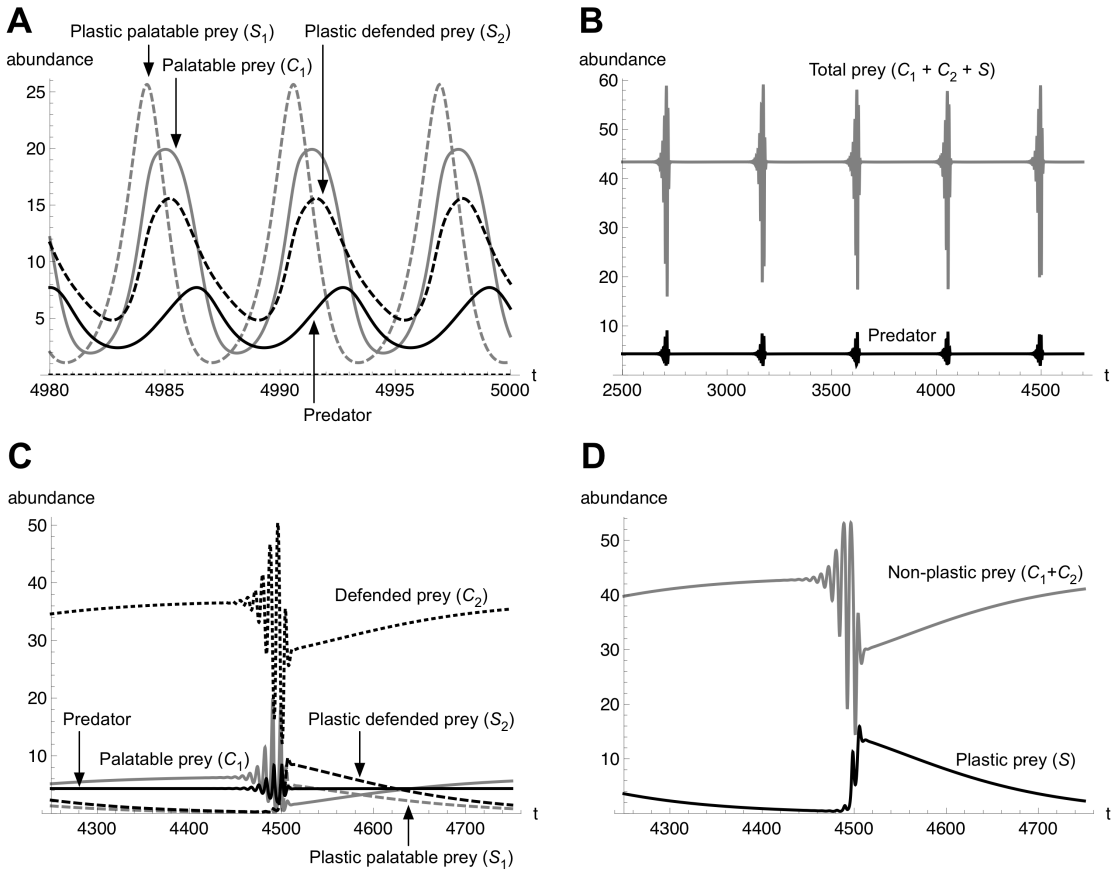

Figure 2.6: Dynamics of model IV in a stable environment. *A*, Limit cycles when the plastic genotype coexists with the palatable genotype (s_{12} = 0.05, δ = 1.2). *Black solid line* = predator, *gray solid line* = palatable genotype, *gray dashed line* = palatable phenotype of plastic genotype, and *black dashed line* = defended phenotype of plastic genotype. *B*, Intermittent cycles when the plastic genotype coexists with both palatable and defended genotypes (s_{12} = 0.1, δ = 1.0). *Gray line* = sum of prey, and *black line* = predator. *C*, Close look at the intermittent cycle. *Black dotted line* = defended genotype. The other lines are the same as in *A*. *D*, Dissection of *C*. *Gray line* = sum of nonplastic genotypes, and *black line* = plastic genotype.

when nutrient fluctuation amplitude j is small, advantages of plasticity decrease (i.e., the area where the plastic genotype excludes the specialist genotypes becomes smaller; fig. S10). Also, when nutrient fluctuation period length T is too short (e.g., $T \approx 1$), the area where the plastic genotype excludes nonplastic genotypes decreases. This is because the plastic genotypes cannot keep up with such a rapidly changing environment (Stomp et al. 2008). When period length is too long (e.g., $T \approx 10{,}000$), environmental change have

a minimal effect on population dynamics and plasticity is not advantageous (fig. S11).

2.5 Discussion

It is increasingly accepted that phenotypic change in traits affecting ecological dynamics is pervasive in wild populations, so researchers should necessarily include adaptive trait dynamics in models used to develop population management plans (Stockwell et al. 2003, Kinnison and Hairston 2007). However, it is often difficult to distinguish rapid contemporary evolution and phenotypic plasticity in the face of phenotypic polymorphism and rapid phenotypic change in wild populations (e.g., Mittelbach et al. 1999, Charmantier et al. 2008).

Some previous studies represent plasticity and evolution in the same equation (e.g., Taylor and Day 1997, Fox and Vasseur 2008), assuming that an individual has a small probability of changing its phenotype to increase its fitness and that this probability is proportional to the "fitness gradient." The trait change speed is governed by rate parameter v, an additive genetic variance in quantitative genetics modeling (Abrams et al. 1993). Phenotypic plasticity is assumed to have a higher value of rate parameter v, so the trait changes faster than evolution. This may be applicable to the behavioral adjustment of plastic traits by learning (trial-and-error plasticity). However, phenotypic change by reaction norm may have different speed, and there is a possibility that dynamics are not the same as expected under the trait change along fitness gradient. Although many kinds of plasticity, especially morphological plasticity, are controlled by reaction norm, their mechanism-explicit modeling is still challenging (but see Abrams and Matsuda 2004). Here we try to compare the effects of evolution and plasticity with explicit mechanisms modeling of reaction norm.

In this study, we focus on timescale differences and recovery speed of minor traits for phenotypic changes caused by rapid evolution and phenotypic plasticity, and we assess the effects on population and community dynamics. Our analyses indicate that even when identical phenotype pairs are involved, rapid evolution and phenotypic plasticity exert different influences on population dynamics. Thus, we as researchers need to clearly distinguish between evolution and plasticity when predicting population dynamics.

2.5.1 *Stabilizing Effects of Two Mechanisms Involved in Phenotypic Change*

In model IIIA, although plasticity is intergenerational phenomenon as evolution, plasticity stabilizes population dynamics more than evolution. Thus, we can confirm that recovery speed of minor traits alone can enhance ecological stability here. On the other hand, ecological stability of intragenerational plasticity in model IIIB is due to both the operating timescale and recovery speed of minor traits.

The difference in population dynamics observed between models II and III indicates that the speed of adaptation is a crucial factor in stabilizing population dynamics. Previous theoretical studies have shown that a faster evolutionary rate of foraging or defensive traits has the effect of stabilizing population dynamics (Kondoh 2003, Yamauchi and Yamamura 2005, Mougi and Nishimura 2008). Our results support these earlier studies: phenotypic plasticity gives rise to faster changes than does "rapid" evolution, hence there is greater population stability with plasticity than with rapid evolution. We further corroborate this by assessing changes to defense induction parameter f in another plastic function of model IIIB. When f is small, defense induction speed is so slow that the system does not stabilize (fig. S8*A*), but when f is large the system stabilizes (fig. S8*C*; table 2).

Plasticity destabilizes population dynamics (leading to limit cycles), whereas monomorphic (defended) prey stabilizes dynamics (fig. 4*B*, 4*C*) in some regions. This occurs when the defense against predator is intermediate (e.g., $s_{12} = 0.5$ and $\delta = 1.2$; middle regions of the phase diagrams). Because no time lag is assumed in our plasticity model (eqq. [4]), this result is not due to the time lag of defense induction (Underwood 1999), so we speculate that plastic response overshoot could account for this instability (Kopp and Gabriel 2006). In the genetic diversity model, palatable genotypes cannot increase soon after depletion simply because abundance is too low (fig. 4*B*). However, in the plasticity model, palatable types are quickly recovered by plastically produced defended types; this rapid negative feedback would cause the population to cycle if threshold predator density in reaction norm are close to the equilibrium value (fig. 4*C*). Overshooting in model III do not occur when the threshold parameter (g) is small (fig. S6), when the sensitivity parameter (b) is large (fig. S7), or when the defense induction speed parameter (f) of model IIIB is small (fig. S8). These observations support our earlier speculation.

Placing these arguments together in perspective, we conclude that trait

differences between palatable and defended phenotypes do matter. When there is little difference between types, population dynamics are much the same. When the defended genotype is fairly different from the palatable genotype, the mechanisms affect population dynamics in different ways. Consider colony formation in green algae, whose cell numbers of the colony determine the defense ability. The palatable types are unicellular or bicellular. When the defended types consist of groups of 8–16 cells, the defense is effective and this situation corresponds to the left regions of the phase diagrams (fig. 3*B*, 3*C*). In this region, the regulatory effect of the defended type on predators is so strong that plasticity stabilizes the oscillation, but evolution fails to stabilize the system because of the temporal low abundance of either genotype and the resulting time delay. When defended types consist of four cell groups (the middle regions of the phase diagrams), plasticity tends to destabilize the system by overshooting, whereas evolution does not destabilize the system (fig. 4*B*, 4*C*). This prediction is experimentally testable because there are various reaction norms in strains of *Scenedesmus* (Verschoor et al. 2004a).

2.5.2 *Competition of Plastic and Nonplastic Genotypes in Stable and Fluctuating Environments*

Without evolutionary fine-tuning of the plasticity function, even when the overall fitness of a certain phenotype is greater than that of others, such that nonplastic populations achieve the compositional state of only best-fit phenotypes, a plastic genotype must produce maladaptive phenotypes according to its reaction norm. When two nonplastic genotypes stably coexist (i.e., the fitness of the two genotypes is nearly equal), the plastic genotype can coexist as well (because having two phenotypes does not reduce its fitness; fig. S9*A*). However, when it incurs a plasticity maintenance cost (γ), the plastic genotype cannot coexist with nonplastic genotypes in a stable equilibrium. For a plastic genotype to survive, the population must exhibit a limit cycle within which predator density is changing (fig. 5*A*).

Although the evolution of reaction norm is not the main scope of this study, it is possible to underestimate the competitive ability of the plastic genotype as our model did not allow evolution of the reaction norm parameters (DeAngelis et al. 2007). To further corroborate the competitive ability of the plastic genotypes, we determined the fittest reaction norm (i.e., with the evolutionarily stable threshold parameter g for a

given sensitivity parameter b) under different conditions (δ and s_{12}) by numerical simulations (figs. S12, S13). We varied g from 0.1 to 50 in increments of 0.1. After the competition simulation between various genotypes with local mutation, the most abundant genotype was chosen for the competition against nonplastic genotypes (for detail, see the legend of fig. S13). We confirmed that there is no evolutionary branching and that chosen g does not fluctuate through time from the evolutionary simulations and pairwise invasibility plot analysis. Then we examined the effects of fine-tuning of the reaction norm parameters on the competition against nonplastic genotypes (fig. S14). Even without the maintenance cost of plasticity (γ), the plastic genotype can outcompete the nonplastic genotypes only in a small region (ca. 12%) of the parameter space, though it can coexist with the specialist genotype(s) in all other regions (data not shown). Furthermore, with a small cost of plasticity ($\gamma = 0.01$), the parameter regions where the plastic genotype can competitively exclude the nonplastic genotypes were about 2% (fig. S14). Thus, the specialist genotypes are almost always better competitors in the parameter space (the plastic genotype was competitively excluded in about 89% of the parameter space; fig. S14).

Note that we do not try to determine the evolutionarily stable strategy (ESS) here. Evolutionary stability was originally defined under the assumption that a population does not undergo population dynamics (e.g., Geritz et al. 1998, Vincent and Brown 2005). Recent studies showed that when population dynamics are considered, it is possible for mutants to coexist with residents even if the residents use ESS at each population density (Křivan and Cressman 2009, Cressman and Křivan 2010). In our study, however, the plastic genotype cannot coexist with fixed genotypes in most parameter regions even when population dynamics are considered (and even when there is no cost of plasticity; see fig. S9*A*).

We examine the ecological outcomes of competition between plastic and fixed genotypes in fluctuating environments (similar to Stomp et al. 2008) and demonstrate that plastic genotypes can exclude fixed genotypes. Svanbäck et al. (2009) tested the effect of population fluctuation on the evolution of phenotypic plasticity, using an individual-based stochastic predator-prey model. The model was formerly used to test evolutionary branching due to frequency-dependent selection. They observed that the evolution of plasticity is generally more likely to occur than evolutionary branching when ecological dynamics exhibit pronounced predator-prey cycles, whereas the

opposite is true when conditions are stable. Our results, as well as those of Svanbäck et al. (2009), confirm that genetic variation is favored in stable environments, whereas phenotypic plasticity is favored in unstable and fluctuating environments, including those marked by intrinsic fluctuations and forced oscillations.

An interesting perspective presented by our models involves the interplay between evolution and the ecology of plasticity; from an ecological perspective, plasticity of prey (inducible defense) promotes population stability, whereas from an evolutionary perspective, environmental or demographic fluctuation promotes the evolution of plasticity. Thus, there is a sort of "catch-22" in the evolution of plasticity, and the result of this dilemma is demonstrated by eco-evolutionary bursting of plastic prey (fig. 6*B*–6*D*). For these parameter conditions, nonplastic genotypes at first oscillate with the predator, but when the amplitude of oscillation grows too large, plasticity increases because of its advantage in a changing environment. However, stabilizing the oscillation results in the reduction of the advantages of the plastic genotype. This intermittent cycle (eco-evolutionary bursting) is a unique and an intriguing example of eco-evolutionary dynamics. Unfortunately, few models have been developed to study the interplay between the evolution and ecology of phenotypic plasticity. Most evolutionary ecology studies of plasticity have focused on identifying conditions that favor the evolution of plasticity (e.g., de Jong 1995, Leimar 2005) but not on its effect on population dynamics; recent eco-evolutionary studies, on the other hand, have largely neglected the effects of plasticity. Thus, forthcoming studies can take the next interesting step of looking at the eco-evolutionary dynamics of phenotypic plasticity.

Our result provides an interesting insight into evolution in *Scenedesmus* and *Desmodesmus*. *Desmodesmus* are green algae and congeners of *Scenedesmus*, but they have fewer inducible defenses than *Scenedesmus*: they are either always defended (colony forming) or always palatable (unicellular; Verschoor et al. 2004a, Verschoor et al. 2004b). The difference between plastic *Scenedesmus* and nonplastic *Desmodesmus* is sometimes explained by alternative defensive traits, such as the presence of a spine. Whereas *Desmodesmus* has a spine, *Scenedesmus* does not; thus, unicellular *Desmodesmus* do not need to defend themselves by forming a colony (Verschoor et al. 2004a). But this explanation cannot account for the permanent defensive state of *Desmodesmus*. Our models indicate that nonplastic defense (as *Desmodesmus*) is advantageous in stable environments, whereas inducible defense (as *Scenedesmus*) is

advantageous in fluctuating environments. Thus, it may be interesting to investigate whether *Scenedesmus* is living in a more fluctuating habitat than *Desmodesmus* in future studies.

2.5.3 *Conclusion and Future Perspective*

In conclusion, our models show that mechanisms that cause adaptive phenotypic changes of prey can greatly influence the population dynamics of a predator-prey system. Plastic response can stabilize population dynamics more so than rapid evolution by responding to environmental changes faster than nonplastic genotypes. Our results suggest that an explicit consideration of phenotypic change may be essential in understanding population dynamics in wild populations. Although plasticity promotes ecological stability, it is not advantageous in stable environments. When plastic genotypes compete with fixed genotypes, a faster response is advantageous only in fluctuating environments, thus plastic genotypes can outcompete nonplastic ones under externally oscillating predation pressure. Nonplastic genotypes enjoy advantages over plastic genotypes when an environment is stable. Thus, we conclude that environmental fluctuations are essential for the evolution of plasticity. A particularly interesting situation arises from the feedback between the stabilizing effects of plasticity and the effects of stable or fluctuating environments on competition between nonplastic and plastic genotypes. This eco-evolutionary bursting is an excellent example of the need to reconsider eco-evolutionary feedbacks.

One promising direction for future work is testing our theoretical predictions using laboratory experiments. Because our models are constructed based on rotifer-algae chemostat system, it will be straightforward to examine our predictions experimentally. Theoretically, our study deals only with biclonal models of rapid evolution to mimic rotifer-algae chemostat systems. However, multiclonal models (Jones et al. 2009), adaptive dynamics models that allow for the study of a continuum of traits (Geritz et al. 1998, Cortez and Ellner 2010), and one-locus and quantitative genetic models (Abrams 2001, Fussmann et al. 2007) are also possible candidates for describing eco-evolutionary dynamics. Thus, it is important to choose an appropriate model to describe a focal system (Abrams 2005), and researchers must examine whether these evolutionary mechanisms affect population dynamics in different ways.

2.6 Appendix

2.6.1 Local Stability Analysis of Model I

Because predator mortality m is negligibly small relative to the dilution rate δ, we eliminate it in the following local stability analysis for the sake of simplicity (Jones and Ellner 2007). Rescaling the variables as $x = N/N_I$, $y = C/(\varepsilon_1 N_I)$, $z = B/(\varepsilon_1 \varepsilon_2 N_I)$ and $T = \delta t$,

$$\frac{dx}{dT} = 1 - x - \frac{A_1 yx}{a_1 + x}, \tag{A1a}$$

$$\frac{dy}{dT} = y\left(\frac{A_1 x}{a_1 + x} - \frac{A_2 z}{a_2 + y} - 1 \right), \tag{A1b}$$

$$\frac{dz}{dT} = z\left(\frac{A_2 y}{a_2 + y} - 1 \right), \tag{A1c}$$

where $A_1 = 1/(h_1\delta)$, $A_2 = 1/(h_2\delta)$, $a_1 = 1/(h_1 s_1 N_I)$ and $a_2 = 1/(\varepsilon_1 h_2 s_2 N_I)$. The sum of scaled concentrations $x + y + z$ converges to 1 because $d(x + y + z)/dT = 1 - (x + y + z)$. After initial transient the dynamics are described as

$$\frac{dy}{dT} = y\left[\frac{A_1\left(1 - y - z\right)}{a_1 + 1 - y - z} - \frac{A_2 z}{a_2 + y} - 1 \right], \tag{A2a}$$

$$\frac{dz}{dT} = z\left(\frac{A_2 y}{a_2 + y} - 1 \right). \tag{A2b}$$

There are three equilibria: (1) wipe-out equilibrium E_0: $y = z = 0$; (2) predator wipe-out equilibrium E_1: $y^* = 1 - a_1/(A_1 - 1)$ and $z^* = 0$; (3) coexistence equilibrium E_2: $\hat{y} = a_2/(A_2 - 1)$ and $\hat{z} = \hat{w} - \hat{y}$, where

$$\hat{w} = \frac{1}{2}\left[A_1\hat{y} + a_1 + 1 - \sqrt{(A_1\hat{y} + a_1 + 1)^2 - 4A_1\hat{y}} \right]. \tag{A3}$$

The expression in the square root is always positive, because $(A_1\hat{y} + a_1 + 1)^2 - 4A_1\hat{y} = (A_1\hat{y} - 1)^2 + a_1(2A_1\hat{y} + a_1 + 2)$; $\hat{w} = \hat{y} + \hat{z}$ satisfies $f(\hat{w}) = \hat{w}^2 - (A_1\hat{y} + a_1 + 1)\hat{w} + A_1\hat{y} = 0$. As $f(w)$ is convex, $f(0) = A_1\hat{y} > 0$, and $f(1) = -a_1 < 0$, there is one root of $f(w) = 0$ defined above in the range $0 < w < 1$. For the existence of coexistence equilibrium,

$$\hat{z} = \hat{w} - \hat{y} = \frac{1}{2}\left[A_1\hat{y} + a_1 + 1 - \sqrt{(A_1\hat{y} + a_1 + 1)^2 - 4A_1\hat{y}} \right] - \hat{y}, \tag{A4}$$

must be positive, or

$$A_2 > 1 + \frac{a_2}{1 - a_1/\left(A_1 - 1\right)}, \tag{A5}$$

or $1 > a_1/(A_1 - 1) + a_2/(A_2 - 1)$.

The Jacobian at the wipe-out equilibrium E_0 is

$$\mathbf{J}_0 = \begin{pmatrix} \frac{A_1}{1+a_1} - 1 & 0 \\ 0 & -1 \end{pmatrix}. \tag{A6}$$

According to Routh-Hurwitz criterion, E_0 is stable if $A_1 < 1 + a_1$ (Kot 2001).

The Jacobian at the predator wipe-out equilibrium E_1 is

$$\mathbf{J}_1 = \begin{pmatrix} -\frac{A_1 a_1 y^*}{\left(a_1 + 1 - y^*\right)^2} & -\frac{A_1 a_1 y^*}{\left(a_1 + 1 - y^*\right)^2} - \frac{A_2 y^*}{a_2 + y^*} \\ 0 & \frac{A_2 y^*}{a_2 + y^*} - 1 \end{pmatrix}. \tag{A7}$$

The equilibrium is stable if

$$A_2 < \frac{a_2 + y^*}{y^*} = 1 + \frac{a_2}{1 - a_1 / \left(A_1 - 1\right)} \tag{A8}$$

Comparing this with equation (A5), we see that whenever the predator wipe-out equilibrium is stable, there is no coexistence stable equilibrium; or, whenever coexistence stable equilibrium exists, the predator wipe-out equilibrium is unstable.

The Jacobian at the coexistence equilibrium is

$$\mathbf{J}_2 = \begin{pmatrix} \hat{y}\left[-\frac{A_1 a_1}{(a_1 + 1 - \hat{y} - \hat{z})^2} + \frac{A_2 \hat{z}}{(a_2 + \hat{y})^2}\right] & \hat{y}\left[-\frac{A_1 a_1}{(a_1 + 1 - \hat{y} - \hat{z})^2} - \frac{A_2}{a_2 + \hat{y}}\right] \\ \frac{A_2 a_2 \hat{z}}{(a_2 + \hat{y})^2} & 0 \end{pmatrix}. \tag{A9}$$

As the determinant of $\mathbf{J}_2$ is always positive, E_2 is stable if the trace of $\mathbf{J}_2$ is negative, or

$$\frac{A_2 \hat{z}}{(a_2 + \hat{y})^2} - \frac{A_1 a_1}{(a_1 + 1 - \hat{y} - \hat{z})^2} < 0. \tag{A10}$$

The Hopf bifurcation occurs when the left term of equation (A10) equals 0, because the Hopf bifurcation requires that there is a pair of imaginary eigenvalues and the real parts of the eigenvalues pass through 0 (Kot 2001). The result is shown in supplementary figure S1*A*. The small difference between the local stability analysis (fig. S1*A*) and the

numerical simulation (fig. 3*A*) in low dilution rate is due to the absence of predator death rate in the local stability analysis.

2.6.2 Local Stability Analysis of Model II

Rescaling variables as in model I, we can get

$$\frac{dx}{dT} = 1 - x - \sum_{i=1}^{2} \frac{A_1 x y_i}{a_{1i} + x}, \tag{B1a}$$

$$\frac{dy_1}{dT} = y_1 \left(\frac{A_1 x}{a_{11} + x} - \frac{A_2 p_1 z}{a_2' + p_1 y_1 + p_2 y_2} - 1 \right), \tag{B1b}$$

$$\frac{dy_2}{dT} = y_2 \left(\frac{A_1 x}{a_{12} + x} - \frac{A_2 p_2 z}{a_2' + p_1 y_1 + p_2 y_2} - 1 \right), \tag{B1c}$$

$$\frac{dz}{dT} = z \left[\frac{A_2 \left(p_1 y_1 + p_2 y_2 \right)}{a_2' + p_1 y_1 + p_2 y_2} - 1 \right], \tag{B1d}$$

where $a_{11} = 1/(h_1 s_{11} N_I)$, $a_{12} = 1/(h_1 s_{12} N_I)$, $a_2' = 1/(\varepsilon_1 h_2 N_I)$, $p_1 = s_{21}$, and $p_2 = s_{22}$. Here y_1 is the palatable prey, and y_2 is the defended prey. Searching efficiency for predator to get the defended genotype (s_{22}) is less than that of the palatable genotype (s_{21}). Because of the trade-off assumption (eq. [2]), the half saturation parameter for the defended genotype to get nutrient (a_{12}) is larger than that of the palatable genotype (a_{11}). The sum of scaled concentrations of nutrient, prey, and predator approaches 1. Substituting $x = 1 - y_1 - y_2 - z$, again, after initial transient dynamics, equations (B1) reduce to

$$\frac{dy_1}{dT} = y_1 \left[\frac{A_1 \left(1 - Y - z \right)}{a_{11} + 1 - Y - z} - \frac{A_2 p_1 z}{a_2' + Q} - 1 \right], \tag{B2a}$$

$$\frac{dy_2}{dT} = y_2 \left[\frac{A_1 \left(1 - Y - z \right)}{a_{12} + 1 - Y - z} - \frac{A_2 p_2 z}{a_2' + Q} - 1 \right], \tag{B2b}$$

$$\frac{dz}{dT} = z \left(\frac{A_2 Q}{a_2' + Q} - 1 \right), \tag{B2c}$$

where $Y = y_1 + y_2$ and $Q = p_1 y_1 + p_2 y_2$. There are five equilibria: (1) wipe-out equilibrium E_0: $y_1 = y_2 = z = 0$, (2) predator wipe-out equilibrium E_1: $y_1^* = 1 - a_{11}/(A_1 - 1)$ and $y_2^* = z^* = 0$, (3) palatable prey-predator coexistence equilibrium E_2: $\hat{y}_1 = a_2'$

/[$p_1(A_2 - 1)$], $\hat{y}_2 = 0$, and $\hat{z} = \hat{w}_1 - \hat{y}_1$, (4) defended prey-predator coexistence equilibrium E_3: $\bar{y}_1 = 0$, $\bar{y}_2 = a_2' /[p_2(A_2 - 1)]$ and $\bar{z} = \bar{w}_2 - \bar{y}_2$, and (5) two prey-predator coexistence equilibrium E_4: $\tilde{y}_1, \tilde{y}_2, \tilde{z} > 0$. Note that due to the larger half-saturation parameter for defended prey ($a_{11} < a_{12}$), only palatable prey exists in the predator wipe-out equilibrium E_1.

For E_0, E_1, E_2, and E_3, single genotype dynamics is analyzed in the previous section (app. A). For the stability of extinction equilibrium E_0, $A_1 < 1 + a_{11}$. The predator-free equilibrium E_1 exists if $A_1 > 1 + a_{11}$ and is stable against the invasion of predator if $A_2 < A_{2ci} = (a_2' + p_1 y_1^*)/(p_1 y_1^*)$, where $y_1^* = 1 - a_{11}/(A_1 - 1)$. The region for the stability of predator-free equilibrium in (A_1, A_2) parameter space lies below the hyperbola: $a_{11}/(A_1 - 1) + a_2' /[p_1(A_2 - 1)] > 1$. If the predation rate A_2 is greater than the threshold, the predator can invade the palatable genotype population. The palatable prey-predator coexistence equilibrium E_2 with $\hat{y}_1 > 0$ and $\hat{z} > 0$ exist when $A_2 > A_{2ci}$ and is stable when A_2 is below the curve defined as

$$\frac{A_2 \hat{z}}{(a_2' / p_1 + \hat{y}_1)^2} < \frac{A_1 a_{11}}{(a_{11} + 1 - \hat{y}_1 - \hat{z})^2}, \tag{B3}$$

where $\hat{y}_1 = a_2' /[p_1(A_2 - 1)]$ and $\hat{w}_1 = \hat{y}_1 + \hat{z}$ is the smaller root of ${w_1}^2 - (A_1 y_1 + a_{11} + 1)w_1 + A_1 y_1 = 0$. Cycles emerge through a Hopf bifurcation when A_2 becomes above the curve (eq. [B3]). In the same way, the defended prey-predator coexistence equilibrium E_3 with $\bar{y}_2 > 0$ and $\bar{z} > 0$ exist when $A_2 > (a_2' + p_2 y_2')/(p_2 y_2')$, where $y_2' = 1 - a_{12}/(A_1 - 1)$ and is stable when A_2 is below the curve defined as

$$\frac{A_2 \bar{z}}{\left(a_2' / p_2 + \bar{y}_2\right)^2} < \frac{A_1 a_{12}}{\left(a_{12} + 1 - \bar{y}_2 - \bar{z}\right)^2} \tag{B4}$$

where $\bar{y}_2 = a_2' /[p_2(A_2 - 1)]$ and $\bar{w}_2 = \bar{y}_2 + \bar{z}$ is the smaller root of ${w_2}^2 - (A_1 y_2 + a_{12} + 1)w_2 + A_1 y_2 = 0$. Cycles emerge through a Hopf bifurcation when A_2 becomes above the curve (eq. [B4]).

For the two prey-predator coexistence equilibrium E_4, we derive the conditions where a prey at a low density can invade the community with the other prey. For palatable prey invasion, we calculate the condition where per capita growth rate of palatable prey in the defended prey-predator equilibrium E_3 equal 0:

$$\frac{1}{y_1}\frac{dy_1}{dT} = \frac{A_1\left(1 - \bar{y}_2 - \bar{z}\right)}{a_{11} + 1 - \bar{y}_2 - \bar{z}} - \frac{A_2 p_1 \bar{z}}{a_2' + p_2 \bar{y}_2} - 1 = 0 \tag{B5}$$

where y_1 nearly equal 0. Then we get the invasion condition of palatable prey substituting $\bar{y}_2 = a_2'/[p_2(A_2-1)]$ 1 and $\bar{z} = \bar{w}_2 - \bar{y}_2$:

$$\frac{A_1\left(1-\bar{w}_2\right)}{a_{11}+1-\bar{w}_2} - p_1\left[\frac{\left(A_2-1\right)\bar{w}_2}{a_2'} - \frac{1}{p_2}\right] - 1 = 0 \qquad \text{(B6)}$$

In the same way, we calculate the condition where per capita growth rate of defended prey in the palatable prey-predator equilibrium E_2 equals 0:

$$\frac{1}{y_2}\frac{dy_2}{dT} = \frac{A_1(1-\hat{y}_1-\hat{z})}{a_{12}+1-\hat{y}_1-\hat{z}} - \frac{A_2 p_2 \hat{z}}{a_2' + p_1\hat{y}_1} - 1 = 0. \qquad \text{(B7)}$$

Again we get the invasion condition of defended prey substituting $\hat{y}_1 = a_2'/[p_1(A_2 - 1)]$ and $\hat{z} = \hat{w}_1 - \hat{y}_1$,

$$\frac{A_1(1-\hat{w}_1)}{a_{12}+1-\hat{w}_1} - p_2\left[\frac{(A_2-1)\hat{w}_1}{a_2'} - \frac{1}{p_1}\right] - 1 = 0. \qquad \text{(B8)}$$

For the Hopf bifurcation, we use Routh-Hurwitz criterion. When the characteristic equation is represented as $\lambda^3 + a\lambda^2 + b\lambda + c = 0$, the system is stable if $a > 0$, $c > 0$, and $ab > c$ (Kot 2001). Hopf bifurcation occurs when $a > 0$, $c > 0$, and $ab = c$. The result is shown in supplementary figure S1B. The boundaries between regions C_1 E and C_1 O, regions C_{12} E and C_{12} O, and regions C_2 E and C_2 O are for Hopf bifurcations towards limit cycles occurred in regions C_1 O, C_{12} O, and C_2 O. The dotted line between regions C_1 O and C_{12} O is the numerically obtained boundary of the transition between two limit-cycle attractors. Because the invasion condition for defended prey (eq. [B8]) assumes the stable palatable prey-predator equilibrium E_2, our analysis cannot distinguish cycling regions C_1 O and C_{12} O.

2.6.3 Evolution of Reaction Norm Function

Here we consider evolution of the threshold parameter, g, in the reaction norm function assuming the demographic equilibrium of predator and prey. Rescaling variables as 2.6.1 and 2.6.2, dynamics of resource (x), resident palatable prey (Y_1), resident defended prey (Y_2), and predator (z) are described as

$$
\begin{aligned}
\frac{dx}{dt} &= 1-x-F_1\left(Y_1+y_1\right)-F_2\left(Y_2+y_2\right),\\
\frac{dY_1}{dt} &= \left(1-Q\right)\left(F_1Y_1+F_2Y_2\right)-p_1HY_1-Y_1,\\
\frac{dY_2}{dt} &= Q\left(F_1Y_1+F_2Y_2\right)-p_2HY_2-Y_2,\\
\frac{dz}{dt} &= H\left[p_1\left(Y_1+y_1\right)+p_2\left(Y_2+y_2\right)\right]-\left(1+m\right)z,
\end{aligned}
\tag{C1}
$$

where

$$
\begin{aligned}
F_1 &= \frac{A_1x}{a_{11}+x}, F_2 = \frac{A_1x}{a_{12}+x},\\
Q &= \frac{\left(z/G\right)^b}{1+\left(z/G\right)^b}, q = \frac{\left(z/g\right)^b}{1+\left(z/g\right)^b},\\
H &= \frac{A_2z}{a_2'+p_1\left(Y_1+y_1\right)+p_2\left(Y_2+y_2\right)}, H_0 = \frac{A_2z}{a_2'+p_1Y_1+p_2Y_2},
\end{aligned}
$$

y_1 and y_2 are palatable and defended prey of mutant, A_1 and A_2 are feeding rates of prey and predator, a_{11}, a_{12}, and a_2' are saturation constants for palatable prey, defended prey and predator, p_1 and p_2 are palatability of palatable and defended prey for predator, G and g are the threshold parameters for resident and mutant, b is the sensitivity parameter, and m is predator death rate. The mutant dynamics is given by

$$
\begin{aligned}
\frac{dy_1}{dt} &= \left(1-q\right)\left(F_1y_1+F_2y_2\right)-p_1Hy_1-y_1,\\
\frac{dy_2}{dt} &= q\left(F_1y_1+F_2y_2\right)-p_2Hy_2-y_2.
\end{aligned}
\tag{C2}
$$

Because the first mutant is very rare, linearized equation around $y_1 = y_2 = 0$ is

$$
\begin{aligned}
\frac{dy_1}{dt} &= \left(1-q\right)\left(F_1y_1+F_2y_2\right)-p_1H_0y_1-y_1,\\
\frac{dy_2}{dt} &= q\left(F_1y_1+F_2y_2\right)-p_2H_0y_2-y_2.
\end{aligned}
\tag{C3}
$$

The Jacobian matrix of equation (C3) with the demographic equilibrium is

$$
\mathbf{J} = \begin{pmatrix} \left(1-\overline{q}\right)\overline{F}_1-p_1\overline{H}_0-1 & \left(1-\overline{q}\right)\overline{F}_2 \\ \overline{q}\overline{F}_1 & \overline{q}\overline{F}_2-p_2\overline{H}_0-1 \end{pmatrix},
\tag{C4}
$$

where

$$\bar{F}_1 = \frac{A_1 \bar{x}}{a_{11} + \bar{x}}, \bar{F}_2 = \frac{A_1 \bar{x}}{a_{12} + \bar{x}},$$
$$\bar{q} = \frac{\left(\bar{z}/g\right)^b}{1 + \left(\bar{z}/g\right)^b}, \bar{H}_0 = \frac{A_2 \bar{z}}{a_2' + p_1 \bar{Y}_1 + p_2 \bar{Y}_2},$$

and $\bar{x}$, $\bar{y}_1$, $\bar{y}_2$, and $\bar{z}$ are variables in the stable equilibrium. Thus the trace and determinant of the Jacobian matrix (C4) are

$$\begin{aligned} \mathrm{tr}(\mathbf{J}) &= (1-\bar{q})\bar{F}_1 + \bar{q}\bar{F}_2 - (p_1 + p_2)\bar{H}_0 - 2, \\ \Delta \equiv \det(\mathbf{J}) &= (1 + p_1 \bar{H}_0)(1 + p_2 \bar{H}_0) - (1 + p_2 \bar{H}_0)(1-\bar{q})\bar{F}_1 - (1 + p_1 \bar{H}_0)\bar{q}\bar{F}_2. \end{aligned} \tag{C5}$$

The first and second orders of differential equations are

$$\begin{aligned} \frac{\partial \Delta}{\partial q} &= (1 + p_2 \bar{H}_0)\bar{F}_1 - (1 + p_1 \bar{H}_0)\bar{F}_2, \\ \frac{\partial^2 \Delta}{\partial q^2} &= 0. \end{aligned} \tag{C6}$$

Therefore, the evolutionarily singular strategy is realized when $\frac{\partial \Delta}{\partial q} = 0$. This condition can be rewritten as $(1 + p_2 \bar{H}_0)\bar{F}_1 = (1 + p_1 \bar{H}_0)\bar{F}_2$. Because the second order is zero, it is not strictly evolutionarily stable, but neutrally stable in the demographic equilibrium of predator and prey (see the legend of fig. S13). Then the pairwise invasibility plot (PIP) should be like fig. S13*D*.

2.6.4 Supplemental Figures

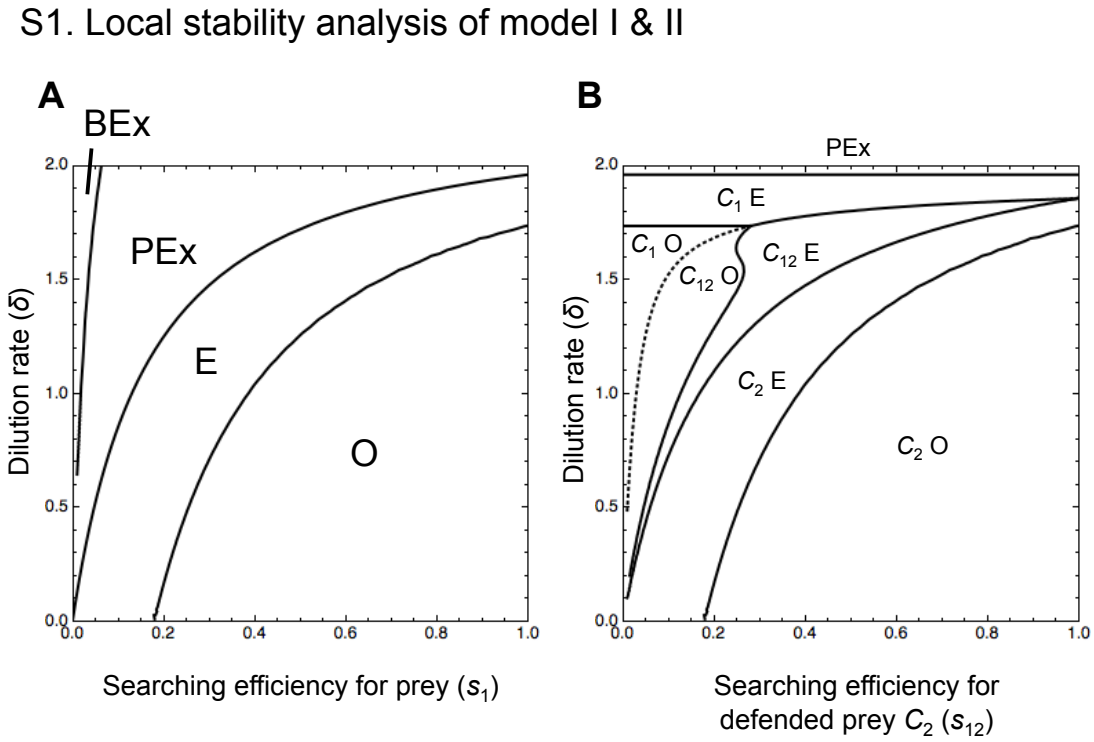

Figure 2.S1: *A*, Local stability analysis of model I. The abbreviated letters are the same as figure 3*A*. For details of analysis, see Appendix 2.6.1. *B*, Local stability analysis of model II. The abbreviated letters are the same as figure 3*B*. For details of analysis, see Appendix 2.6.2. The dotted line between regions C_1 O and C_{12} O is obtained assuming stable equilibria. However, those two regions are both limit-cycle attractors, thus this boundary should be obtained numerically.

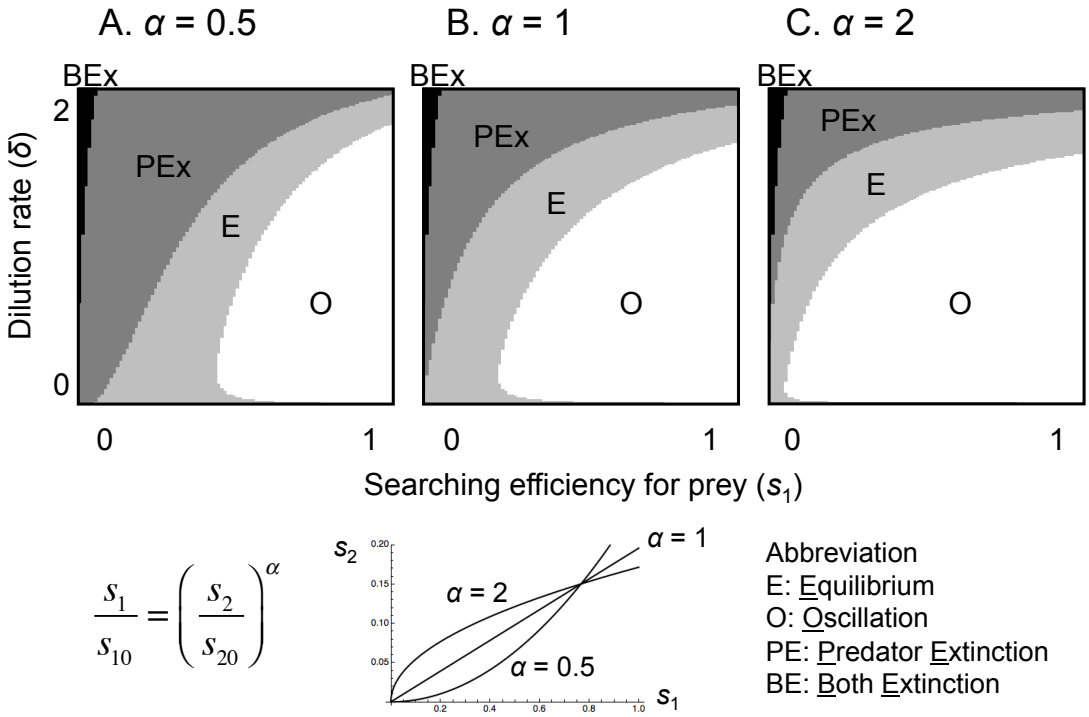

Figure 2.S2: Effects of the trade-off function parameter α in model I. *A*, $\alpha = 0.5$. The trade-off function is convex. *B*, $\alpha = 1$. The trade-off function is linear. *C*, $\alpha = 2$. The trade-off function is concave. The abbreviated letters are the same as figure 3*A*.

S3. Effects of α in model II (simulation started from right side)

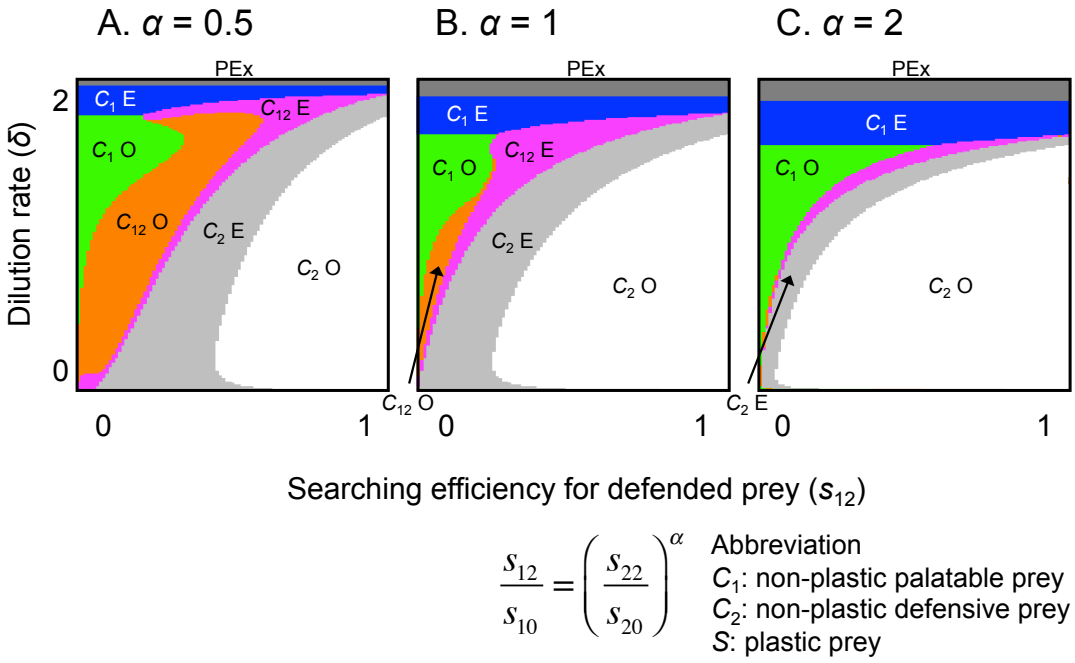

$$\frac{s_{12}}{s_{10}} = \left(\frac{s_{22}}{s_{20}}\right)^{\alpha}$$

Figure 2.S3: Effects of the trade-off function parameter α in model II. Because model II has bistability regions, the simulation results are affected by the initial conditions. Here we extended the equilibrium points from right side (s_{12} = 0.99). *A*, α = 0.5. The trade-off function is convex. *B*, α = 1. The trade-off function is linear. *C*, α = 2. The trade-off function is concave. The abbreviated letters are the same as figure 3*B*.

S4. Effects of α in model II (simulation started from left side)

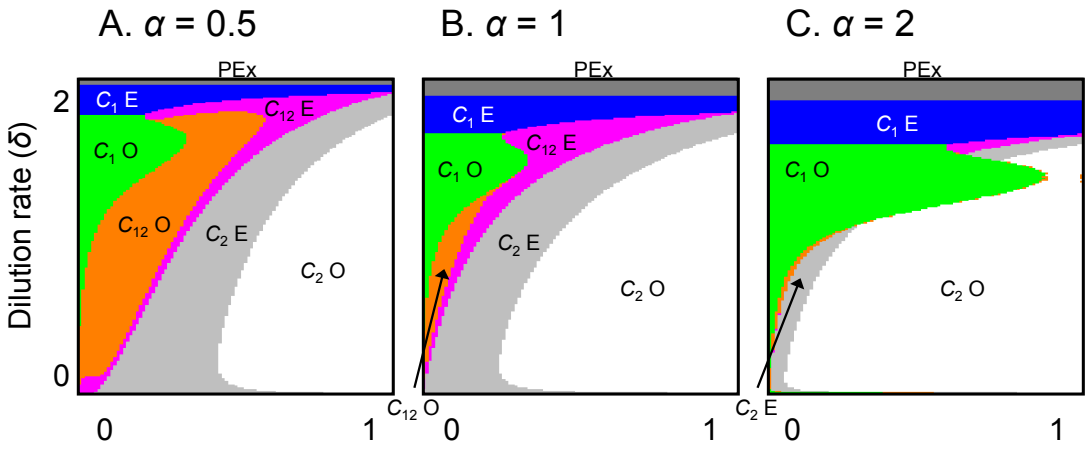

$$\frac{s_{12}}{s_{10}} = \left(\frac{s_{22}}{s_{20}} \right)^{\alpha}$$

Figure 2.S4: Effects of the trade-off function parameter α in model II. Because model II has bistability regions, the simulation results are affected by the initial conditions. Here we extended the equilibrium points from left side (s_{12} = 0.01). *A*, α = 0.5. The trade-off function is convex. *B*, α = 1. The trade-off function is linear. *C*, α = 2. The trade-off function is concave. The abbreviated letters are the same as figure 3*B*.

S5. Effects of α in model IIIA (b = 2, g = 5)

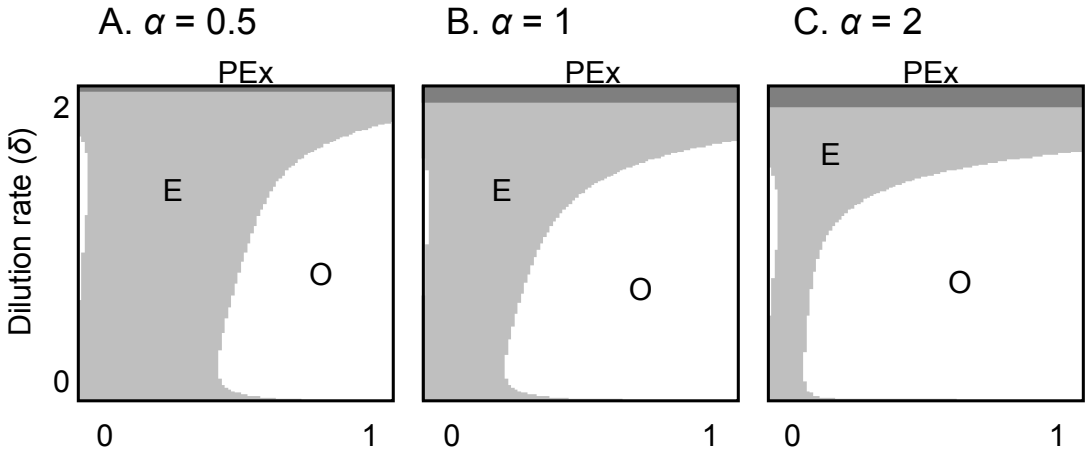

$$\frac{s_{12}}{s_{10}} = \left(\frac{s_{22}}{s_{20}} \right)^{\alpha}$$

Figure 2.S5: Effects of the trade-off function parameter α in model IIIA. Here reaction norm parameters were set as b = 2 and g = 5. *A*, α = 0.5. The trade-off function is convex. *B*, α = 1. The trade-off function is linear. *C*, α = 2. The trade-off function is concave. The legend is the same as figure 3*C*.

S6. Effects of g in model IIIA (α = 1, b = 2)

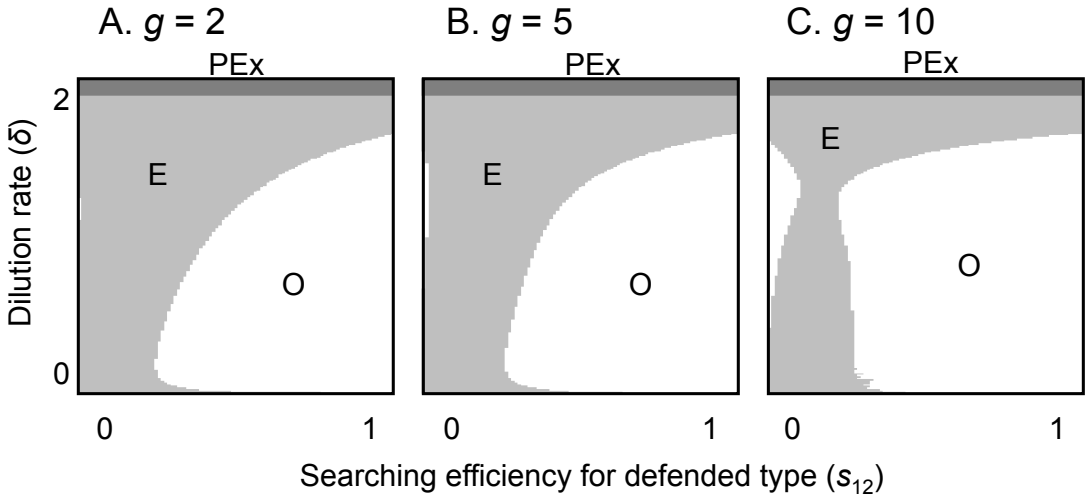

$$Q_1(B)=\frac{1}{1+(B/g)^b},Q_2(B)=\frac{(B/g)^b}{1+(B/g)^b}$$

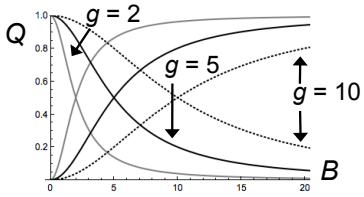

Figure 2.S6: Effects of the threshold parameter of reaction norm g in model IIIA. Here trade-off is linear ($\alpha = 1$) and $b = 2$. *A*, $g = 2$. *B*, $g = 5$. *C*, $g = 10$. The abbreviated letters are the same as figure 3*C*.

S7. Effects of b in model IIIA (α = 1, g = 5)

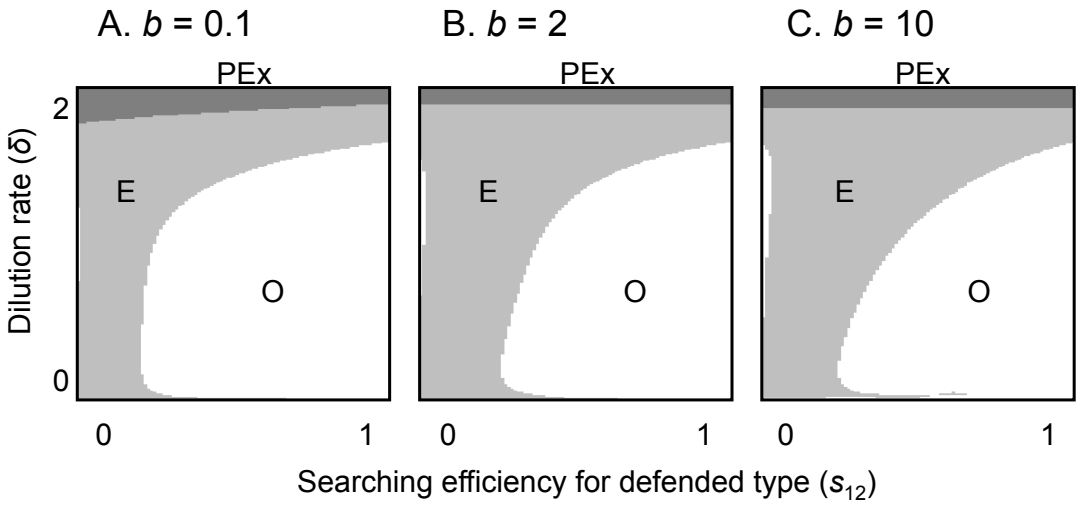

$$Q_1(B) = \frac{1}{1+(B/g)^b}, Q_2(B) = \frac{(B/g)^b}{1+(B/g)^b}$$

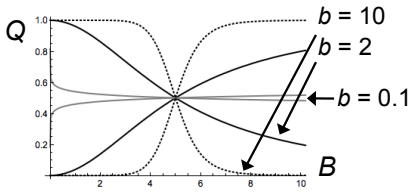

Figure 2.S7: Effects of the sensitivity parameter of reaction norm b in model IIIA. Here trade-off is linear (α = 1) and g = 5. *A*, b = 0.1. *B*, b = 2. *C*, b = 10. The abbreviated letters are the same as figure 3*C*.

S8. Effects of *f* in model IIIB (*b* = 2, *g* = 5)

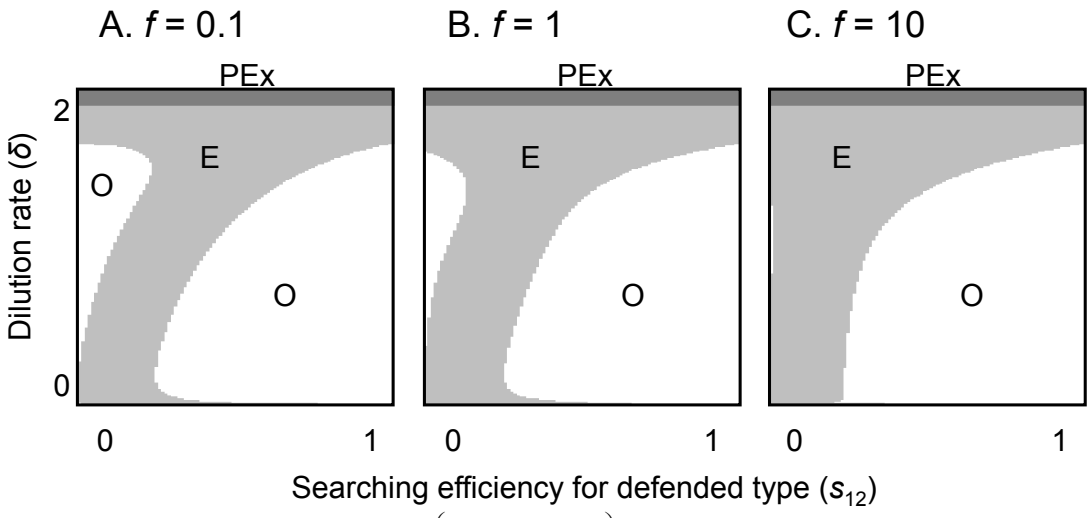

$$\frac{dS_1}{dt} = \frac{s_{11}NS_1}{1+h_1 s_{11}N} - \frac{1}{\varepsilon_2}\left(\frac{s_{21}S_1 B}{1+h_2\sum_{j=1}^{2} s_{2j}S_j}\right) - \delta S_1 - fQ_2(B)S_1 + fQ_1(B)S_2$$

$$\frac{dS_2}{dt} = \frac{s_{12}NS_2}{1+h_1 s_{12}N} - \frac{1}{\varepsilon_2}\left(\frac{s_{22}S_2 B}{1+h_2\sum_{j=1}^{2} s_{2j}S_j}\right) - \delta S_2 + fQ_2(B)S_1 - fQ_1(B)S_2$$

Figure 2.S8: Effects of the response parameter of phenotypic plasticity *f* in model IIIB. Here trade-off is linear (α = 1), *b* = 2, and *g* = 5. *A*, *f* = 0.1. *B*, *f* = 1. *C*, *f* = 10. The abbreviated letters are the same as figure 3*C*.

S9. Effects of γ in model IV

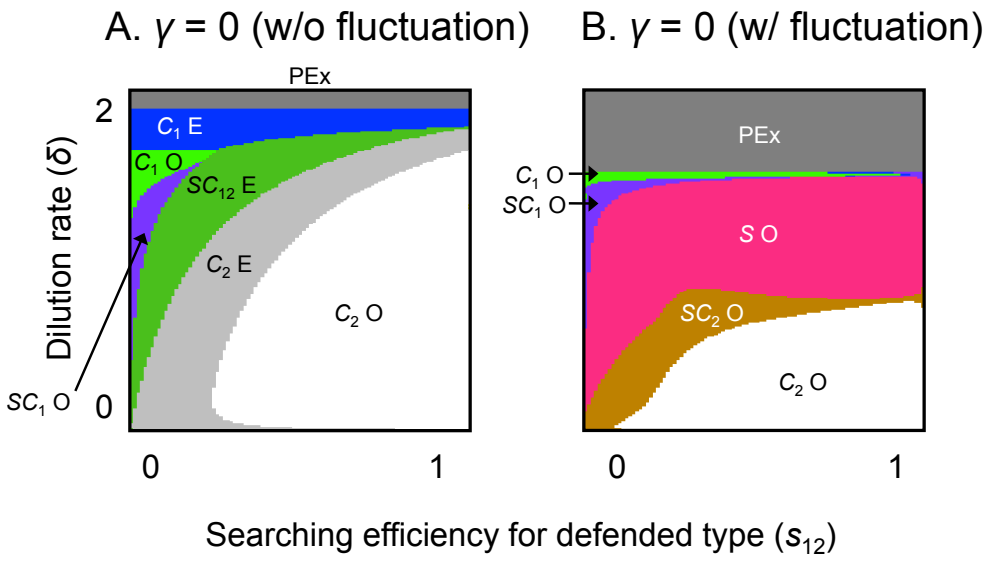

$$\frac{dS_i}{dt} = Q_i(B)\left(\sum_{j=1}^{2}\frac{s_{1j}NS_j}{1+h_1 s_{1j}N}\right) - \frac{1}{\varepsilon_2}\left[\frac{s_{2i}S_iB}{1+h_2\sum_{j=1}^{2}s_{2j}\left(C_j+S_j\right)}\right] - (\gamma+\delta)S_i, (i=1,2)$$

Figure 2.S9: Effects of the maintenance cost of phenotypic plasticity γ in model IV. Here trade-off is linear ($\alpha = 1$), $b = 2$, and $g = 5$. *A*, $\gamma = 0$ and the nutrient inflow N_I is constant. *B*, $\gamma = 0$ and the nutrient inflow N_I is fluctuating ($\sigma = 0.99$ and $T = 100$). Region SC_{12} E (S, C_1, and C_2 Equilibrium; moss green): palatable, defended and plastic prey coexist in a stable equilibrium. The other abbreviated letters are the same as figure 5.

S10. Effects of σ in model IV (T = 100)

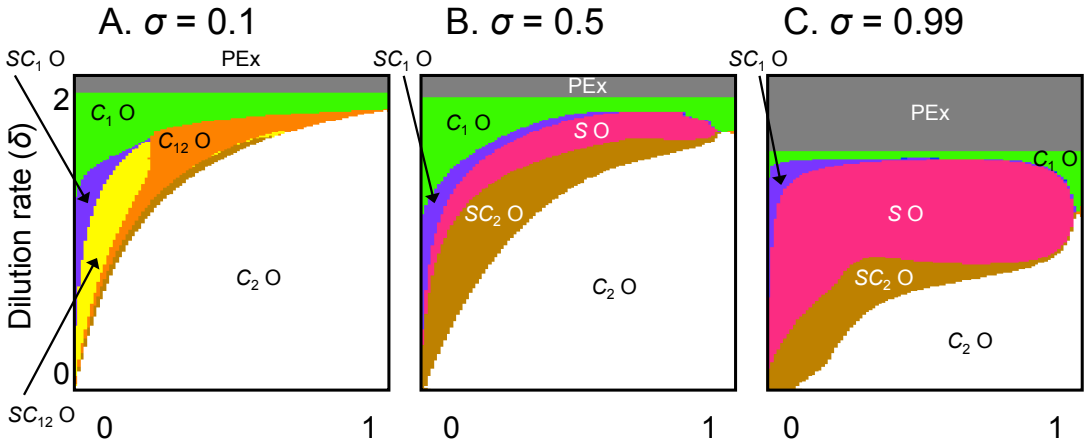

$$N_I(t) = N_I\left[1+\sigma\sin\left(\frac{2\pi t}{T}\right)\right]$$

Figure 2.S10: Effects of the nutrient fluctuation amplitude parameter σ in model IV. Here trade-off is linear ($\alpha = 1$), $b = 2$, $g = 5$, and $T = 100$. *A*, $\sigma = 0.1$. *B*, $\sigma = 0.5$. *C*, $\sigma = 0.99$ (same as fig. 5*B*). The abbreviated letters are the same as figure 5.

S11. Effects of T in model IV (σ = 0.99)

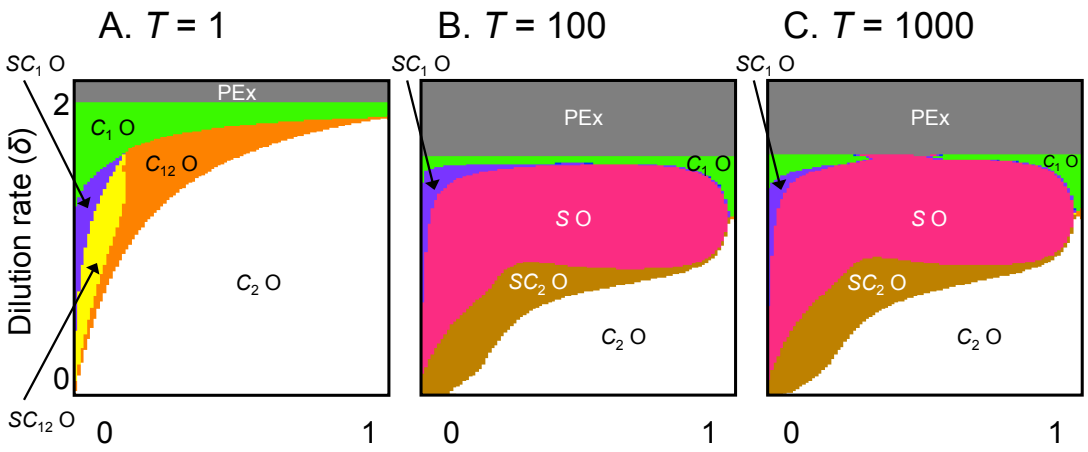

$$N_I(t) = N_I\left[1+\sigma\sin\left(\frac{2\pi t}{T}\right)\right]$$

Figure 2.S11: Effects of the nutrient fluctuation period length parameter T in model IV. Here trade-off is linear ($\alpha = 1$), $b = 2$, $g = 5$, and $\sigma = 0.99$. *A*, $T = 1$. *B*, $T = 100$ (same as fig. 5*B*). *C*, $T = 1{,}000$. The abbreviated letters are the same as figure 5.

S12. The fittest threshold parameter *g* in model IIIA

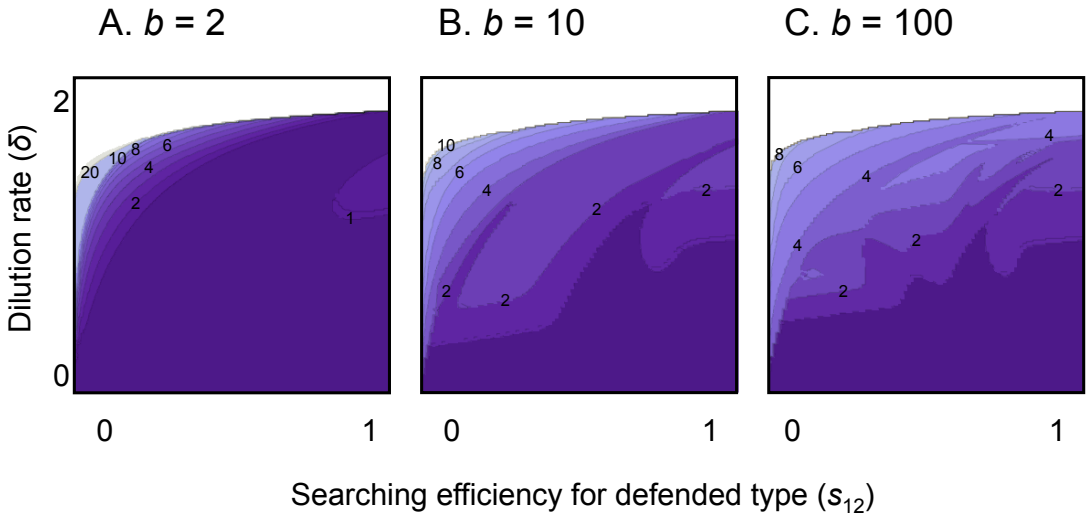

Figure 2.S12: The fittest threshold parameter of reaction norm g in model IIIA. Here trade-off is linear ($\alpha = 1$). *A*, $b = 2$. *B*, $b = 10$. *C*, $b = 100$. The contour plots show the fittest values of g (from 0.1 to 50) for each condition (each combination of s_{12} and δ). For the detail of simulation to find out the fittest g, see the legend of figure S13.

S13. Examples of the fittest threshold parameter g (b = 10)

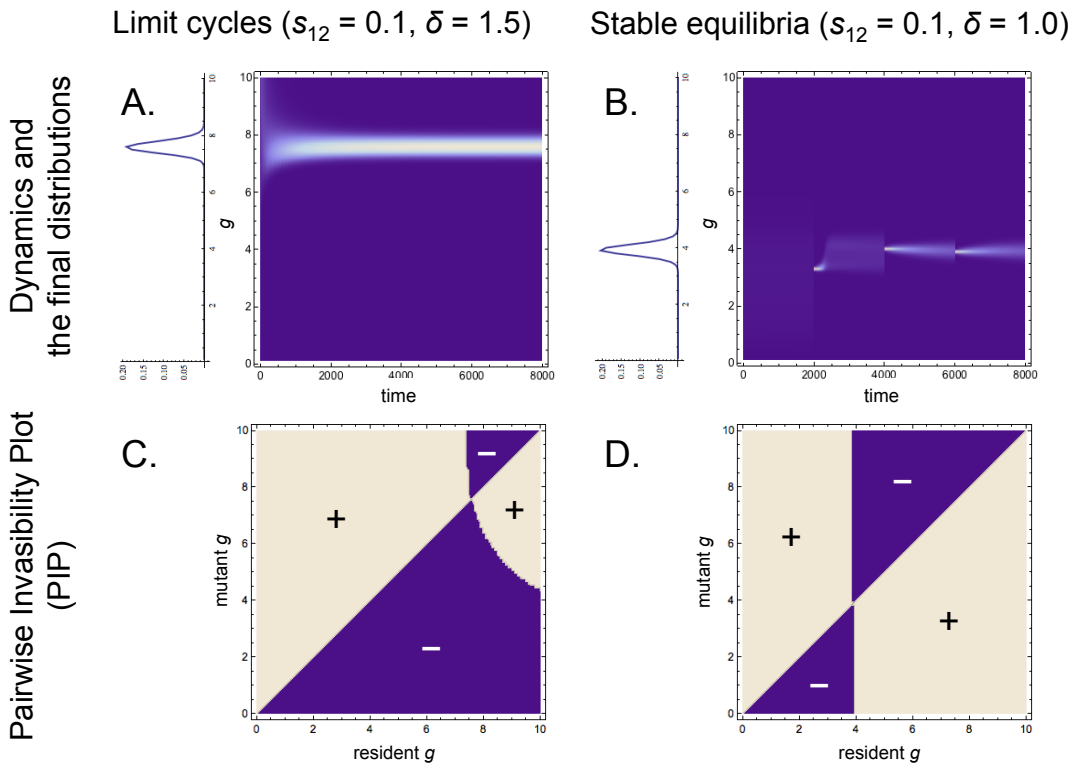

Figure 2.S13: Examples of the fittest threshold parameter g. Here trade-off is linear (α = 1). *A*, An example of the evolutionary simulation (density plot) and the final phenotypic distribution (at t = 8,000) in limit cycles (s_{12} = 0.1, δ = 1.5). *B*, An example of the evolutionary simulation (density plot) and the final phenotypic distribution (at t = 8,000) in stable equilibria (s_{12} = 0.1, δ = 1.0). *C*, An example of pairwise invasibility plots (PIP) in limit cycles (s_{12} = 0.1, δ = 1.5). *D*, An example of PIP in stable equilibria (s_{12} = 0.1, δ = 1.0). The resident g is x-axis and the mutant g is y-axis. Purple regions (−): the mutant cannot invade when it is rare. Off-white regions (+): the mutant can invade when it is rare. Note that the evolutionary stable g values are the same as the most abundant g in the final distributions.

To determine the fittest reaction norm parameters, we at first set 500 genotypes ($S_1 \sim S_{500}$) with g varying from 0.1 to 50 (the difference between the neighboring genotypes is 0.1) with the same abundance. The 500 plastic genotypes competed until t = 8,000 in numerical simulations. Through this process, local mutation can occur to neighboring genotypes (i.e., from i to $i - 1$ and $i + 1$). The mutation rate was set as 10^{-3}. After the competition, the most abundant genotype was chosen for the

competition against non-plastic genotypes.

There are two cases for the final genotype distribution of plastic prey. (i) In the case where the evolution of g value ended up with prey-predator cycles, the genotype distribution had a steep peak at an intermediate g value, $g = g^*$. This g value is chosen as the fittest reaction norm parameter, and used in the competition between plastic and non-plastic prey. PIP drawn in figure S13*C* for such case clearly shows that $g = g^*$ is both convergence and evolutionarily stable. To draw PIP, we detected the sign of the mean initial growth rate of mutant reaction norm genotype in the population when it is rare, where the resident reaction norm genotype already converges to a stable limit cycle, for each combination of mutant and resident reaction norm parameters. (ii) In the case where the evolution ended up with the stable demographic equilibrium of prey and predator, the final genotype distribution for g had a broad humped curve around an intermediate value g^{**}. If PIP is plotted for such case, we have a vertical line at $g = g^{**}$ as the invasibility boundary (fig. S13*D*). This implies that, although $g = g^{**}$ is convergence stable and hence g value evolves towards g^{**} when the resident population is nearly monomorphic, g^{**} itself is not strictly evolutionarily stable (it is neutrally evolutionarily stable), and hence the genotypes other than g^{**} can constitute the evolutionary stable population. Exactly the same situation arises when PIP is drawn for analyzing Fisherian sex ratio. PIP has a vertical line at sex ratio $R = 1/2$, implying that, as long as the population mean sex ratio is kept 1:1, many genotypes with different sex ratios can constitute an evolutionary stable population. Nonetheless, 1:1 sex ratio is called the evolutionary stable sex ratio. In the same vein we call $g = g^{**}$ evolutionarily stable, and used as the fittest genotype in our simulation for the competition of plastic and non-plastic prey.

There are two ways to obtain $g = g^{**}$ in the case (ii). First is to draw PIP as we did in figure S13*D*. To do this for every combination of parameters is time consuming, though. Alternative way we used to draw the evolutionarily stable g in figure S12 and S14 was the following. Though g^{**} in demographic equilibrium is only neutrally evolutionary stable, it is still convergence stable. This implies that, as long as the wild type population is monomorphic, g value should always evolve towards g^{**}. This obvious fact is used to obtain g^{**}. We picked up the most abundant genotype at regular time intervals (t = 2,000, 4,000, and 6,000) where an evolutionary equilibrium is reached. The prey population is set monomorphic each time, and started evolving

towards g^{**} again by selection and mutation. By repeating this procedure, the prey genotype distribution evolves to have a steep peak at $g = g^{**}$ as shown in figure S13*B*. The values obtained by these two ways were compared and, not surprisingly, showed very good agreement.

There is a clear reason why we have a neutral evolutionarily stability for reaction norm parameter when population is in demographic equilibrium. There is an optimum ratio of defended and palatable prey at the equilibrium, and various combination of plastic genotypes can attain the desired defended/palatable ratio for a given predator density.

We here obtained the evolutionary stable threshold parameter g^* in model III (through competition between the plastic genotypes) and then we let the plastic genotype with g^* compete with non-plastic genotypes in model IV. We should note, however, that the evolutionarily stable g^* values may be slightly different if we let the plastic genotypes to evolve in model IV (through competition between the plastic *and* non-plastic genotypes). This possible complication is beyond the scope of the present study and we leave it for future studies.

S14. Effects of the fittest threshold parameter *g* in model IV

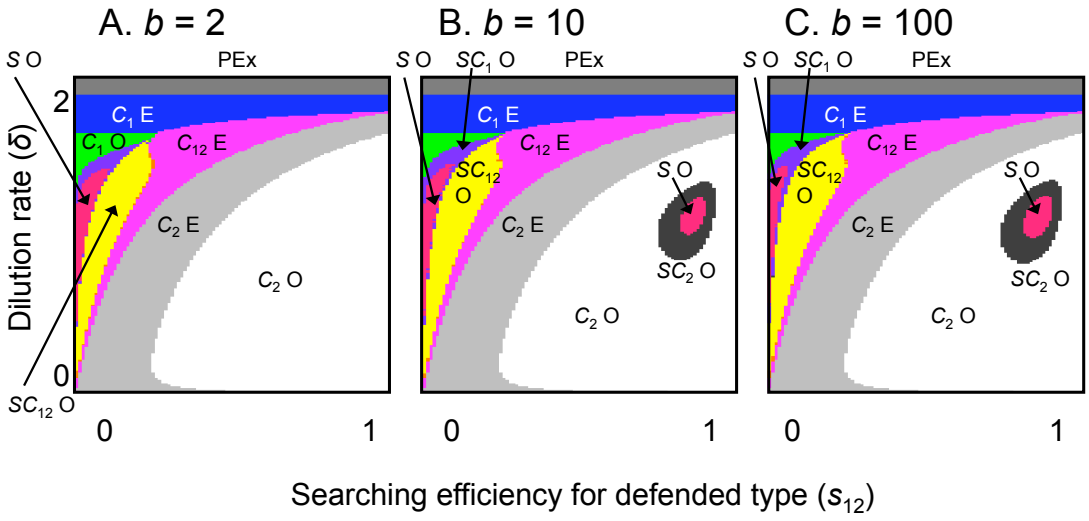

Figure 2.S14: Effects of the threshold parameter of reaction norm *g* in model IV. Here trade-off is linear ($\alpha = 1$). *A*, $b = 2$. *B*, $b = 10$. *C*, $b = 100$. The dynamics of competition between the plastic prey with the fittest threshold *g* (fig. S12) and non-plastic genotypes are shown. The abbreviated letters are the same as figure 5.

2.7 Acknowledgments

We are grateful to M. Kondoh, A. Mougi, and anonymous reviewers for their valuable comments and suggestions. M.Y. is supported by a Research Fellowship of the Japan Society for the Promotion of Science (JSPS) for Young Scientists (21-7611). A.S. is supported by the Precursory Research for Embryonic Science and Technology (PRESTO) Program of the Japan Science and Technology Agency (JST), a Grant-in-Aid for Scientific Research from JSPS, and the Graduate University for Advanced Studies (Sokendai). T.Y. is supported by PRESTO JST and Ministry of Education, Culture, Sports, Science, and Technology/ JSPS Grants-in-Aid for Scientific Research (19687002, 20370009).

Chapter 3. Ecological speciation via functional pleiotropy

Masato Yamamichi, Akira Sasaki

3.1 Abstract

A conventional theory proposes that single-gene speciation would be difficult, because selection acts against a mutation that causes reproductive isolation. An excellent example of single-gene speciation is, however, found in snails, in which a gene for left-right reversal of polarity could have given rise to new species multiple times, and this might be facilitated by a small population size and a maternal effect ('delayed inheritance' (DI), in which an individual's phenotype is determined by its mother's genotype). Recently, evidence suggests that a pleiotropic effect of the speciation gene on anti-predator survival due to right-handed predators (functional pleiotropy) may also promote speciation. Here we examine the effects of the three factors and allele dominance to understand single-gene speciation process. It appears that the recessive mutant allele with DI has higher fixation probability when reproductive isolation is strong and functional pleiotropy is weak, but in large populations, both alleles have the same fixation probability. On the other hand, the dominant mutant allele without DI has higher one when reproductive isolation is weak and pleiotropy is strong. Our results underline the conflicting effects of viability selection and positive frequency-dependent selection due to reproductive isolation on the mutant phenotype, providing insight into single-gene speciation.

3.2 Introduction

Darwin tried to explain the origin of species by natural selection (Darwin 1859), but he did not know the detail of genetic basis. Since then, understanding speciation from the genic level to the ecological level is an ongoing challenge in evolutionary biology (Coyne and Orr 2004). One of the longstanding debates in speciation studies concerns how many genes causing reproductive isolation (speciation genes) are required for speciation to occur. A classic theory, the Bateson-Dobzhansky-Muller (BDM) model, predicts that two or more genes must be involved in speciation, because a new allele with strong effects on viability of heterozygotes or mating compatibility without epistasis to other genes should decrease the fitness of variants, and therefore has difficulty in fixing in the populations. On the other hand, negative epistatic interactions

between independently derived alleles (A and B) at two loci can establish reproductive isolation between descendant genotypes (AAbb and aaBB) without reproductive isolation between ancestral genotype (aabb) and daughter lineages (Bateson 1909, Dobzhansky 1936, Muller 1942).

Although the classical BDM incompatibility model has been influential in explaining the speciation process (Orr 1996, Gavrilets 2004), the BDM model cannot explain the evolution of reproductive isolation by a single gene without incompatible gene interaction. The speciation as a result of genetic substitution at a single locus is sometimes called as 'single-gene speciation' (Orr 1991). There are some empirical supports such as single-locus determination of mating behavior in animals (Tauber et al. 2003, Ueshima and Asami 2003) or flowering traits in plants (Bradshaw and Schemske 2003, see Gavrilets 2004, Servedio et al. 2011 for review). In addition, because "one-locus models are a natural starting point for theoretical approaches to many evolutionary phenomena" (Gavrilets 2004), several studies have theoretically investigated speciation models by a single locus (Moore 1979, 1981, Slatkin 1982, Orr 1991, Gregorius 1992, van Batenburg and Gittenberger 1996, Stone and Björklund 2002, Davison et al. 2005). On the other hand, a single gene that pleiotropically contributes to both reproductive isolation and divergent adaptation is of special interest as it can potentially promote ecological speciation (evolution of reproductive isolation as a result of ecologically divergent selection) with gene flow (Rundle and Nosil 2005). This is because recombination cannot break down the association of the two functions (Felsenstein 1981). We call this type of pleiotropy 'functional pleiotropy' as the speciation gene needs not to affect two or more traits: when the speciation gene determines a single trait that influences both reproductive isolation and ecologically divergent adaptation, it is also functional pleiotropy (Jordan and Otto 2012). In spite of these intensive interests, the process of single-gene speciation is not consistently understood, partly because previous studies relied heavily on numerical simulations (Kirkpatrick and Ravigné 2002, Gavrilets 2004). Here we use new analytical results to investigate the effects of functional pleiotropy, allele dominance, population size, and maternal effect on the fixation process of the speciation gene in single-gene speciation.

An excellent example of single-gene speciation is found in snails (see Schilthuizen and Davison 2005, Okumura et al. 2008 for review): handedness of snails is shown to be controlled by two alleles at a single locus (Boycott et al. 1930, Degner

1952, Murray and Clarke 1966, Freeman and Lundelius 1982) and mating between opposite coiling individuals rarely occurs (Johnson 1982, Gittenberger 1988, Asami et al. 1998). Thus the handedness gene is responsible for premating isolation. Despite the positive frequency-dependent selection against rare mutants predicted by the BDM model (Johnson 1982, Asami et al. 1998), it was revealed that evolutionary transitions from original and abundant dextral (clockwise coiling) species to mutant sinistral (counter-clockwise coiling) species have occurred multiple times (Ueshima and Asami 2003, Davison et al. 2005, Hoso et al. 2010, Gittenberger et al. 2012).

Why is single-gene speciation possible in snails? Orr (1991) proposed that, after Gittenberger (1988), a small population size and a maternal effect (delayed inheritance: Fig. 1) in snail populations could promote single-gene speciation. Because of the low mobility of snails, local populations tend to be isolated from each other, causing repeated extinction and colonization. This results in small effective population size and strong genetic drift (e.g., Arnaud and Laval 2004, Hoso 2012). Delayed inheritance of snail handedness is a sort of maternal effect, in which an individual's phenotype is determined by its mother's genotype (Fig. 1: Boycott et al. 1930, Freeman and Lundelius 1982, Utsuno and Asami 2010). Subsequent theoretical studies about snail coiling evolution fundamentally attributed the cause of single-gene speciation to these two factors (van Batenburg and Gittenberger 1996, Stone and Björklund 2002, Davison et al. 2005).

A recent study proposed a novel explanation concerning the effects of functional pleiotropy in single-gene speciation of snails, so-called the 'right-handed predator' hypothesis (Hoso et al. 2010). The research showed that a gene controlling coiling direction of snails could pleiotropically affect not only reproductive isolation but also anti-predator adaptation due to predator's 'handedness'. Because most snails are dextral (Vermeij 1975), predators tend to be 'right-handed' (specializing in the abundant dextral type of prey). Such predators include box crabs (Shoup 1968, Ng and Tan 1985, Dietl and Hendricks 2006), larvae of water-scavenger beetle (Inoda et al. 2003), and snail-eating snakes (Hoso et al. 2007, Hoso et al. 2010). Behavioral experiments revealed that those predators tend to fail in attempts to eat sinistral snails, due to left-right asymmetry of their feeding apparatuses and behaviors (Inoda et al. 2003, Dietl and Hendricks 2006, Hoso et al. 2007). Although a mating disadvantage still exists, sinistral individuals will have a survival advantage under such right-handed

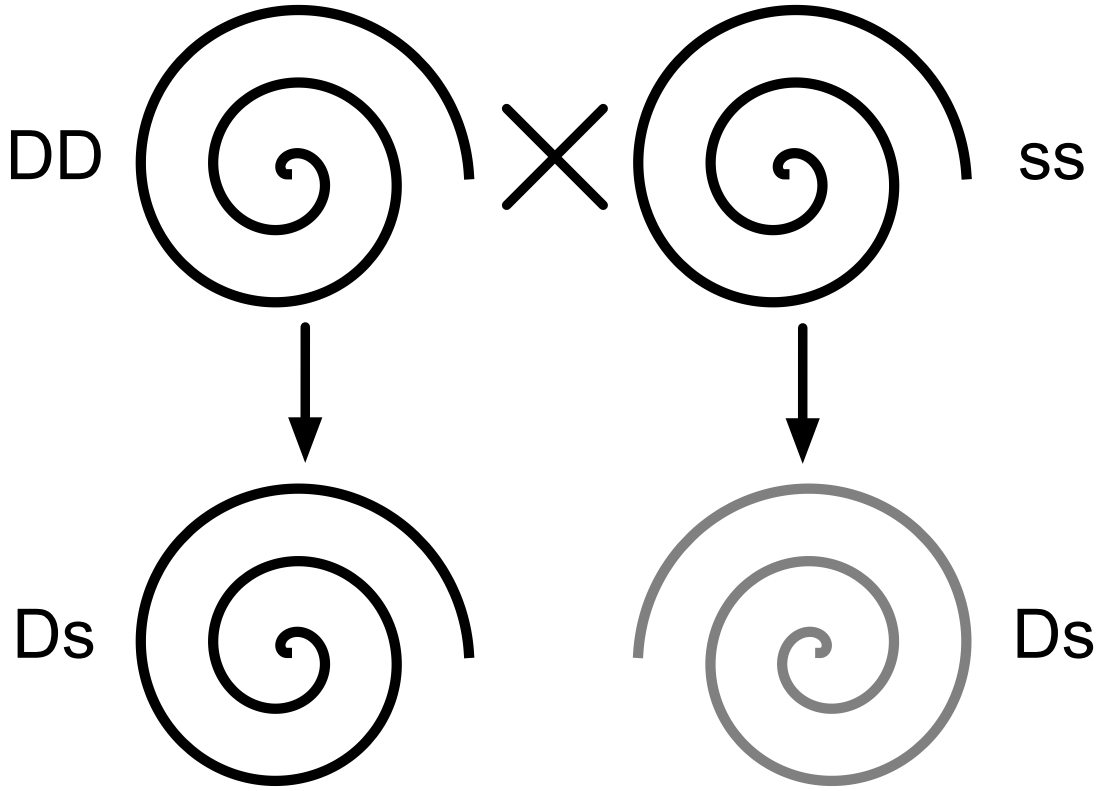

Figure 3.1: Chirality inheritance determined by maternal effects of dominant dextral (D) and recessive sinistral (s) alleles at a single nuclear locus (delayed inheritance). Black and gray spirals indicate dextral and sinistral phenotypes. In the second generation, individuals of the same genotype (Ds) develop into the opposite enantiomorph depending on the maternal genotype (DD or ss). Note that snails are androgynous.

predation. This can potentially promote the fixation of a sinistral allele, and indeed Hoso et al. (2010) found a positive correlation between right-handed predator (snake) distribution and the proportion of sinistral lineages. Although Hoso et al. (2010) found the correlating *pattern*, the underlying fixation *process* of the mutant allele in the speciation gene with functional pleiotropy has not been fully investigated.

Here we theoretically investigate the fixation process of the mutant allele in the speciation gene in single-gene speciation with or without functional pleiotropy. Our specific questions are: (1) how do allele dominance, population size, and delayed inheritance affect single-gene speciation? What kind of allele dominance has the highest fixation probability? How do population size and delayed inheritance affect this

tendency? (2) How does functional pleiotropy affect the process of single-gene speciation? When the mutant frequency is low, it would be better for heterozygotes to have the resident phenotype to mate with common resident genotypes (positive frequency-dependent selection). On the other hand, the mutant phenotype is advantageous under strong viability selection. Because of the conflicting factors, the effects of allele dominance and delayed inheritance can be changed by functional pleiotropy.

3.3 Models

To examine the questions, we consider a general allopatric speciation model. When a panmictic population split into two geographically divided subpopulations, it is sufficient to compare fixation probabilities of a mutant allele in a single subpopulation to understand the likelihood of speciation (Orr 1991). We construct Wright-Fisher models of haploid or diploid individuals without delayed inheritance and diploid individuals with delayed inheritance, to study the mutant allele frequency change through generations with reproductive isolation and viability selection.

We first consider the deterministic invasion condition of a mutant allele in infinite populations. Then we calculate the mutant fixation probability in finite populations by diffusion approximation analysis for large populations (Kimura 1962). Because diffusion approximation analysis assumes large populations, we also perform numerical calculations of the exact fixation probability for small populations by using a first step analysis (Pinsky and Karlin 2010), as well as Monte Carlo simulations (as Fig. 2). The first step analysis is also applicable to large populations, but the calculation is time-consuming when N is large. Therefore we show only the results for $N = 3$.

3.3.1 Model 1. *Haploid model*

Assume the case where mating occurs randomly, but mating between different phenotypes fails with probability r (Table 1). A common phenotype is advantageous because mating is more likely to be successful. In contrast, a rare phenotype tends to have a reduced probability of mating success (positive frequency-dependent selection). We denote the frequency of the mutant allele (A) by p, and that of the wild-type allele (a) by $1 - p$. The frequency after mating, $\tilde{p}$, is

$$\tilde{p} = \frac{p^2 + (1-r)p(1-p)}{p^2 + 2(1-r)p(1-p) + (1-p)^2}, \tag{3.1}$$

where r is an intensity of reproductive isolation ($0 \le r \le 1$, Table 1). Reproductive isolation is complete if $r = 1$, the mating is random if $r = 0$, and reproductive isolation is partial if $0 < r < 1$. The mutant frequency after one generation, p', is given by

$$p' = \frac{(1+s)\tilde{p}}{(1+s)\tilde{p} + 1 \cdot (1-\tilde{p})}, \tag{3.2}$$

where s is a positive viability selection coefficient. For example, if a mutant snail is sinistral then s represents the relative survival advantage of sinistral snails due to right-handed predation by snakes (Hoso et al. 2010).

3.3.2 Model 2. *Diploid model without delayed inheritance*

We consider the situation in which a single heterozygous mutant (Aa) appears by a mutation in the resident population (aa). We denote the degree of dominance of allele as h. $h = 0$ and $h = 1$ correspond to completely recessive and dominant mutant alleles, respectively. Under partial dominance ($0 < h < 1$), we consider two models: the first one is a three-phenotype model in which heterozygotes have an intermediate phenotype of the homozygous phenotypes, and intensities of reproductive isolation and viability selection are determined by the phenotype (h), although this does not apply to snails (Table 1). The second one is a model with only two phenotypes (A and a) and the heterozygous phenotype is A with probability h and a with probability $1 - h$ (Appendix S8). We introduce the first model here. The frequencies of genotypes AA (= x) and Aa (= y) after mating, $\tilde{x}$ and $\tilde{y}$, are given by

$$\begin{aligned} T\tilde{x} &= x^2 + \left[1-(1-h)r\right]xy + \frac{y^2}{4}, \\ T\tilde{y} &= \left[1-(1-h)r\right]xy + 2(1-r)xz + \frac{y^2}{2} + (1-hr)yz, \end{aligned} \tag{3.3}$$

where $T = 1 - 2r\left[(1-h)xy + xz + hyz\right]$ and z (= $1 - x - y$) is the frequency of the resident allele homozygote, aa (Table 1). The frequencies in the next generation, x' and y', are

Table 3.1: The diploid model without delayed inheritance (h = 0: a is a dominant allele, h = 1: A is a dominant allele).

Mating comb.	Mating prob.	AA	Aa	aa
AA × AA	x^2	1	0	0
AA × Aa	$2[1-(1-h)r]xy$	1/2	1/2	0
AA × aa	$2(1-r)xz$	0	1	0
Aa × Aa	y^2	1/4	1/2	1/4
Aa × aa	$2(1-hr)yz$	0	1/2	1/2
aa × aa	z^2	0	0	1

$$x' = \frac{(1+s)\tilde{x}}{(1+s)\tilde{x}+(1+hs)\tilde{y}+1\cdot\tilde{z}},$$
$$y' = \frac{(1+hs)\tilde{y}}{(1+s)\tilde{x}+(1+hs)\tilde{y}+1\cdot\tilde{z}}, \quad (3.4)$$

where $\tilde{z} = 1-\tilde{x}-\tilde{y}$.

3.3.3 Model 3. *Diploid model with delayed inheritance*

There are three genotypes (AA, Aa, and aa) and two phenotypes (A and a), thus six combinations are possible (i.e., AA_A, AA_a, Aa_A, Aa_a, aa_A, and aa_a). Here AA_A represents a genotype AA with phenotype A. However, as we assume complete dominance here, only five combinations arise: for example, AA_a is not realizable when A is dominant (Table S1). We assume that the mutation in the speciation gene occurs in an embryo, therefore the first mutant's phenotype is the same as its wild-type mother. We denote the frequencies of each combination of genotypes and phenotypes as follows: AA_A: x_A, Aa_A: y_A, Aa_a: y_a, aa_A: z_A, aa_a: z_a (= $1 - x_A - y_a - z_A - z_a$). Let p (= $x_A + (y_A + y_a)/2$) and q (= $1 - p = (y_A + y_a)/2 + z_A + z_a$) be the frequencies of dominant (A) and recessive (a) alleles. Frequencies after mating are

$$
\begin{aligned}
T\tilde{x}_{\mathrm{A}} &= p^2 - ry_{\mathrm{a}}\left(x_{\mathrm{A}} + \frac{y_{\mathrm{A}}}{2}\right),\\
T\tilde{y}_{\mathrm{A}} &= p(1-x_{\mathrm{A}}) - r\left[z_{\mathrm{a}}\left(x_{\mathrm{A}} + \frac{y_{\mathrm{A}}}{2}\right) + y_{\mathrm{a}}\left(x_{\mathrm{A}} + y_{\mathrm{A}} + \frac{z_{\mathrm{A}}}{2}\right)\right],\\
T\tilde{y}_{\mathrm{a}} &= p(1+x_{\mathrm{A}} - 2p) - r\left[z_{\mathrm{a}}\left(x_{\mathrm{A}} + \frac{y_{\mathrm{A}}}{2}\right) + \frac{y_{\mathrm{a}}z_{\mathrm{A}}}{2}\right],\\
T\tilde{z}_{\mathrm{A}} &= (p-x_{\mathrm{A}})(1-p) - \frac{r}{2}\left[y_{\mathrm{A}}(y_{\mathrm{a}}+z_{\mathrm{a}}) + y_{\mathrm{a}}z_{\mathrm{A}}\right],
\end{aligned}
\tag{3.5}
$$

where $T = 1 - 2r(x_{\mathrm{A}} + y_{\mathrm{A}} + z_{\mathrm{A}})(y_{\mathrm{a}} + z_{\mathrm{a}})$. Frequencies in the next generation are determined after viability selection and these depend on allelic dominance of the mutant. When the mutant allele is dominant,

$$
x'_{\mathrm{A}} = \frac{(1+s)\tilde{x}_{\mathrm{A}}}{W},\ y'_{\mathrm{A}} = \frac{(1+s)\tilde{y}_{\mathrm{A}}}{W},\ y'_{\mathrm{a}} = \frac{\tilde{y}_{\mathrm{a}}}{W},\ z'_{\mathrm{A}} = \frac{(1+s)\tilde{z}_{\mathrm{A}}}{W},\ z'_{\mathrm{a}} = \frac{\tilde{z}_{\mathrm{a}}}{W},
\tag{3.6}
$$

where $W = 1 + s(\tilde{x}_{\mathrm{A}} + \tilde{y}_{\mathrm{A}} + \tilde{z}_{\mathrm{A}})$ is the mean fitness of the population. See Appendix S2 for the recessive mutant allele.

3.4 Results

At first, we consider the case where there is no viability selection (s = 0). In snails, this corresponds to single-gene speciation without right-handed predation. Then, we show the results for the case with functional pleiotropy (s > 0).

3.4.1 *Single-gene speciation without functional pleiotropy*

Through deterministic analysis of infinite populations, we confirm that the system is bistable by positive frequency-dependent selection due to reproductive isolation (Fig. 3). Therefore a rare mutant allele cannot invade in infinite populations as predicted by the classic theory (Bateson 1909, Dobzhansky 1936, Muller 1942). Thus, genetic drift in finite populations is a prerequisite for single-gene speciation without functional pleiotropy (Gavrilets 2004). For example, the frequency change in one generation, $\Delta p = p' - p$, in the haploid model is

$$
\Delta p = \frac{p(1-p)\left[r(2p-1) + s - sr(1-p)\right]}{(1+s\tilde{p})\left[1 - 2rp(1-p)\right]},
\tag{3.7}
$$

from equations (1) and (2). Assuming large population size and small r and s, we can consider a continuous time model of allele frequency change for the whole range of p. Neglecting the higher order terms of r and s, we have the deterministic dynamics,

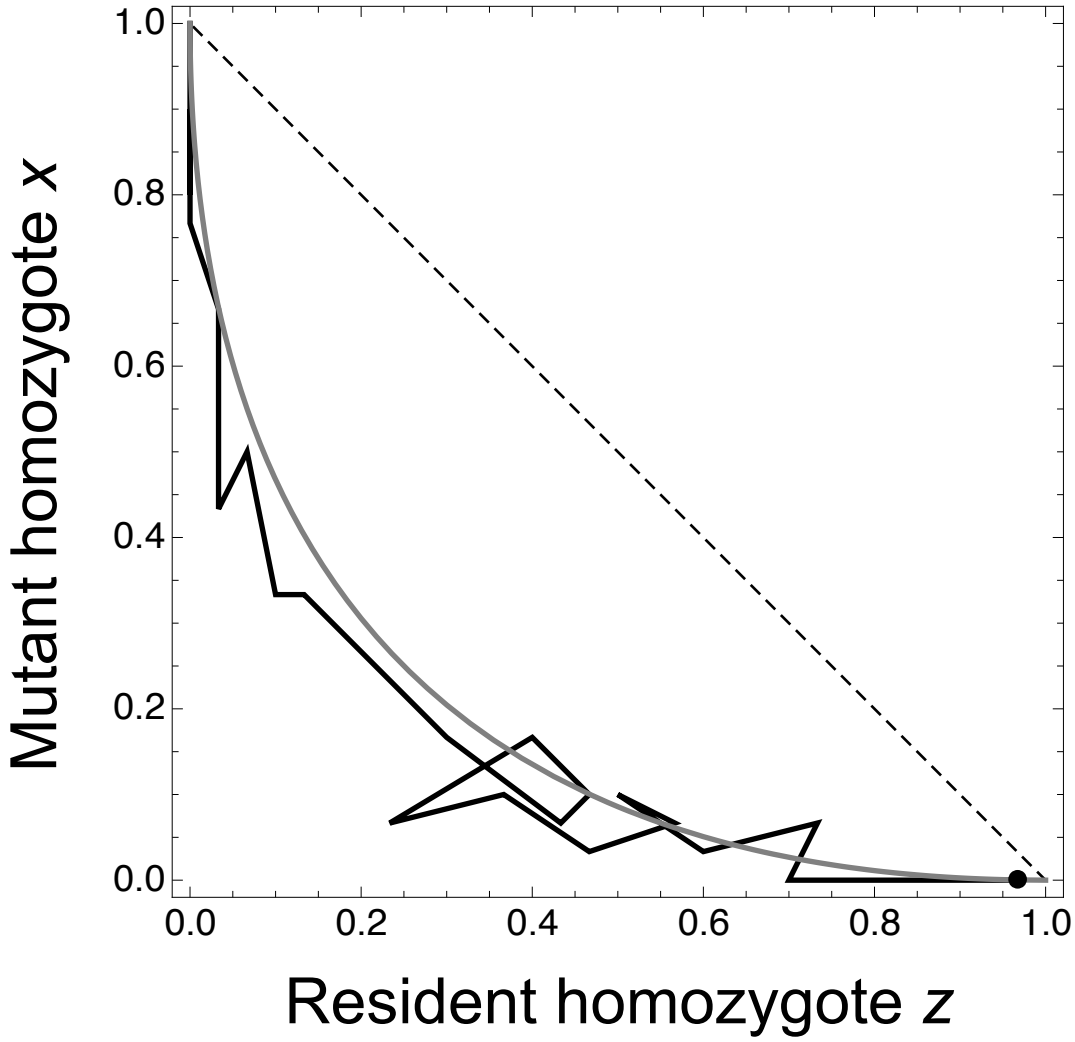

Figure 3.2: An example of fixation process of the mutant allele starting from a single heterozygote in the diploid model without delayed inheritance. *X*-axis: frequency of the resident allele homozygotes, aa (z). *Y*-axis: frequency of the mutant allele homozygotes, AA (x). Note that $x + z \leq 1$ (the dashed line). The initial condition is at $(z, x) = (1 - 1/N, 0)$ (the black point). The gray curve ($x = 1 + z - 2\sqrt{z}$) indicates the HW equilibrium. Parameter values are $N = 30$, $r = 0.1$, $s = 0.1$, and $h = 1$.

$$\dot{p} = p(1-p)\big[r(2p-1)+s\big]. \tag{3.8}$$

The dynamics have two stable equilibria at $p = 0$ and $p = 1$, and an internal unstable equilibrium at $p = (1 - s/r)/2$ when $r > s$. When $s = 0$, the unstable equilibrium is at $p = 1/2$ and the derivative of allele frequency dynamics is negative when p is smaller than 1/2 and is positive when p is larger than 1/2 (the solid gray line in Fig. 3A).

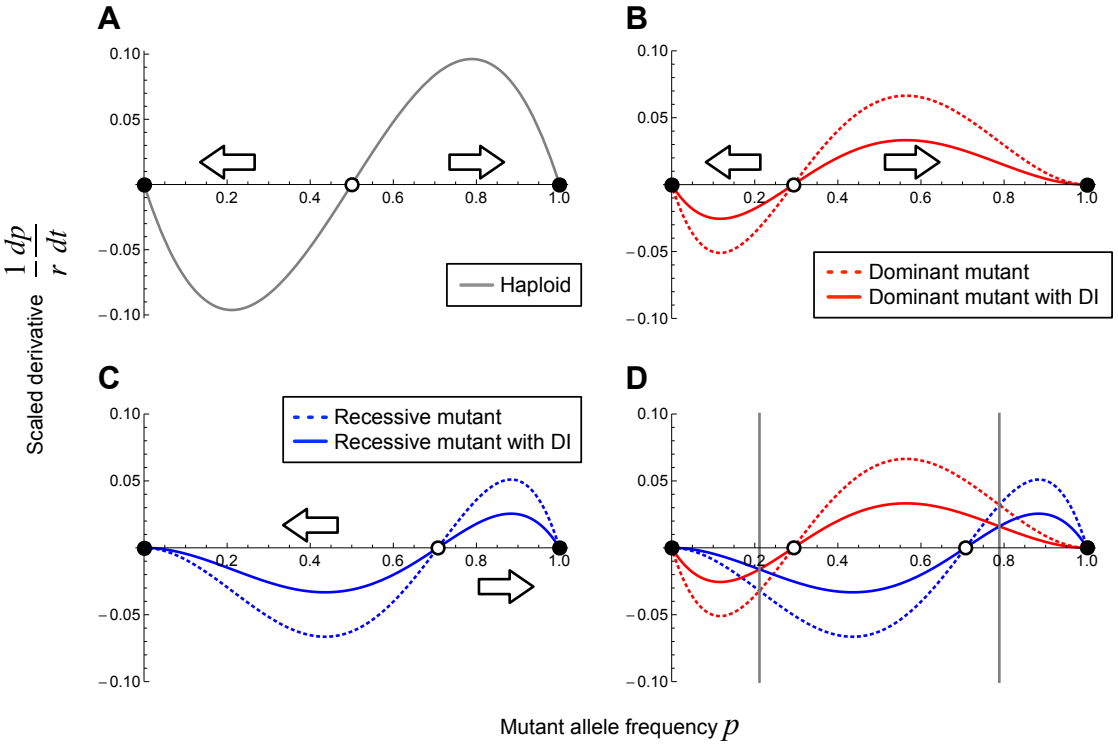

Figure 3.3: Allele frequency dynamics affected by positive frequency-dependent selection due to reproductive isolation (indicated by white arrows). *X*-axis: the mutant allele frequency (p). *Y*-axis: scaled derivatives of the mutant allele ($\dot{p}/r$). A: The haploid model (the solid gray line, eq. 8 when $s = 0$). An unstable equilibrium at $p = 1/2$ (the white point) divides two basins of attraction. Stable equilibria are at $p = 0$ and 1 (black points). B: The diploid models with the dominant mutant allele without delayed inheritance (the dotted red line, eq. 10 when $s = 0$ and $h = 1$) and with delayed inheritance (the solid red line, eq. 17 when $s = 0$). An unstable equilibrium is at $p = 1-1/\sqrt{2}$. C: The diploid models with the recessive mutant allele without delayed inheritance (the dotted blue line, eq. 10 when $s = 0$ and $h = 0$) and with delayed inheritance (the solid blue line, eq. 18 when $s = 0$). An unstable equilibrium is at $p = 1/\sqrt{2}$. D: Comparison of the diploid models with the dominant (red) and recessive (blue) alleles. Intersection points are at $p = 1/2-\sqrt{3}/6$ and $1/2+\sqrt{3}/6$ (gray lines).

The dynamics of the dominant and recessive alleles in the diploid models also show positive frequency-dependent selection, but their patterns are contrasting, providing insights into the fixation processes: the dominant allele is more favored in intermediate frequencies whereas the recessive allele has higher derivatives in low and

high frequencies (Fig. 3D). To show this, we approximate two-dimensional genotype frequency dynamics of the diploid model to one-dimensional allele frequency dynamics. The frequency dynamics of the genotypes is not strictly on the Hardy-Weinberg (HW) equilibrium, and the deviation is caused by reproductive isolation and viability selection (Fig. 2). We show that, if both r and s are small, the frequency dynamics first approaches the HW equilibrium, and then slowly converges to one of the stable equilibria, $p = 0$ or 1 (Crow and Kimura 1970). Assuming that both s and r are of the order of ε, a small positive constant, we expand the dynamics (3) and (4) in Taylor series with respect to ε. The leading order dynamics for the zygote frequencies are then

$$\begin{aligned} x' &= p^2 + O(\varepsilon), \\ y' &= 2p(1-p) + O(\varepsilon). \end{aligned} \tag{3.9}$$

Thus, in the leading order, genotype frequencies are in the HW equilibrium. From this it also follows that the allele frequencies do not change with time, $p' = p$, up to the leading order. By assuming large population size, small values of r and s, and the HW equilibrium, we have the approximated deterministic allele frequency dynamics,

$$\dot{p} = p(1-p)\left\{r\left[p(2p^2-1) - h(6p^2-6p+1)\right] + s\left[p + h(1-2p)\right]\right\}. \tag{3.10}$$

The scaled derivatives of the frequency dynamics when h = 0, 1/2, and 1 without viability selection (s = 0) are shown by dotted lines (Figs. 3, S1).

In spite of the different dynamics of the dominant and recessive alleles, surprisingly, they cancel out and both alleles have the same fixation probability in large populations (Figs. 4H, 4I). Fixation probabilities are calculated by diffusion approximation as follows: with random genetic drift, the diffusion process for the change in allele frequency is characterized by infinitesimal mean and variance of the frequency change:

$$\begin{aligned} M(p) &= E\left[\Delta p \middle| p\right] = p(1-p)\left[r(2p-1) + s\right], \\ V(p) &= E\left[(\Delta p)^2 \middle| p\right] = \frac{p(1-p)}{N}, \end{aligned} \tag{3.11}$$

in Model 1. The fixation probability of the allele A with the initial frequency p, denoted by $u(p)$, then satisfies the backward equation,

$$M(p)u'(p) + \frac{1}{2}V(p)u''(p) = 0, \tag{3.12}$$

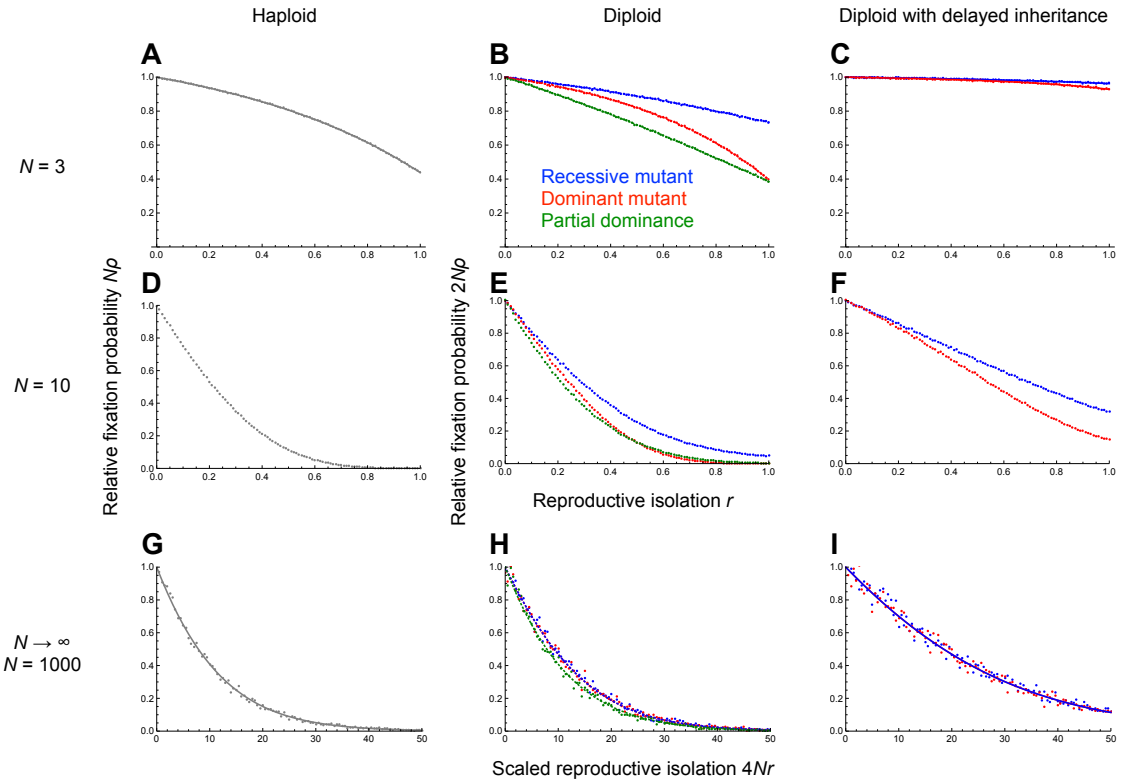

Figure 3.4: Relative fixation probabilities of a single mutant with reproductive isolation to that of a neutral mutant. Here is no viability selection (s = 0). A-F: X-axis is the reproductive isolation parameter (r). G-I: X-axis is four times the product of the reproductive isolation parameter and the effective population size ($4Nr$). Y-axis is the product of fixation probability and effective population size ($N\rho$ in the haploid model and $2N\rho$ in the diploid models). A-C: N = 3 (first step analyses and Monte Carlo simulations), D-F: N = 10 (Monte Carlo simulations), G-I: $N \rightarrow \infty$ (diffusion approximations) and N = 1000 (Monte Carlo simulations). A, D, G: Solid gray lines: the haploid model. Others: Blue lines: the recessive mutant allele, red lines: the dominant mutant allele, green lines: the partial dominance model with two phenotypes (h = 1/2), solid lines: with delayed inheritance, dotted lines: without delayed inheritance. The solid gray line in Fig. 4G and the dotted green line in Fig. 4H are the same. The dotted blue and red lines (the diploid model without delayed inheritance) are overlapping in Fig. 4H. The solid blue and red lines (the diploid model with delayed inheritance) are also overlapping in Fig. 4I.

with the boundary condition, $u(0) = 0$ and $u(1) = 1$ (Kimura 1962). This yields

$$u(p)=\frac{\int_0^p \exp\left[-\int_0^y \frac{2M(z)}{V(z)}dz\right]dy}{\int_0^1 \exp\left[-\int_0^y \frac{2M(z)}{V(z)}dz\right]dy} \tag{3.13}$$

as the solution. From equations (11) and (13), the fixation probability of a single mutant, $\rho = u(1/N)$, is

$$\rho=\frac{1/N}{\int_0^1 \exp\left\{\frac{y}{2}\left[R(1-y)-S\right]\right\}dy}, \tag{3.14}$$

where $R = 4Nr$ and $S = 4Ns$. The relative fixation rate of a single mutant to that of a neutral mutant is given by $\phi = N\rho$ (Figs. 4G-4I). In the same way, the fixation probability of a single recessive ($h = 0$) mutant allele, $\rho_0 = u(1/2N)$, is

$$\rho_0=\frac{1/(2N)}{\int_0^1 \exp\left[\frac{Ry^2}{2}(1-y^2)\right]dy}, \tag{3.15}$$

whereas that of the dominant mutant allele ($h = 1$), $\rho_1 = u(1/2N)$, is

$$\rho_1=\frac{1/(2N)}{\int_0^1 \exp\left[\frac{Ry}{2}(2-y)(1-y)^2\right]dy}. \tag{3.16}$$

It is easy to show that the equations (15) and (16) are equivalent (Appendix S3).

When population size is small, on the other hand, the recessive mutant allele has higher fixation probabilities than the dominant allele. We show this result by Monte Carlo simulations (Figs. 4E, 4F) as well as numerical calculations of exact fixation probabilities by the first step analysis (Figs. 4B, 4C, Appendix S5, S6, S7). This difference could be due to the different contribution of absolute individual numbers to frequency dynamics. Although we assume that the first mutant is always a single heterozygous individual in the diploid model, initial frequency of the mutant is higher in small populations. Thus, the first heterozygous individual with the dominant mutant allele is more strongly selected against in small populations (Fig. 3D).

Delayed inheritance halves the strength of positive frequency-dependent selection (Fig. 3), thereby doubles fixation probability in large populations (Figs. 4H, 4I). Assuming the HW equilibrium when r and s are small (Appendix S4), the approximated frequency dynamics of the dominant mutant allele in Model 3 is given by

$$\dot{p} = \frac{1}{2} p(1-p)^2 \left[-r(2p^2 - 4p + 1) + s \right]. \quad (3.17)$$

In the same way, the frequency dynamics of the recessive mutant allele in Model 3 is

$$\dot{q} = \frac{1}{2} q^2 (1-q) \left[r(2q^2 - 1) + s \right]. \quad (3.18)$$

In comparing with equation (10), strength of selection in equation (17) is a half of that in equation (10) when h = 1 and the right-hand side of equation (18) scales by 1/2 compared with equation (10) when h = 0 as shown by solid lines (Fig. 3). For this reason, the fixation probabilities of mutants in Model 3 are twice as high as those in Model 2 (Figs. 4H, 4I, Appendix S4). This indicates that delayed inheritance effectively halves the effective population size. This is probably due to the fact that a phenotype is determined only by the mother's genotype with no contribution from the father. The tendency that the model with delayed inheritance has higher fixation probabilities is the same in small populations (Figs. 4B, 4C, 4E, 4F).

We consider two cases of the partial dominance (h = 0.5) in Model 2. By comparing the allele frequency dynamics, the strength of positive frequency-dependent selection in the first model with three phenotypes is always smaller than that in the second model with two phenotypes, in which selection coefficient values are a half of the haploid model (Fig. S1). Therefore the model with three phenotypes has higher fixation probabilities. Interestingly, the fixation probability of the model with three phenotypes is between those of the completely dominant and recessive alleles in small populations (Figs. S2A, S2B), whereas it is higher than those of the dominant and recessive alleles in large populations (Figs. S2C, S3). For the model with two phenotypes, on the other hand, the fixation probability of an allele with partial dominance is almost always smaller than those of the completely dominant and recessive alleles (Figs. 4B, 4E, 4H, S2, S3). Specifically, the partial dominance model with h = 1/2 in large populations have the same fixation probability as the haploid model (Fig. 4H).

3.4.2 *Single-gene speciation with functional pleiotropy*

We theoretically show that functional pleiotropy can promote single-gene speciation as proposed by Hoso et al. (2010). Although functional pleiotropy can keep linkage between adaptation and reproductive isolation, it can also cause positive

frequency-dependent selection. Therefore, pleiotropy needs a sufficient level of selective force to promote ecological speciation (Fig. 5). The required selection coefficient for the mutant allele to invade is $s > r/(1-r)$ in the haploid and diploid models with complete dominance and $s > r/(1-hr)$ for the diploid models with partial dominance (Appendix S1, S2, S8). In the haploid model, equations (1) and (2) are approximated as $p' \approx (1+s)(1-r)p$ if the mutant frequency is small ($p \approx 0$). When $(1 + s)(1 - r) < 1$, the system is bistable and the positive frequency-dependent selection excludes rare alleles. There are two locally stable equilibria at $p = 0$ and $p = 1$, and a locally unstable equilibrium, $p_c = [r(1+s)-s]/[r(2+s)]$, that divides the two basins of attraction. As the mutant allele is selected for more ($s > 0$), the unstable equilibrium moves toward 0 and vanishes when s is as large as to satisfy $(1 + s)(1 - r) = 1$. When $(1 + s)(1 - r) > 1$, or $s > r/(1 - r)$, there is a globally stable equilibrium at $p = 1$ and the mutant allele increases and eventually fixes irrespective of the initial frequency (Fig. 5). Note that invasion is impossible when reproductive isolation is complete ($r = 1$), and this again suggests the importance of genetic drift in small populations.

For the diploid model, partial dominance makes ecological speciation easier as heterozygotes can obtain mating chance and survival advantage simultaneously. We derive the condition for the mutant allele to be able to invade the wild-type population as $(1 + hs)(1 - hr) > 1$ when $h \neq 0$ by analyzing recursion equations (3) and (4) (Appendix S1). Interestingly, the invasion condition of the complete recessive allele ($h = 0$) differs from $s > r$, that is the limit of $h \to 0$ for the invasion condition of the partially dominant mutant (Appendix S1). The heterozygotes with the completely recessive mutant allele are neutral for viability selection, but the invasion condition is equivalent to that for the completely dominant ($h = 1$) allele (Fig. 5). Also, we found that a locally stable equilibrium in which the mutant allele coexist with the resident allele appears when r is large and h is small (Fig. S4). In this case, the invasion condition (Fig. 5) does not equal a fixation condition with a single globally stable equilibrium. For the diploid model with delayed inheritance, the invasion condition in infinite populations is $(1 + s)(1 - r) > 1$ (Appendix S2), so this is the same as Models 1 and 2 (Fig. 5). However, the eigenvalue of the Jacobian matrix in the linearized system is smaller than that of the dominant allele in Model 2, which corresponds to the fact that the delayed inheritance makes the invasion of a mutant easier in a finite population (Appendix S2).

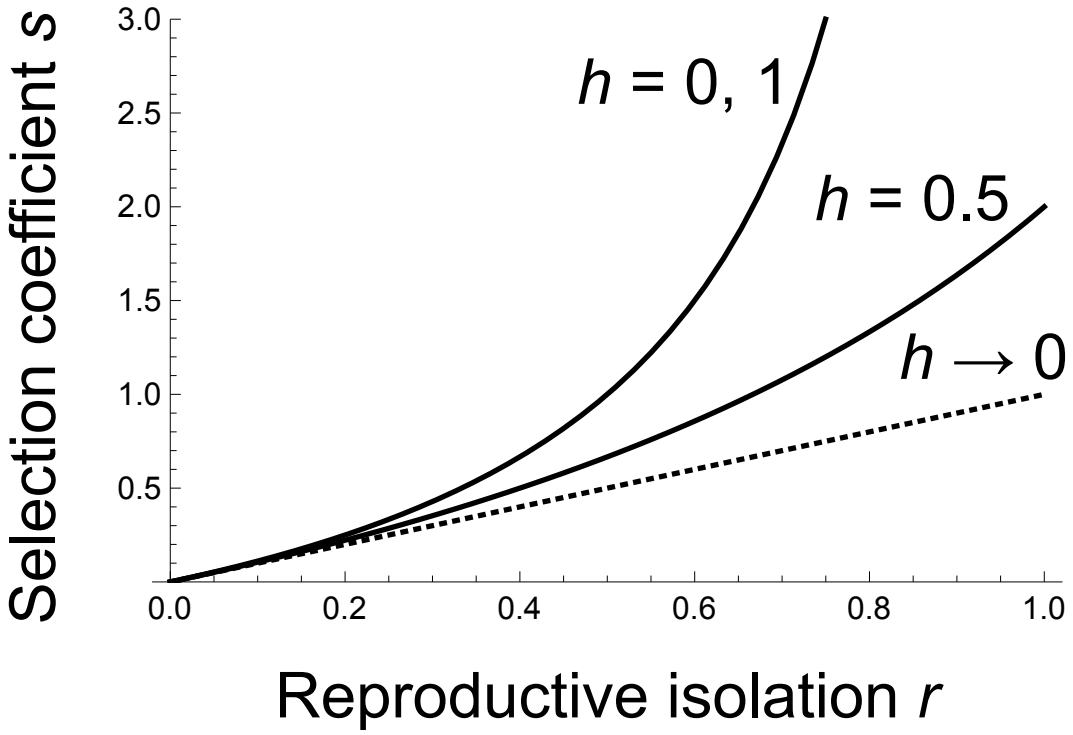

Figure 3.5: Deterministic invasion conditions of a mutant allele. *X*-axis: the reproductive isolation parameter (*r*). *Y*-axis: the viability selection coefficient (*s*). The completely dominant and recessive ($h = 0$ and 1) mutant alleles require a large selection coefficient for invasion whereas the alleles with partial dominance (e.g., $h = 0.5$) require a smaller selection coefficient. Note that the invasion condition of the completely recessive mutant allele differs from the limit of $h \rightarrow 0$ (the dotted line).

In finite populations, the balance between viability selection and positive frequency-dependent selection due to reproductive isolation determines fixation probability: when *r* is small, positive frequency-dependent selection is so weak that the dominant allele without delayed inheritance has the highest fixation probabilities. When *r* is large, on the other hand, the recessive allele with delayed inheritance is better due to strong positive frequency-dependent selection. In intermediate conditions, the dominant allele with delayed inheritance is better (Fig. 6). This is due to conflicting effects of reproductive isolation and viability selection. Positive frequency-dependent selection and viability selection work on the mutant phenotype, thus individuals with the mutant phenotype get conflicting effects from the two selection pressures: when reproductive isolation is weak, the survival advantage of the mutant phenotype exceeds its mating

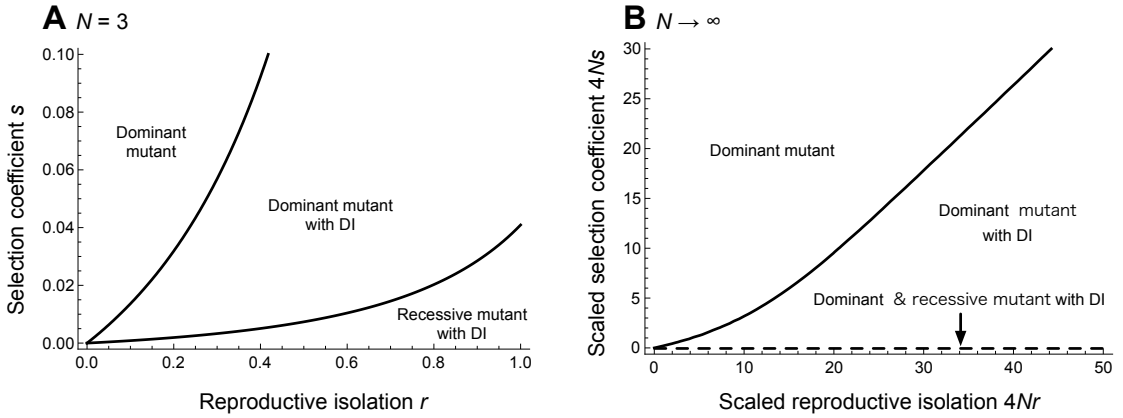

Figure 3.6: The alleles with the highest fixation probabilities given certain strength of reproductive isolation and viability selection. A: $N = 3$ (first step analyses), B: $N \rightarrow \infty$ (diffusion approximations). When $4Ns = 0$, both dominant and recessive mutant alleles with delayed inheritance have the same fixation probability. DI: delayed inheritance.

disadvantage. When reproductive isolation is strong, positive frequency-dependent selection is so strong that the survival advantage of the mutant phenotype cannot overcome the mating disadvantage when the mutant is rare.

With functional pleiotropy, fixation probabilities in the partial dominance model with three phenotypes are larger than those of the completely dominant and recessive mutant alleles when intensity of reproductive isolation and viability selection is intermediate (Fig. S5). In this case, heterozygotes that get intermediate mating and survival advantages simultaneously may work as a bridge between the mutant and wild-type homozygotes. This is consistent with the above interpretation on conflicting effects of viability selection and positive frequency-dependent selection on the mutant phenotype. In the second model with two phenotypes, the fixation probabilities are almost the same as those of the haploid model (data not shown).

3.5 Discussion

Single-gene speciation remains a controversial topic for evolutionary biology: Bateson, Dobzhansky, and Muller theoretically predicted that single-gene speciation is almost impossible (Bateson 1909; Dobzhansky 1936; Muller 1942), but there is some convincing evidence of single-gene speciation (e.g., Ueshima and Asami 2003). In the context of ecological speciation with gene flow, a single gene that pleiotropically

contributes to both reproductive isolation and divergent adaptation is believed to promote speciation (Rundle and Nosil 2005). If one locus is responsible for ecological adaptation and the other one is for reproductive isolation, speciation becomes less probable, because recombination breaks down the association between those two loci (Felsenstein 1981). As a trait that pleiotropically causes reproductive isolation and ecological adaptation provides a simple solution for this problem, it is called an 'automatic magic trait' (Gavrilets 2004, Servedio et al. 2011). An increasing number of studies suggest the involvement of adaptation in speciation (Barton 2010), but evolutionary process of single-gene speciation with adaptation is not fully investigated. In this study we theoretically analyze the poorly understood fixation process of the speciation gene, thereby supporting the idea that viability selection for the speciation gene may resolve the seeming conflict between theory and data on single-gene speciation (Hoso et al. 2010): handedness of snails pleiotropically works as an 'automatic magic trait' for both reproductive isolation and anti-predator adaptation (Gavrilets 2004, Servedio et al. 2011), and thereby right-handed predation promotes single-gene speciation.

In finite populations without pleiotropy, the dominant and recessive alleles have the same fixation probability in large populations whereas the recessive allele has a higher probability in small populations. The effects of population size are contrasting, but most left-right reversals are likely to have occurred in small and isolated populations (Orr 1991, Hoso 2012). Thus we predict that the frequently fixed allele in snails should be recessive in the absence of right-handed predation.

There are conflicting arguments about allele dominance; Orr (1991) wrote "the probability of fixation of a maternal mutation is roughly independent of its dominance" in dioecious populations, but hermaphroditic populations with selfing "*decrease* the chance that a dominant mutation will be fixed." On the other hand, van Batenburg and Gittenberger (1996) showed that the dominant mutant allele has a higher fixation probability, and Ueshima and Asami (2003) speculated allele dominance based on their results. We point out that this discrepancy is mainly due to different assumptions about the initial numbers of the mutant allele. Both Orr (1991) and we computed the fixation probability of a single mutant, whereas van Batenburg and Gittenberger (1996) changed initial numbers of mutants from 2 to 32. These assumptions are responsible for the different results, because the recessive mutant allele

has a higher fitness when it is rare, whereas the dominant mutant allele has a higher derivative when the frequency is intermediate (Fig. 3D). We changed initial numbers of mutants in Monte Carlo simulations and obtained the supporting results (data not shown). van Batenburg and Gittenberger (1996) assumed mass invasion from neighboring sinistral populations, but the fixation probability is usually calculated for a single *de novo* mutation. When the initial mutant is a single heterozygote, we both analytically and numerically showed that the recessive mutant allele has a higher fixation probability in small populations, but both alleles have the same probability in large populations (Fig. 4).

With functional pleiotropy, the balance between viability selection and positive frequency-dependent selection due to reproductive isolation determines the fixation probability of the mutant allele. The frequently fixed allele can be dominant when population size is small and viability selection is strong (fig. 6A), in contrast with speciation without functional pleiotropy. In single-gene speciation in snails, intensity of reproductive isolation, r, should be an important parameter: interchiral mating is almost impossible in flat-shelled snails which perform two-way face-to-face copulation (high r), whereas tall-shelled snails can copulate by shell mounting (small r) (Asami et al. 1998). Therefore, even with the same population size and right-handed predation pressure, the frequently fixed allele dominance in snails can be changed (Fig. 6A): when right-handed predation is weak or absent and reproductive isolation is strong, frequently fixed allele should be recessive. On the other hand, frequently fixed allele can be dominant when right-handed predation is strong and reproductive isolation is weak.

We have calculated fixation probabilities for various N, r, s and dominance of the mutant allele. Phylogenic information (Ueshima and Asami 2003, Hoso et al. 2010) can be used to infer those parameters because the number of left-right reversals in the phylogeny is influenced by fixation probabilities. Let P_S be the duration that the snail phenotype stay sinistral, and P_D be that for dextrality. The expected sojourn time in sinistral phenotype is $P_S = 1/(N\mu\rho_D)$ where μ is the mutation rate of the speciation gene changing to the dextral allele and ρ_D is the fixation probability of the mutant dextral allele. Assuming that the mutation is symmetrical and population size is constant, the ratio of those values is given by $P_S/P_D = (N\mu\rho_D)/(N\mu\rho_S) = \rho_D/\rho_S$. If left-right reversals have occurred frequently, the ratio estimated from phylogeny data should approach the theoretical prediction. The extent of assortative mating, r, (Asami et al.

1998) and biased predation pressure by right-handed predators, *s*, (Hoso et al. 2007, Hoso et al. 2010) are known from experiments. Thus it would be possible to estimate the population size and allele dominance by statistical inference. However, in addition to somewhat arbitrary assumptions about constant population size, symmetrical mutation, and equilibrium states, reconstruction of ancestral states is generally challenging, especially when the trait evolves adaptively (Schluter et al. 1997, Cunningham 1999). Further, we did not consider gene flow between snails of opposite chirality (Davison et al. 2005) or internal selection against left-right reversal (Utsuno et al. 2011). Thus, we propose these estimations as a future research subject.

In conclusion, delayed inheritance and functional pleiotropy of the speciation gene (e.g., right-handed predation on snails) can promote single-gene speciation, which supports the hypothesis about frequent left-right reversal of snails in habitats of specialist snakes (Hoso et al. 2010). Interestingly, population size and functional pleiotropy can change the effects of allele dominance and delayed inheritance on speciation. For example, Ueshima & Asami (2003) constructed a molecular phylogeny and speculated that the dextral allele seems to be dominant for *Euhadra* snails based on the result of van Batenburg and Gittenberger (1996), but caution is needed because reversal could occur by a *de novo* mutation and viability selection might be involved in speciation. Recent technological developments in molecular biology make it possible to investigate the dominance of alleles in ecologically important traits, and their ecological and evolutionary effects (e.g., Rosenblum et al. 2010). Although the challenge to search for a coiling gene (the speciation gene) of snail is still underway (e.g., Grande and Patel 2009, Kuroda et al. 2009), our prediction that the recessive allele has a higher fixation probability in the absence of specialist predators and in the flat-shelled snails whereas the dominant allele can have a higher one in the presence of specialist predators and in the tall-shelled snails will be a testable hypothesis. This would be possible, for example, by analyzing the correlations between the presence of right-handed predators and sinistral allele dominance.

3.6 Appendix

3.6.1 Appendix S1: Invasion condition in the diploid model without delayed inheritance

We denote the frequencies of the genotypes, AA, Aa, and aa by x, y, and z (= $1 - x - y$).

The frequencies after mating are

$$
\begin{aligned}
T\tilde{x} &= x^2 + \left[1-(1-h)r\right]xy + \frac{y^2}{4}, \\
T\tilde{y} &= \left[1-(1-h)r\right]xy + 2(1-r)xz + \frac{y^2}{2} + (1-hr)yz, \\
T\tilde{z} &= \frac{y^2}{4} + (1-hr)yz + z^2,
\end{aligned}
\tag{A1}
$$

where $T = 1-2r\left[(1-h)xy + xz + hyz\right]$ is the sum of the frequencies of three genotypes after mating (see Table 1 for the derivation). The frequencies in the next generation after viability selection favoring a mutant phenotype is

$$
\begin{aligned}
x' &= \frac{(1+s)\tilde{x}}{(1+s)\tilde{x} + (1+hs)\tilde{y} + \tilde{z}}, \\
y' &= \frac{(1+hs)\tilde{y}}{(1+s)\tilde{x} + (1+hs)\tilde{y} + \tilde{z}}, \\
z' &= \frac{\tilde{z}}{(1+s)\tilde{x} + (1+hs)\tilde{y} + \tilde{z}}.
\end{aligned}
\tag{A2}
$$

Here we assume that A is the mutant allele and a is the wild-type allele. When h = 1, the mutant allele is dominant; whereas, it is recessive when h = 0. We first consider the condition for the invasion of the completely or partially dominant mutant ($0 < h \le 1$). We then examine the invasibility condition for the completely recessive mutant ($h = 0$), in which we need to consult the center manifold theorem (Guckenheimer and Holmes 1983).

3.6.1.1 Invasibility of the completely and partially dominant mutant ($0 < h \le 1$)

We linearize the dynamics (A2) for small x and y:

$$
\begin{pmatrix} x' \\ y' \end{pmatrix} = \begin{pmatrix} 0 & 0 \\ 2(1-r)(1+hs) & (1+hs)(1-hr) \end{pmatrix} \begin{pmatrix} x \\ y \end{pmatrix}
\tag{A3}
$$

The largest eigenvalue of the linearized system is $(1+hs)(1-hr)$. Thus the mutant can invade if and only if $(1+hs)(1-hr) > 1$. This condition can be rewritten as $s > r/(1-hr)$.

3.6.1.2 Invasibility of the completely recessive mutant ($h = 0$)

If the mutant allele is completely recessive ($h = 0$), the linearized system is also given

by with $h=0$:

$$\begin{pmatrix} x' \\ y' \end{pmatrix} = A\begin{pmatrix} x \\ y \end{pmatrix} = \begin{pmatrix} 0 & 0 \\ 2(1-r) & 1 \end{pmatrix}\begin{pmatrix} x \\ y \end{pmatrix}. \tag{A4}$$

As the largest eigenvalue is 1, we need to have higher order terms of x and y to examine the local stability of $x=y=0$. The Taylor expansion of (A2) up to the quadratic terms of x and y yields

$$\begin{pmatrix} x' \\ y' \end{pmatrix} = \begin{pmatrix} 0 & 0 \\ 2(1-r) & 1 \end{pmatrix}\begin{pmatrix} x \\ y \end{pmatrix} + \begin{pmatrix} f(x,y) \\ g(x,y) \end{pmatrix}, \tag{A5}$$

with

$$\begin{aligned} f(x,y) &= (1+s)\left[x^2 + (1-r)xy + \frac{y^2}{4}\right], \\ g(x,y) &= -2(1-r)(1-2r)x^2 - (2-3r)xy - \frac{y^2}{2}. \end{aligned} \tag{A6}$$

The linear part of (A5) can be diagonalized by the transformation

$$\begin{pmatrix} x \\ y \end{pmatrix} = P\begin{pmatrix} u \\ v \end{pmatrix}, \text{ with } P = \begin{pmatrix} 0 & -\dfrac{1}{2(1-r)} \\ 1 & 1 \end{pmatrix}, \tag{A7}$$

where the column vectors of P are the eigenvectors corresponding to the eigenvalues 1 and 0 of matrix A. This yields

$$\begin{aligned} \begin{pmatrix} u' \\ v' \end{pmatrix} &= \begin{pmatrix} 1 & 0 \\ 0 & 0 \end{pmatrix}\begin{pmatrix} u \\ v \end{pmatrix} + P^{-1}\begin{pmatrix} f(x,y) \\ g(x,y) \end{pmatrix} \\ &\equiv \begin{pmatrix} 1 & 0 \\ 0 & 0 \end{pmatrix}\begin{pmatrix} u \\ v \end{pmatrix} + \begin{pmatrix} F(u,v) \\ G(u,v) \end{pmatrix}, \end{aligned} \tag{A8}$$

with

$$\begin{aligned} F(u,v) &= -\frac{1}{2}(r-s+rs)u^2 - \frac{r}{2(1-r)}uv + \frac{(2-r)r(1+s)}{2(1-r)}v^2, \\ G(u,v) &= -\frac{1}{2}(1-r)(1+s)u^2 - \frac{(2-r)r(1+s)}{2(1-r)}v^2. \end{aligned} \tag{A9}$$

Define the center manifold $W^c = \{(u,v) \mid v = k(u), k'(0) = k''(0) = 0\}$ on which the trajectory near $u=v=0$ stays throughout the process. The simplest form would be

$k(u) = au^2$. In order that the point (u', v') is also on the center manifold, we should have $v' = k(u')$. Substituting $u' = u + F(u, k(u))$ and $v' = G(u, k(u))$ into this yields

$$G(u, au^2) - a\left[u + F(u, au^2)\right]^2 = 0. \quad \text{(A10)}$$

Equating the coefficient of the leading term to zero, a is determined as

$$a = -\frac{1}{2}(1-r)(1+s). \quad \text{(A11)}$$

The slow dynamic of u restricted on the center manifold is then

$$u' = u + F(u, k(u)) = u - \frac{1}{2}(r - s + rs)u^2, \quad \text{(A12)}$$

and hence u converges to zero if $r - s + rs > 0$, or the mutant can invade if $r - s + rs < 0$ (or $(1-r)(1+s) > 1$). This invasibility condition for the completely recessive mutant is equivalent to that for the completely dominant mutant, but, interestingly, differs from the condition $s > r$ in the limit of $h \to 0$ for the invasibility condition of the partially dominant mutant.

3.6.2 Appendix S2: Invasion condition in the diploid model with delayed inheritance

In the presence of delayed inheritance, a phenotype of an individual is determined by a maternal genotype. We therefore need to keep track the frequencies of 2×3 combination of phenotype $\times$ genotype to describe the genetic dynamics. Here we denote the two alleles as A (dominant allele) and a (recessive allele). An individual has either phenotype A or a (right-handed or left-handed, depending on which is dominant) that is determined by the genotype of its mother. We denote for example an individual with the genotype AA and the phenotype A by AA_A.

As we assume that A is a dominant allele and a is a recessive allele in the diploid model with delayed inheritance, the genotype-phenotype combination AA_a will never be produced (indeed, for an individual to have phenotype a, its mother should be homozygote of the recessive allele, aa). We denote the frequencies of AA_A, Aa_A, Aa_a, aa_A, and aa_a as x_A, y_A, y_a, z_A, and z_a. $x_a \equiv 0$ as noted above. The frequency of phenotype A is $x_A + y_A + z_A$ and that of phenotype a is $y_a + z_a$. Let p_i $(= x_i + y_i/2)$ be the frequency of allele A with phenotype i $(=$ A or a), and q_i $(z_i + y_i/2)$ be the frequency of allele a with phenotype i $(=$ A or a). The frequencies after mating are

calculated from Table S1 as

$$
\begin{aligned}
T\tilde{x}_{\mathrm{A}} &= (p_{\mathrm{A}}+p_{\mathrm{a}})^2 - 2rp_{\mathrm{A}}p_{\mathrm{a}},\\
T\tilde{y}_{\mathrm{A}} &= (p_{\mathrm{A}}+p_{\mathrm{a}})(q_{\mathrm{A}}+q_{\mathrm{a}}) + (p_{\mathrm{A}}+p_{\mathrm{a}})\frac{y_{\mathrm{A}}+y_{\mathrm{a}}}{2} - r(p_{\mathrm{A}}q_{\mathrm{a}}+p_{\mathrm{a}}q_{\mathrm{A}}) - \frac{r}{2}(p_{\mathrm{a}}y_{\mathrm{A}}+p_{\mathrm{A}}y_{\mathrm{a}}),\\
T\tilde{y}_{\mathrm{a}} &= (p_{\mathrm{A}}+p_{\mathrm{a}})(z_{\mathrm{A}}+z_{\mathrm{a}}) - r(p_{\mathrm{a}}z_{\mathrm{A}}+p_{\mathrm{A}}z_{\mathrm{a}}),\\
T\tilde{z}_{\mathrm{A}} &= (q_{\mathrm{A}}+q_{\mathrm{a}})\frac{y_{\mathrm{A}}+y_{\mathrm{a}}}{2} - \frac{r}{2}(q_{\mathrm{a}}y_{\mathrm{A}}+q_{\mathrm{A}}y_{\mathrm{a}}),\\
T\tilde{z}_{\mathrm{a}} &= (q_{\mathrm{A}}+q_{\mathrm{a}})(z_{\mathrm{A}}+z_{\mathrm{a}}) - r(q_{\mathrm{a}}z_{\mathrm{A}}+q_{\mathrm{A}}z_{\mathrm{a}}),
\end{aligned}
\qquad \text{(B1)}
$$

where $T = 1-2r(x_{\mathrm{A}}+y_{\mathrm{A}}+z_{\mathrm{A}})(y_{\mathrm{a}}+z_{\mathrm{a}})$. When there is no reproductive isolation ($r = 0$) or viability selection ($s = 0$), the ratio of two phenotypes for the heterozygous genotype, $\mathrm{Aa_A} : \mathrm{Aa_a}$, is $(1 + p) : (1 – p)$ and that for the homozygous genotype, $\mathrm{aa_A} : \mathrm{aa_a}$, is $p : (1 – p)$ under delayed inheritance assuming the HW equilibrium.

3.6.2.1 Invasibility of a dominant mutant

The frequencies in the next generation are then given by those after the viability selection favoring a dominant handedness mutant (A) with the selection coefficient s:

$$
x'_{\mathrm{A}} = \frac{(1+s)\tilde{x}_{\mathrm{A}}}{W},\ y'_{\mathrm{A}} = \frac{(1+s)\tilde{y}_{\mathrm{A}}}{W},\ y'_{\mathrm{a}} = \frac{\tilde{y}_{\mathrm{a}}}{W},\ z'_{\mathrm{A}} = \frac{(1+s)\tilde{z}_{\mathrm{A}}}{W},\ z'_{\mathrm{a}} = \frac{\tilde{z}_{\mathrm{a}}}{W},
\qquad \text{(B2)}
$$

where $W = 1+s(\tilde{x}_{\mathrm{A}}+\tilde{y}_{\mathrm{A}}+\tilde{z}_{\mathrm{A}})$ is the mean fitness of the population.

We now examine the invasibility of the dominant allele A in the resident population consisting only of the recessive allele a (i.e., $z_{\mathrm{a}} = 1$ and $x_{\mathrm{A}} = y_{\mathrm{A}} = y_{\mathrm{a}} = z_{\mathrm{A}} = 0$). The system (B1)-(B2) is linearized with respect to z_{A}, y_{A}, y_{a}, and x_{A} as

$$
\begin{pmatrix} z'_{\mathrm{A}} \\ y'_{\mathrm{a}} \\ y'_{\mathrm{A}} \\ x'_{\mathrm{A}} \end{pmatrix} =
\begin{pmatrix}
0 & (1+s)/2 & (1-r)(1+s)/2 & 0 \\
0 & 1/2 & (1-r)/2 & 1-r \\
0 & (1+s)/2 & (1-r)(1+s)/2 & (1-r)(1+s) \\
0 & 0 & 0 & 0
\end{pmatrix}
\begin{pmatrix} z_{\mathrm{A}} \\ y_{\mathrm{a}} \\ y_{\mathrm{A}} \\ x_{\mathrm{A}} \end{pmatrix},
\qquad \text{(B3)}
$$

where z_{a} is eliminated by using $z_{\mathrm{a}} = 1-x_{\mathrm{A}}-y_{\mathrm{A}}-y_{\mathrm{a}}-z_{\mathrm{A}}$. The Jacobian matrix in the right hand side of (B3) has three zero eigenvalues and a non-trivial eigenvalue,

$$
\lambda = \frac{1}{2}(2+s-r-rs).
\qquad \text{(B4)}
$$

The population allows the invasion of the dominant mutant if $\lambda > 1$, which gives exactly the same condition $(1-r)(1+s) > 1$ as that for the invasibility of dominant mutant if there was no delayed inheritance. Though the condition for the invasibility is the same, the value (B4) itself is smaller than the dominant eigenvalue, $\lambda' = (1-r)(1+s)$, when there was no delayed inheritance, which corresponds to the fact that the delayed inheritance makes the invasion of a handedness mutant easier in a finite population.

3.6.2.2 Invasibility of a recessive mutant

Let us now consider the invasibility of a recessive handedness mutant that enjoys an ecological advantage in viability with the selection coefficient s. The frequencies after reproduction are given by (B1), and the frequencies in the next generation are

$$x'_{\mathrm{A}} = \frac{\tilde{x}_{\mathrm{A}}}{W}, y'_{\mathrm{A}} = \frac{\tilde{y}_{\mathrm{A}}}{W}, y'_{\mathrm{a}} = \frac{(1+s)\tilde{y}_{\mathrm{a}}}{W}, z'_{\mathrm{A}} = \frac{\tilde{z}_{\mathrm{A}}}{W}, z'_{\mathrm{a}} = \frac{(1+s)\tilde{z}_{\mathrm{a}}}{W}, \tag{B5}$$

where $W = 1 + s(\tilde{y}_{\mathrm{a}} + \tilde{z}_{\mathrm{a}})$ is the mean fitness. As before $\tilde{x}_{\mathrm{a}} = 0$. The resident population consists only of dominant allele A (i.e., $x_{\mathrm{A}} = 1$ and $y_{\mathrm{A}} = y_{\mathrm{a}} = z_{\mathrm{A}} = z_{\mathrm{a}} = 0$). The system (B1), (B5) is linearized with respect to z_{a}, z_{A}, y_{a}, and y_{A} as

$$\begin{aligned}
\begin{pmatrix} z'_{\mathrm{a}} \\ z'_{\mathrm{A}} \\ y'_{\mathrm{a}} \\ y'_{\mathrm{A}} \end{pmatrix} &= A \begin{pmatrix} z_{\mathrm{a}} \\ z_{\mathrm{A}} \\ y_{\mathrm{a}} \\ y_{\mathrm{A}} \end{pmatrix} + \begin{pmatrix} f_1(z_{\mathrm{a}}, z_{\mathrm{A}}, y_{\mathrm{a}}, y_{\mathrm{A}}) \\ f_2(z_{\mathrm{a}}, z_{\mathrm{A}}, y_{\mathrm{a}}, y_{\mathrm{A}}) \\ f_3(z_{\mathrm{a}}, z_{\mathrm{A}}, y_{\mathrm{a}}, y_{\mathrm{A}}) \\ f_4(z_{\mathrm{a}}, z_{\mathrm{A}}, y_{\mathrm{a}}, y_{\mathrm{A}}) \end{pmatrix} \\
&= \begin{pmatrix} 0 & 0 & 0 & 0 \\ 0 & 0 & 0 & 0 \\ (1-r)(1+s) & 1+s & 0 & 0 \\ 1-r & 1 & 1-r & 1 \end{pmatrix} \begin{pmatrix} z_{\mathrm{a}} \\ z_{\mathrm{A}} \\ y_{\mathrm{a}} \\ y_{\mathrm{A}} \end{pmatrix} + \begin{pmatrix} f_1(z_{\mathrm{a}}, z_{\mathrm{A}}, y_{\mathrm{a}}, y_{\mathrm{A}}) \\ f_2(z_{\mathrm{a}}, z_{\mathrm{A}}, y_{\mathrm{a}}, y_{\mathrm{A}}) \\ f_3(z_{\mathrm{a}}, z_{\mathrm{A}}, y_{\mathrm{a}}, y_{\mathrm{A}}) \\ f_4(z_{\mathrm{a}}, z_{\mathrm{A}}, y_{\mathrm{a}}, y_{\mathrm{A}}) \end{pmatrix},
\end{aligned} \tag{B6}$$

where f_i's are quadratic or higher order terms of z_{a}, z_{A}, y_{a}, and y_{A}. The matrix A has eigenvalues $\lambda = 1$ and $\lambda = 0$ (with multiplicity 3). Because the dominant eigenvalue is 1, we need to construct a center manifold to examine the local stability of the equilibrium $(z_{\mathrm{a}}, z_{\mathrm{A}}, y_{\mathrm{a}}, y_{\mathrm{A}})^T = (0,0,0,0)^T$, where superscript T denotes the vector transform.

The eigenvector corresponding to the eigenvalue 1 is found, by solving $(A-1I)\mathbf{b}=\mathbf{0}$, to be $\mathbf{b}_1=(1,0,0,0)^T$, where I is a 4×4 identity matrix. There are two eigenvectors satisfying $(A-0I)\mathbf{b}=A\mathbf{b}=\mathbf{0}$ corresponding to the eigenvalue 0:

$$\mathbf{b}_2=\begin{pmatrix}1\\-(1-r)\\0\\0\end{pmatrix}, \text{ and } \mathbf{b}_3=\begin{pmatrix}0\\0\\1\\-(1-r)\end{pmatrix}. \tag{B7}$$

We now find a nonzero vector $\mathbf{b}_4$ that, together with $\mathbf{b}_2$ and $\mathbf{b}_3$, spans the 3-dimensional generalized eigenspace corresponding to the eigenvalue 0. Such vector $\mathbf{b}_4$ must satisfy $(A-0I)^2\mathbf{b}_4=A^2\mathbf{b}_4=\mathbf{0}$ and be linearly independent of $\mathbf{b}_2$ or $\mathbf{b}_3$, which is obtained as

$$\mathbf{b}_4=\begin{pmatrix}1\\0\\0\\-(1-r)(2+s-r-rs)\end{pmatrix}. \tag{B8}$$

Now we define the transformation matrix P whose columns consist of $\mathbf{b}_1$, $\mathbf{b}_2$, $\mathbf{b}_3$, and $\mathbf{b}_4$:

$$P=\begin{pmatrix}0 & 1 & 0 & 1\\0 & -(1-r) & 0 & 0\\0 & 0 & 1 & 0\\1 & 0 & -(1-r) & -(1-r)(2+s-r-rs)\end{pmatrix}. \tag{B9}$$

We then transform the variables as

$$\begin{pmatrix}z_{\mathrm{a}}\\z_{\mathrm{A}}\\y_{\mathrm{a}}\\y_{\mathrm{A}}\end{pmatrix}=P\begin{pmatrix}u_1\\u_2\\u_3\\u_4\end{pmatrix}. \tag{B10}$$

The dynamics for the transformed variables become

$$\begin{pmatrix} u_1' \\ u_2' \\ u_3' \\ u_4' \end{pmatrix} = P^{-1}AP\begin{pmatrix} u_1 \\ u_2 \\ u_3 \\ u_4 \end{pmatrix} + P^{-1}\begin{pmatrix} f_1 \\ f_2 \\ f_3 \\ f_4 \end{pmatrix}$$
$$= \begin{pmatrix} 1 & 0 & 0 & 0 \\ 0 & 0 & 0 & 0 \\ 0 & 0 & 0 & (1-r)(1+s) \\ 0 & 0 & 0 & 0 \end{pmatrix}\begin{pmatrix} u_1 \\ u_2 \\ u_3 \\ u_4 \end{pmatrix} + \begin{pmatrix} F_1(u_1,u_2,u_3,u_4) \\ F_2(u_1,u_2,u_3,u_4) \\ F_3(u_1,u_2,u_3,u_4) \\ F_4(u_1,u_2,u_3,u_4) \end{pmatrix}. \quad \text{(B11)}$$

Here, $F_i(u_1,u_2,u_3,u_4)$ is the i th row of $P^{-1}\mathbf{f}(\mathbf{x}) = P^{-1}\mathbf{f}(P\mathbf{u})$ where $\mathbf{f} = (f_1,f_2,f_3,f_4)^T$, $\mathbf{x} = (z_a, z_A, y_a, y_A)^T$, and $\mathbf{u} = (u_1,u_2,u_3,u_4)^T$. We now define the center manifold

$$W^c = \{(u_1,u_2,u_3,u_4) \mid u_2 = f(u_1), u_3 = g(u_1), u_4 = h(u_1)\}, \quad \text{(B12)}$$

where f, g, and h are functions with the following properties: $f(0) = g(0) = h(0) = 0$ and $f'(0) = g'(0) = h'(0) = 0$. The simplest forms for such functions are $f(u) = au^2$, $g(u) = bu^2$, and $h(u) = cu^2$ where a, b, and c are constants. Substituting these into (B11), and requiring that the variables u_2', u_3', and u_4' in the next generation must lie on the center manifold ($u_2' = f(u_1')$, $u_3' = g(u_1')$, and $u_4' = h(u_1')$), we now have

$$\begin{aligned} u_1' &= u_1 + F_1(u_1, au_1^2, bu_1^2, cu_1^2), \\ a\left[u_1 + F_1(u_1, au_1^2, bu_1^2, cu_1^2)\right]^2 &= F_2(u_1, au_1^2, bu_1^2, cu_1^2), \\ b\left[u_1 + F_1(u_1, au_1^2, bu_1^2, cu_1^2)\right]^2 &= (1-r)(1+s)cu_1^2 + F_3(u_1, au_1^2, bu_1^2, cu_1^2), \\ c\left[u_1 + F_1(u_1, au_1^2, bu_1^2, cu_1^2)\right]^2 &= F_4(u_1, au_1^2, bu_1^2, cu_1^2). \end{aligned} \quad \text{(B13)}$$

The coefficients a, b, and c are determined from the leading order terms of the second to the forth equations of (B13) as

$$a=-\frac{1}{4(1-r)},\quad b=\frac{1+s}{4},\quad c=\frac{1}{4(1-r)}. \tag{B14}$$

Substituting this into the first equation of (B13), we have a slow dynamics on the center manifold:

$$u_1'=u_1+\frac{1}{4}(s-r-rs)u_1^2+O\left(u_1^3\right). \tag{B15}$$

Thus, u_1 converges to zero if and only if $s(1-r)-r<0$ or $s<r/(1-r)$. Conversely, the recessive mutant can invade the population if $s>r/(1-r)$. This condition is the same as the condition $(2+s-r-rs)/2>1$ or $(1-r)(1+s)>1$ for the invasibility of the dominant mutant.

The center manifold $u_2=-u_1^2/\left[4(1-r)\right]$, $u_3=(1+s)u_1^2/4$, and $u_4=u_1^2/\left[4(1-r)\right]$ in the original coordinate is defined in a parametric form with a parameter $\xi=u_1$ as

$$\begin{aligned}
z_{\mathrm{a}}&=O\left(\xi^3\right),\\
z_{\mathrm{A}}&=\frac{1}{4}\xi^2+O\left(\xi^3\right),\\
y_{\mathrm{a}}&=\frac{1+s}{4}\xi^2+O\left(\xi^3\right),\\
y_{\mathrm{A}}&=\xi-\frac{3+2s-2r-2rs}{4}\xi^2+O\left(\xi^3\right).
\end{aligned} \tag{B16}$$

3.6.3 Appendix S3: Diffusion approximation analysis of the diploid model without delayed inheritance

We here derive the approximate one-dimensional diffusion process describing the allele frequency dynamics in a finite population of effective population size *N* without delayed inheritance. The discrete-generation genotype dynamics in infinite population are derived as (A1)-(A2) of Appendix S1. As is usual in diffusion approximation, we take the limit of weak fecundity and viability selections, $r\to 0$, $s\to 0$, and large population $N\to\infty$ with the products *Nr* and *Ns* being kept finite.

Assuming that both *s* and *r* are of the order of ε, a small positive constant, we expand the dynamics (A1)-(A2) in Taylor series with respect to ε. The leading order

dynamics for the zygote frequencies x, y, and z of genotypes AA, Aa, and aa are then

$$\begin{aligned} x' &= p^2 + O(\varepsilon), \\ y' &= 2pq + O(\varepsilon), \\ z' &= q^2 + O(\varepsilon), \end{aligned} \tag{C1}$$

where $p = x + y/2$ and $q = z + y/2$ respectively is the frequency of allele A and a. Thus, in the leading order, genotype frequencies are in the Hardy-Weinberg equilibrium. From this it also follows that the allele frequencies do not change with time, $p' = p$ and $q' = q$, up to the leading order.

Now we derive the slow allele frequency dynamics as the first order expansion of the equations (A1) and (A2). The change in the allele frequency p of the mutant allele A is then

$$\Delta p = p(1-p)\left\{r\left[p(2p^2-1) - h(6p^2-6p+1)\right] + s\left[p + h(1-2p)\right]\right\} + O(\varepsilon^2). \tag{C2}$$

Note that s in (C2) is the selection coefficient favoring the phenotype A. From (C2) we have the frequency dynamics:

$$\dot{p} = p(1-p)\left\{r\left[p(2p^2-1) - h(6p^2-6p+1)\right] + s\left[p + h(1-2p)\right]\right\}. \tag{C3}$$

The dynamics has two stable equilibria at p = 0 and p = 1, and an internal unstable equilibrium when $r > s$.

With random genetic drift, the diffusion process for the change in the allele frequency is characterized by infinitesimal mean and variance of the frequency change:

$$\begin{aligned} M(p) &= E\left[\Delta p | p\right] = p(1-p)\left\{r\left[p(2p^2-1) - h(6p^2-6p+1)\right] + s\left[p + h(1-2p)\right]\right\}, \\ V(p) &= E\left[(\Delta p)^2 | p\right] = \frac{p(1-p)}{2N}. \end{aligned} \tag{C4}$$

The fixation probability of the allele A with the initial frequency p then satisfies the backward equation (12) with the boundary condition $u(0) = 0$ and $u(1) = 1$. This yields equation (13). The fixation probability of a single mutant $\rho = u(1/2N)$ is then

$$\rho = \frac{1/(2N)}{\int_0^1 \exp\left\{4Nry(1-y)\left[\frac{y}{2}(1+y) - h(2y-1)\right] - 4Nsy\left[\frac{y}{2} + h(1-y)\right]\right\} dy}, \tag{C5}$$

The relative fixation rate of a single mutant relative to that of a neutral mutant is given by $\phi = 2N\rho$:

$$\phi = \frac{1}{\int_0^1 \exp\left\{ Ry(1-y)\left[\frac{y}{2}(1+y) - h(2y-1)\right] - Sy\left[\frac{y}{2} + h(1-y)\right]\right\} dy}, \qquad \text{(C6)}$$

where $R = 4Nr$ and $S = 4Ns$. Here we consider three cases: (i) h = 0 (the recessive mutant), (ii) h = 1 (the dominant mutant), (iii) h = 0.5 (the partially dominant mutant).

3.6.3.1 h = 0 (the recessive mutant)

After factorization, the deterministic dynamics is

$$\dot{p} = p^2(1-p)\left[r(2p^2-1) + s\right], \qquad \text{(C7)}$$

when h = 0. This can be written as

$$\dot{p} = 2rp^2(1-p)\left(p - \sqrt{\frac{r-s}{2r}}\right)\left(p + \sqrt{\frac{r-s}{2r}}\right),$$

when $r > 0$ and $r > s$. Thus the dynamics has an internal unstable equilibrium at $p_c = \sqrt{(r-s)/2r}$ when $r > s$. When s = 0, therefore, the dynamics has two stable equilibria at p = 0 and p = 1, and an internal unstable equilibrium at $p_c = 1/\sqrt{2}$ (the dotted blue line in Fig. 3).

The relative fixation rate is

$$\phi_0 = \frac{1}{\int_0^1 \exp\left\{\frac{y^2}{2}\left[R(1-y^2) - S\right]\right\} dy}. \qquad \text{(C8)}$$

When s = 0, for the relative fixation rate, $\phi_0 = 1/\int_0^1 \exp\left[\frac{Ry^2}{2}(1-y^2)\right] dy$, we can show the following properties. Firstly, at the limit of $R \to 0$ the fixation probability is equal to that of a neutral allele:

$$\phi_0\big|_{R=0} = 1. \qquad \text{(C9)}$$

Secondly we see that $1/\phi_0$ is convex with respect to R because

$$\frac{\partial^2}{\partial R^2}\left(\frac{1}{\phi_0}\right) = \frac{1}{4}\int_0^1 \left(y^2 - y^4\right)^2 \exp\left[\frac{R}{2}\left(y^2 - y^4\right)\right] dy > 0. \qquad \text{(C10)}$$

Thirdly we see that the sign of the initial slope of $1/\phi_0$ from

$$\frac{\partial}{\partial R}\left(\frac{1}{\phi_0}\right)\bigg|_{R=0} = \frac{1}{15}. \qquad \text{(C11)}$$

Because the right-hand side of equation (C11) is positive, ϕ_0 is smaller than 1 for any $R > 0$. The fixation probability of a dominant mutant allele is always smaller than that, $1/(2N)$, of a neutral allele (i.e. the native recessive allele is the finite population size ESS, ESS_N, in the sense of Nowak et al. (2004) (Nowak et al. 2004)). In addition, this value is smaller than the haploid model (1/12), implying that the reduction rate of fixation probability is more moderate in the diploid model.

3.6.3.2 $h = 1$ (the dominant mutant)

The frequency dynamics of dominant mutant is obtained from equation (C3):

$$\dot{p} = p(1-p)^2\left[-r\left(2p^2-4p+1\right)+s\right]. \tag{C12}$$

This can be written as

$$\dot{p} = 2rp(1-p)^2\left[p-\left(1-\sqrt{\frac{r+s}{2r}}\right)\right]\left[\left(1+\sqrt{\frac{r+s}{2r}}\right)-p\right].$$

If $r > s$, this has an internal unstable equilibrium at $p_c = 1-\sqrt{(r+s)/2r}$. When $s = 0$, the dynamics has an internal unstable equilibrium at $p_c = 1-1/\sqrt{2}$ (the dotted red line in Fig. 3).

Therefore the relative fixation rate of a recessive mutant to that of a neutral allele $\phi_1 = 2N\rho_1$ then satisfies

$$\phi_1 = \frac{1}{\int_0^1 \exp\left\{\frac{y}{2}(2-y)\left[R(1-y)^2-S\right]\right\}dy}. \tag{C13}$$

If $s = 0$, we can show that the function $(1/\phi_1)$ is convex with respect to R, $\phi_1\big|_{R=0} = 1$, and $\left(\partial(1/\phi_1)/\partial R\right)\big|_{R=0} = 1/15$. Actually, ϕ_1 and ϕ_0 are equivalent ($\phi_0 = \phi_1$) when $s = 0$, though it is different when $s > 0$. This is obvious from equations (C8) and (C13); if we represent the frequency of the recessive allele as p and that of the dominant allele as q, then

$$\begin{aligned} p^2\left(1-p^2\right) &= (1-q)^2\left[1-(1-q)^2\right] \\ &= q(2-q)(1-q)^2. \end{aligned} \tag{C14}$$

3.6.3.3 h = 0.5 (the partially dominant mutant)

The frequency dynamics of mutant with partial dominance is obtained from equation (C3):

$$\dot{p} = \frac{1}{2} p(1-p)\left[r(2p-1)\left(2p^2 - 2p + 1\right) + s \right]. \qquad \text{(C15)}$$

This has an internal unstable equilibrium at

$$p_c = \frac{1}{2} + \frac{1}{2}\left(\sqrt{\frac{1}{27} + \left(\frac{s}{r}\right)^2} - \frac{s}{r} \right)^{\frac{1}{3}} - \frac{1}{6}\left(\sqrt{\frac{1}{27} + \left(\frac{s}{r}\right)^2} - \frac{s}{r} \right)^{-\frac{1}{3}},$$

when $r > s$. Equation (C15) has an internal unstable equilibrium at $p_c = 1/2$ when $s = 0$ (the dotted lime-green line in Fig. S1). The relative fixation rate is

$$\phi_2 = \frac{1}{\int_0^1 \exp\left\{ \frac{y}{2}\left[R(1 - 2y + 2y^2 - y^3) - S \right] \right\} dy}. \qquad \text{(C16)}$$

If $s = 0$, we can show that the function $(1/\phi_2)$ is convex with respect to R, $\phi_2\big|_{R=0} = 1$, and $\left(\partial(1/\phi_2)/\partial R\right)\big|_{R=0} = 1/15$.

These analytical expressions for the relative fixation rates ϕ_0, ϕ_1 and ϕ_2 obtained from one-dimensional diffusion approximation showed good agreements with the simulation results when N = 1,000 (Fig. 4H). When s = 0, we found that ϕ_0 and ϕ_1 are equivalent as shown in equation (C14) (Fig. 4H) and that ϕ_2 is higher than ϕ_0 and ϕ_1 when R is not small, implying that partial dominance can promote fixation of the mutant allele in the diploid model with three phenotypes (Figs. 4H, S2C).

3.6.4 Appendix S4: Diffusion approximation analysis of the diploid model with delayed inheritance

We here derive the approximate one-dimensional diffusion process describing the allele frequency dynamics of snail handedness alleles in a finite population of effective population size N with delayed inheritance. The discrete-generation genotype-phenotype dynamics in infinite population are derived as (B1) and (B2) or (B1) and (B5) of Appendix S2. As is usual in diffusion approximation, we take the limit of weak fecundity and viability selections, $r \to 0$, $s \to 0$, and large population $N \to \infty$ with the products Nr and Ns being kept finite.

Assuming that both s and r are of the order of ε, a small positive constant, we expand the dynamics (B1) and (B2)/(B5) in Taylor series with respect to ε. The leading order dynamics for the zygote frequencies $x = x_{\mathrm{A}} + x_{\mathrm{a}}$, $y = y_{\mathrm{A}} + y_{\mathrm{a}}$, $z = z_{\mathrm{A}} + z_{\mathrm{a}}$ of genotypes AA, Aa, and aa are then

$$\begin{aligned} x' &= p^2 + O(\varepsilon), \\ y' &= 2pq + O(\varepsilon), \\ z' &= q^2 + O(\varepsilon), \end{aligned} \tag{D1}$$

where $p = x + y/2$ and $q = z + y/2$ respectively is the frequency of allele A and a. Thus, in the leading order, genotype frequencies are in the Hardy-Weinberg equilibrium. From this it also follows that the allele frequencies do not change with time, $p' = p$ and $q' = q$, up to the leading order. The frequencies of phenotype-genotype combinations are thus kept constant for a given allele frequency p (or q) up to the leading order:

$$\begin{aligned} x_{\mathrm{A}} &= p^2 + O(\varepsilon), \\ x_{\mathrm{a}} &= 0, \\ y_{\mathrm{A}} &= pq(1+p) + O(\varepsilon), \\ y_{\mathrm{a}} &= pq^2 + O(\varepsilon), \\ z_{\mathrm{A}} &= pq^2 + O(\varepsilon), \\ z_{\mathrm{a}} &= q^3 + O(\varepsilon). \end{aligned} \tag{D2}$$

Now we derive the slow allele frequency dynamics as the first order expansion of the equations (B1) and (B2)/(B5). The change in the allele frequency p of the dominant allele A is then

$$\Delta p = \frac{1}{2} p(1-p)^2 \left[-r(2p^2 - 4p + 1) - s \right] + O(\varepsilon^2). \tag{D3}$$

For the frequency q of the recessive allele, we have

$$\Delta q = \frac{1}{2} q^2 (1-q) \left[r(2q^2 - 1) + s \right] + O(\varepsilon^2). \tag{D4}$$

Note that s in (D3) and (D4) is the selection coefficient favoring phenotype a. If phenotype A is selected for, the sign must be changed before s in the right hand side of (D3) and (D4).

3.6.4.1 The dominant mutant alleles

If the dominant mutant is selected for in the viability selection, we change the sign before s in the right hand side of (D3) to have the deterministic dynamics,

$$\dot{p} = \frac{1}{2} p(1-p)^2 \left[-r(2p^2 - 4p + 1) + s \right]. \qquad \text{(D5)}$$

This rate of change in the allele frequency of dominant allele is exactly a half of that for the diploid model without delayed inheritance with $h = 1$ (eq. C12). In other words, the delayed inheritance does not change allele frequency dynamics at all except for its halved rate. Therefore, the position of internal unstable equilibrium, $p_c = 1 - 1/\sqrt{2}$, is the same as in the model without delayed inheritance (the solid red line in Fig. 3).

The relative fixation rate of a dominant mutant to that of a neutral allele $\phi_A = 2N\rho_A$ then satisfies

$$\phi_A = \frac{1}{\int_0^1 \exp\left\{ \frac{y}{4}(2-y)\left[R(1-y)^2 - S \right] \right\} dy}. \qquad \text{(D6)}$$

3.6.4.2 The recessive mutant allele

If the recessive allele is selected for in the viability selection, we have from (D4) the deterministic dynamics,

$$\dot{q} = \frac{1}{2} q^2 (1-q) \left[r(2q^2 - 1) + s \right]. \qquad \text{(D7)}$$

Again, the right hand side is exactly a half of that for the diploid model without delayed inheritance with $h = 0$ (eq. C7). Thus, two stable equilibria at $q = 0$ and $q = 1$, and an internal unstable equilibrium at $q_c = 1/\sqrt{2}$ are exactly the same as in the model without delayed inheritance (the solid blue line in Fig. 3). The relative fixation rate of a recessive mutant to that of a neutral allele $\phi_a = 2N\rho_a$ then satisfies

$$\phi_a = \frac{1}{\int_0^1 \exp\left\{ \frac{z^2}{4}\left[R(1-z^2) - S \right] \right\} dz}. \qquad \text{(D8)}$$

Note that ϕ_A and ϕ_a are equivalent when $s = 0$, which can be shown by changing the variables in the integral in (D8) from z to $y = 1 - z$. When $s = 0$, the initial slope of

$1/\phi_A$ and $1/\phi_a$ is $\left(\partial(1/\phi_A)/\partial R\right)\big|_{R=0} = 1/30$. This value is smaller than the haploid model (1/12) and the diploid model without delayed inheritance (1/15), implying that the reduction rate of fixation probability is more moderate in the diploid model with delayed inheritance.

The analytical formula for the relative fixation probabilities, (D6) and (D8), by one dimensional diffusion approximation showed good agreements with the Monte Carlo simulation results for the original 4 dimensional genotype-phenotype dynamics for sufficiently large N (N = 1,000, Fig. 4I).

3.6.5 Appendix S5: Exact fixation probabilities in the haploid model

We calculated exact fixation probabilities in the Markov process without any approximation by the first step analysis. Consider a finite population with N haploid individuals. Recursion equations of fixation probabilities can be written as

$$u(i) = \sum_{j=0}^{N} P_{i,j} u(j), \tag{E1}$$

where $u(i)$ is the probability that a mutant allele starting with i individuals in the initial population eventually goes to fixation, and $P_{i,j}$ is the transition probability that the number of mutant allele change from i to j in one generation ($0 \le i, j \le N$). Note that u here is a function of number of individuals, but u in Appendix S3 and S4 is a function of frequencies. With the boundary conditions $u(0) = 0$ and $u(N) = 1$, the fixation probability can be obtained by solving linear equations with $N - 1$ unknown variables. This can be written in a matrix form:

$$A\mathbf{u} = \mathbf{b}, \tag{E2}$$

where

$$A = \begin{pmatrix} P_{1,1}-1 & P_{1,2} & \cdots & P_{1,(N-1)} \\ P_{2,1} & P_{2,2}-1 & \cdots & P_{2,(N-1)} \\ \vdots & \vdots & \ddots & \vdots \\ P_{(N-1),1} & P_{(N-1),2} & \cdots & P_{(N-1),(N-1)}-1 \end{pmatrix},$$

$$\mathbf{u} = \begin{pmatrix} u(1) \\ u(2) \\ \vdots \\ u(N-1) \end{pmatrix},$$

$$\mathbf{b} = \begin{pmatrix} -P_{1,N} \\ -P_{2,N} \\ \vdots \\ -P_{(N-1),N} \end{pmatrix}.$$

The solution can be obtained by multiplying the inverse of matrix A in the both sides of (E1): $\mathbf{u} = A^{-1}\mathbf{b}$. The transition probability $P_{i,j}$ is given by the binomial distribution when there is no selection ($r = s = 0$):

$$P_{i,j} = \binom{N}{j} p^j (1-p)^{N-j}, \tag{E3}$$

where $p = i/N$. When there is positive frequency-dependent selection due to reproductive isolation ($r > 0$ and $s = 0$), the expected frequency in the next generation in equation (E3), p, is replaced by equation (1):

$$P_{i,j} = \binom{N}{j} \left(\frac{p[1-r(1-p)]}{1-2rp(1-p)} \right)^j \left(1 - \frac{p[1-r(1-p)]}{1-2rp(1-p)} \right)^{N-j}. \tag{E4}$$

When there is viability selection for the mutant ($r > 0$ and $s > 0$), equation (E3) is replaced by

$$P_{i,j} = \binom{N}{j} \left(\frac{(1+s)\tilde{p}}{1+s\tilde{p}} \right)^j \left(1 - \frac{(1+s)\tilde{p}}{1+s\tilde{p}} \right)^{N-j}, \tag{E5}$$

where $\tilde{p}$ is from equation (1). The graphs of $u(1)$ are in good agreement with the simulation results when $N = 3$ (Fig. 4A).

One drawback of this method is that calculating the inverse matrix of the transition probability matrix, A, is time-consuming or almost impossible when N is large. In the diploid models, the dimension is two without delayed inheritance and four with delayed inheritance. Due to the 'curse of dimensionality,' therefore, calculation is especially difficult in the diploid models. For sufficiently small population size, however, this method is practical and gives accurate results for very small N when diffusion approximation fails.

3.6.6 Appendix S6: Exact fixation probabilities in the diploid model without delayed inheritance

Consider a finite population with diploid N individuals. The fixation probability can be calculated as

$$u(i,j)=\sum_{k=0}^{N}\sum_{l=0}^{N}P_{ij,kl}u(k,l), \tag{F1}$$

where $u(i, j)$ is the fixation probability when there are i individuals of AA homozygote and j individuals of aa homozygote (we call this as state (i, j) hereafter) and $P_{ij,kl}$ is the transition probability from state (i, j) to state (k, l) in one generation ($0 \le i, j, k, l \le N$). Note that the number of heterozygous individuals Aa is $(N - i - j)$ or $(N - k - l)$. With the boundary conditions $u(0, N) = 0$ and $u(N, 0) = 1$ where the mutant allele is A and the wild-type allele is a, the fixation probability of a mutant allele, $u(0, N - 1)$, can be obtained by solving linear equations for $(N+1)(N+2)/2-2$ unknowns $u(i,j)$ for $i=0,1,\cdots,N-1,\quad j=0,1,\cdots,N-1$, with $i+j\le N$. This can be rewritten in a matrix form $A\mathbf{u}=\mathbf{b}$:

$$\begin{pmatrix} P_{00,00}-1 & P_{00,01} & \cdots & P_{00,(N-1)1} \\ P_{01,00} & P_{01,01}-1 & \cdots & P_{01,(N-1)1} \\ \vdots & \vdots & \ddots & \vdots \\ P_{(N-1)1,00} & P_{(N-1)1,01} & \cdots & P_{(N-1)1,(N-1)1}-1 \end{pmatrix}\begin{pmatrix} u(0,0) \\ u(0,1) \\ \vdots \\ u(N-1,1) \end{pmatrix}=\begin{pmatrix} -P_{00,N0} \\ -P_{01,N0} \\ \vdots \\ -P_{(N-1)1,N0} \end{pmatrix}.$$

The solution is obtained by multiplying the inverse of matrix A in the both sides: $\mathbf{u}=A^{-1}\mathbf{b}$. The transition probability is given by the multinomial distribution,

$$P_{ij,kl}=\frac{N!}{k!(N-k-l)!l!}\left[\left(x+\frac{y}{2}\right)^2\right]^k\left[2\left(x+\frac{y}{2}\right)\left(\frac{y}{2}+z\right)\right]^{N-k-l}\left[\left(\frac{y}{2}+z\right)^2\right]^l, \tag{F2}$$

where $x = i/N$, $y = 1 - (i + j)/N$, and $z = j/N$. When there is positive frequency-dependent selection due to reproductive isolation or viability selection for the mutant in addition to reproductive isolation, the expected frequencies of genotypes in the next generation in equation (F2) is replaced by equation (A1) or (A2).

3.6.7 Appendix S7: Exact fixation probabilities in the diploid model with delayed inheritance

Consider a finite population with diploid N individuals. The fixation probability can be

calculated as

$$u(a,b,c,d)=\sum_{i=0}^{N}\sum_{j=0}^{N}\sum_{k=0}^{N}\sum_{l=0}^{N}P_{abcd,ijkl}u(i,j,k,l), \qquad \text{(G1)}$$

where $u(a, b, c, d)$ is the fixation probability when there are a individuals of AA_A, b individuals of Aa_A, c individuals of Aa_a, and d individuals of aa_A (we call this as state (a, b, c, d) hereafter) and $P_{abcd,ijkl}$ is the transition probability from state (a, b, c, d) to state (i, j, k, l) in one generation ($0 \le a, b, c, d, i, j, k, l \le N$). Note that the number of aa_a individuals is ($N - a - b - c - d$) or ($N - i - j - k - l$). The frequencies of AA_A, Aa_A, Aa_a, and aa_A are x_A (= a/N), y_A (= b/N), y_a (= c/N), z_A (= d/N). With the boundary conditions $u(0, 0, 0, 0) = u(0, 0, 0, 1) = \ldots = u(0, 0, 0, N) = 0$ and $u(N, 0, 0, 0) = 1$ where the dominant mutant allele is A and the recessive wild-type allele is a, the fixation probability of a mutant allele, $u(0, 0, 1, 0)$, can be obtained by solving linear equations for $u(i,j,k,l)$ with $i,j,k,l=0,1,\cdots,N$ and $i+j+k+l\le N$. This can be rewritten in a matrix form $A\mathbf{u}=\mathbf{b}$:

$$\begin{pmatrix} P_{1000,1000}-1 & P_{1000,2000} & \cdots & P_{1000,00N0} \\ P_{2000,1000} & P_{2000,2000}-1 & \cdots & P_{2000,00N0} \\ \vdots & \vdots & \ddots & \vdots \\ P_{00N0,1000} & P_{00N0,2000} & \cdots & P_{00N0,00N0}-1 \end{pmatrix}\begin{pmatrix} u(1,0,0,0) \\ u(2,0,0,0) \\ \vdots \\ u(0,0,N,0) \end{pmatrix}=\begin{pmatrix} -P_{1000,N000} \\ -P_{2000,N000} \\ \vdots \\ -P_{00N0,N000} \end{pmatrix}.$$

The solution is obtained as: $\mathbf{u}=A^{-1}\mathbf{b}$. The transition probability is given by the multinomial distribution,

$$P_{abcd,ijkl}=\frac{N!}{i!j!k!l!(N-i-j-k-l)!}\bar{x}_A^i\bar{y}_A^j\bar{y}_a^k\bar{z}_A^l\left(1-\bar{x}_A-\bar{y}_A-\bar{y}_a-\bar{z}_A\right)^{N-i-j-k-l}, \qquad \text{(G2)}$$

where

$$\bar{x}_A=\left(\frac{a}{N}+\frac{b+c}{2N}\right)^2,\bar{y}_A=\left(\frac{a}{N}+\frac{b+c}{2N}\right)\left(1-\frac{a}{N}\right),\bar{y}_a=\left(\frac{a}{N}+\frac{b+c}{2N}\right)\frac{d+e}{N},$$
$$\bar{z}_A=\frac{b+c}{2N}\left(\frac{b+c}{2N}+\frac{d+e}{N}\right).$$

The expected frequencies in the next generation in equation (G2) are replaced by equations (B1)-(B2) when there is positive frequency-dependent selection due to reproductive isolation and viability selection for the mutant.

When the recessive mutant allele is a and the wild-type allele is A, we solved the equation,

$$\begin{pmatrix} P_{1000,1000}-1 & P_{1000,2000} & \cdots & P_{1000,00N0} \\ P_{2000,1000} & P_{2000,2000}-1 & \cdots & P_{2000,00N0} \\ \vdots & \vdots & \ddots & \vdots \\ P_{00N0,1000} & P_{00N0,2000} & \cdots & P_{00N0,00N0}-1 \end{pmatrix}\begin{pmatrix} u(1,0,0,0) \\ u(2,0,0,0) \\ \vdots \\ u(0,0,N,0) \end{pmatrix}=\begin{pmatrix} -P_{1000,0000} \\ -P_{2000,0000} \\ \vdots \\ -P_{00N0,0000} \end{pmatrix},$$

to obtain the fixation probability of a single mutant, $u(N-1, 1, 0, 0)$, with the boundary conditions: $u(N, 0, 0, 0) = 0$ and $u(0, 0, 0, 0) = u(0, 0, 0, 1) = \ldots = u(0, 0, 0, N) = 1$. The expected frequencies in the next generation in equation (G2) are replaced by equations (B1) and (B5) when there is positive frequency-dependent selection due to reproductive isolation and viability selection for the mutant.

3.6.8 Appendix S8: The partial dominance model with two phenotypes

Thus far we considered the model in which h is a parameter that determines the intermediate phenotype of heterozygote (Appendix S1, S3). Here we consider the case where there are only two phenotypes (A and a) and the heterozygous phenotype is A with probability h and a with probability $1-h$. In this case, the mating probability between heterozygote (Aa × Aa) is

$$\left[h^2+(1-h)^2+2h(1-h)(1-r)\right]y^2=\left[1-2h(1-h)r\right]y^2. \qquad \text{(H1)}$$

Therefore the frequencies after mating are

$$\begin{aligned} T\tilde{x} &= x^2+\left[1-(1-h)r\right]xy+\frac{1}{4}\left[1-2h(1-h)r\right]y^2, \\ T\tilde{y} &= \left[1-(1-h)r\right]xy+2(1-r)xz+\frac{1}{2}\left[1-2h(1-h)r\right]y^2+(1-hr)yz, \\ T\tilde{z} &= \frac{1}{4}\left[1-2h(1-h)r\right]y^2+(1-hr)yz+z^2, \end{aligned} \qquad \text{(H2)}$$

where $T=1-2r(x+hy)\left[(1-h)y+z\right]$. This is the same as (A1) when $h = 0$ or 1. By linearizing the dynamics (H2) after viability selection (A2) for small x and y, we have the same result as equation (3) in Appendix S1. The largest eigenvalue of the linearized system is $(1+hs)(1-hr)$, and the mutant can invade if and only if $(1+hs)(1-hr) > 1$. This condition ($s > r/(1-hr)$) is the same as the original diploid model (Appendix S1).

For diffusion approximation analysis, we take the limit of weak fecundity and viability selections, $r \to 0$, $s \to 0$, and large population $N \to \infty$ with the products Nr and Ns being kept finite (Appendix S3). Assuming that both s and r are the order of e, a small positive constant, the change in the allele frequency p of the mutant allele A is

$$\Delta p = p(1-p)\left[-p+h(2p-1)\right]\left\{r\left[1-2p^2-4hp(1-p)\right]-s\right\}+O(\varepsilon^2). \quad \text{(H3)}$$

Note that s in (H3) is the selection coefficient favoring the phenotype A. From (H3) we have the frequency dynamics:

$$\dot{p} = p(1-p)\left[-p+h(2p-1)\right]\left\{r\left[1-2p^2-4hp(1-p)\right]-s\right\}. \quad \text{(H4)}$$

When h = 1/2, this is a half of the haploid model (equation 8). The dynamics has two stable equilibria at p = 0 and p = 1, and an internal unstable equilibrium at $p_c = \frac{h}{2h-1} - \frac{\sqrt{(2h^2-2h+1)r+(2h-1)s}}{\sqrt{2r}(2h-1)}$ when $r > s$. The relative fixation rate of a single mutant relative to that of a neutral mutant is given by $\phi = 2N\rho$:

$$\phi = \frac{1}{\int_0^1 \exp\left\{\frac{y}{2}\left[y+2h(1-y)\right]\left[R(1-y)(1-2hy+y)-S\right]\right\}dy}. \quad \text{(H5)}$$

where R = 4Nr and S = 4Ns. As shown in Figure S3, the lowest fixation probability is obtained when h = 1/2. When h = 1/2, the fixation probability is exactly the same as the haploid model (Figs. 4G, 4H).

Exact fixation probabilities without approximation in small populations are also calculated as Appendix S6. Results are shown in Fig. 4B (the dotted dark-green line).

Table 3.S1: The diploid model with delayed inheritance (when A is a dominant allele)

Mating comb.	Mating probability	AA_A	Aa_A	Aa_a	aa_A	aa_a
$AA_A \times AA_A$	x_A^2	1	0	0	0	0
$AA_A \times Aa_A$	$2x_A y_A$	1/2	1/2	0	0	0
$AA_A \times Aa_a$	$2(1-r)x_A y_a$	1/2	1/2	0	0	0
$AA_A \times aa_A$	$2x_A z_A$	0	1/2	1/2	0	0
$AA_A \times aa_a$	$2(1-r)x_A z_a$	0	1/2	1/2	0	0
$Aa_A \times Aa_A$	y_A^2	1/4	1/2	0	1/4	0
$Aa_A \times Aa_a$	$2(1-r)y_A y_a$	1/4	1/2	0	1/4	0
$Aa_A \times aa_A$	$2y_A z_A$	0	1/4	1/4	1/4	1/4
$Aa_A \times aa_a$	$2(1-r)y_A z_a$	0	1/4	1/4	1/4	1/4
$Aa_a \times Aa_a$	y_a^2	1/4	1/2	0	1/4	0
$Aa_a \times aa_A$	$2(1-r)y_a z_A$	0	1/4	1/4	1/4	1/4
$Aa_a \times aa_a$	$2y_a z_a$	0	1/4	1/4	1/4	1/4
$aa_A \times aa_A$	z_A^2	0	0	0	0	1
$aa_A \times aa_a$	$2(1-r)z_A z_a$	0	0	0	0	1
$aa_a \times aa_a$	z_a^2	0	0	0	0	1

3.6.9 Supplemental Figures

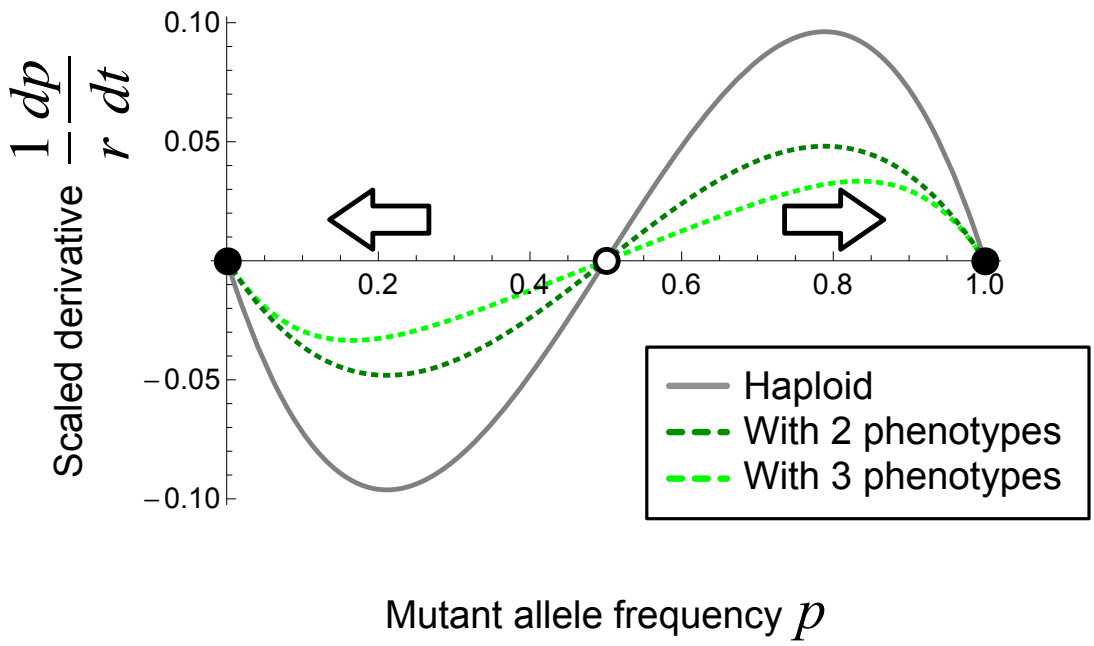

Figure 3.S1: Allele frequency dynamics affected by positive frequency-dependent selection due to reproductive isolation (indicated by white arrows). *X*-axis: the mutant allele frequency (p). *Y*-axis: scaled derivatives of the mutant allele ($\dot{p}/r$). The haploid model (the solid gray line, eq. 8 when $s = 0$), the partial dominance model with two phenotypes (the dotted dark-green line, eq. H5 when $s = 0$ and $h = 1/2$), and the partial dominance model with three phenotypes (the dotted lime-green line, eq. 10 when $s = 0$ and $h = 1/2$). An unstable equilibrium at $p = 1/2$ (the white point) divides two basins of attraction. Stable equilibria are at $p = 0$ and 1 (the black points).

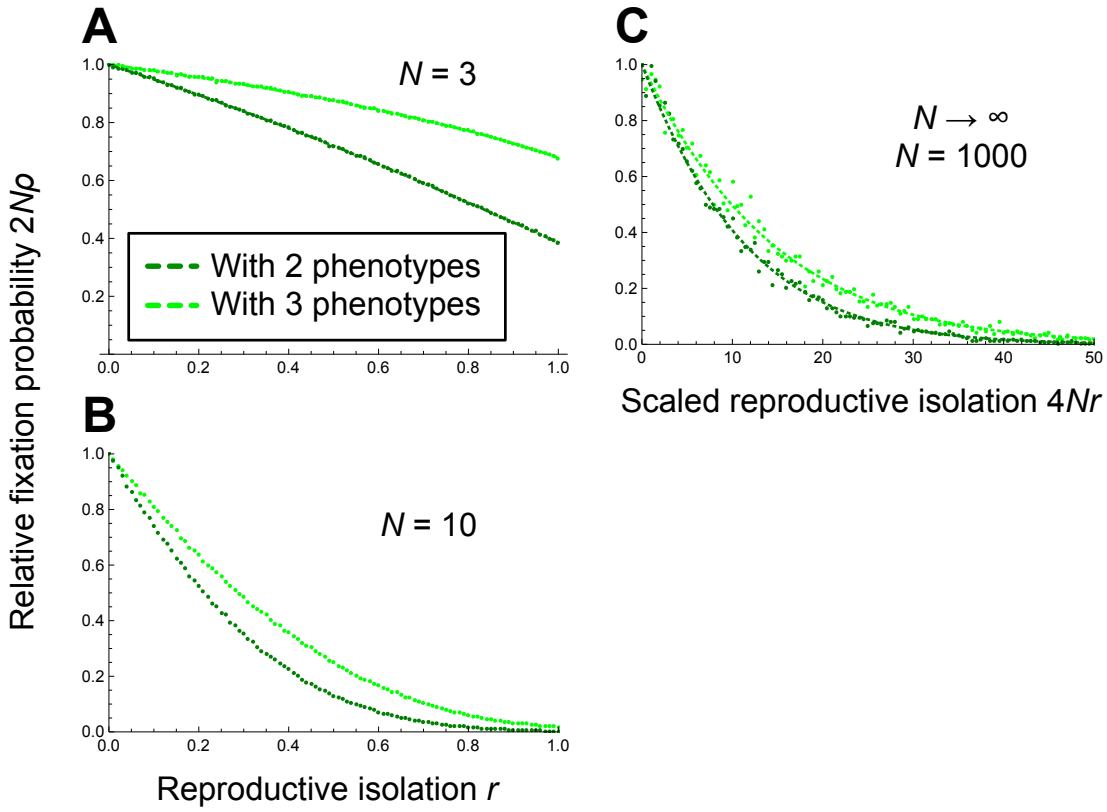

Figure 3.S2: Relative fixation probabilities of a single mutant with reproductive isolation (and without viability selection: $s = 0$) to that of a neutral mutant. A, B: X-axis is the reproductive isolation parameter (r). C: X-axis is four times the product of the reproductive isolation parameter and the effective population size ($4Nr$). Y-axis is the product of fixation probability and effective population size ($2N\rho$). A: $N = 3$ (the first step analysis and Monte Carlo simulations), C: $N = 10$ (Monte Carlo simulations), C: $N \to \infty$ (diffusion approximation) and $N = 1000$ (Monte Carlo simulations). Dotted dark-green lines: the partial dominance model with two phenotypes. Dotted lime-green lines: the partial dominance model with three phenotypes.

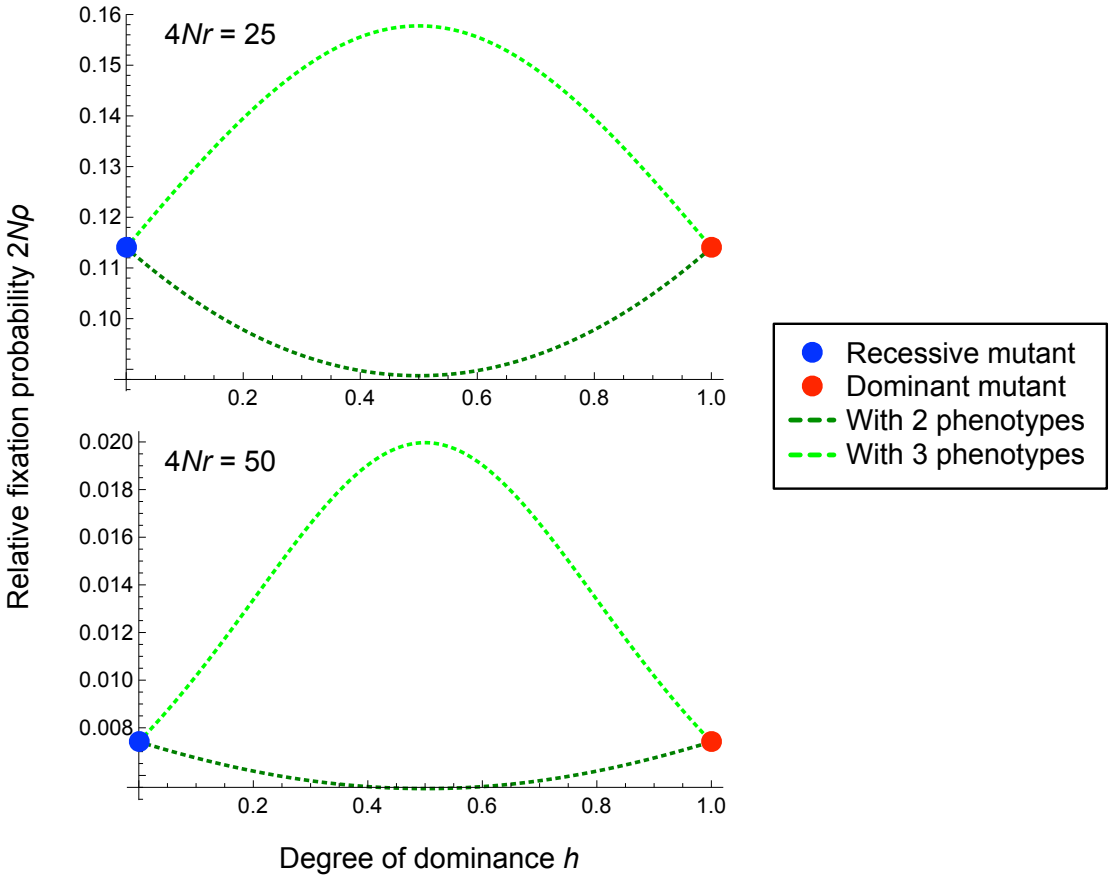

Figure 3.S3: Effects of partial dominance in the diploid model without delayed inheritance in large populations. Blue points: the recessive mutant (h = 0). Red points: the dominant mutant (h = 1). Dotted dark-green lines: the partial dominance model with two phenotypes. Dotted lime-green lines: the partial dominance model with three phenotypes. When R (= $4Nr$) = 0, the fixation probability is 1 regardless of h values.

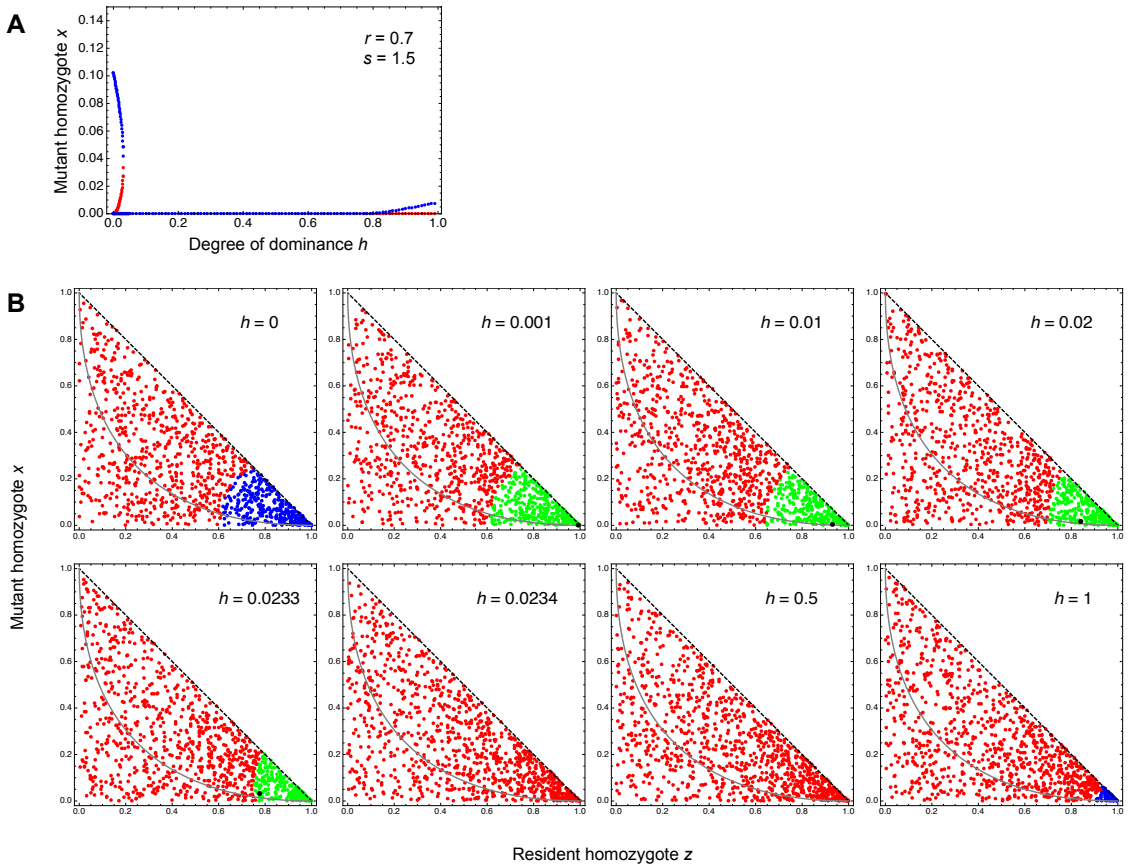

Figure 3.S4: A: The bifurcation plot along the degree of dominance parameter (h). Y-axis is the frequency of the mutant homozygote (x). Red points: stable equilibria. Blue points: unstable equilibria. The equilibrium with the mutant allele ($x = 1$) is always stable. B: Simulation results of deterministic recursion equations (3)-(4). Red points: basin of attraction toward a stable equilibrium of the mutant allele. Blue points: basin of attraction toward a stable equilibrium of the resident allele. Green points: basin of attraction toward a stable equilibrium of both the mutant and resident alleles. The coexistence equilibria are shown as black points. The parameter condition is $r = 0.7$ and $s = 1.5$.

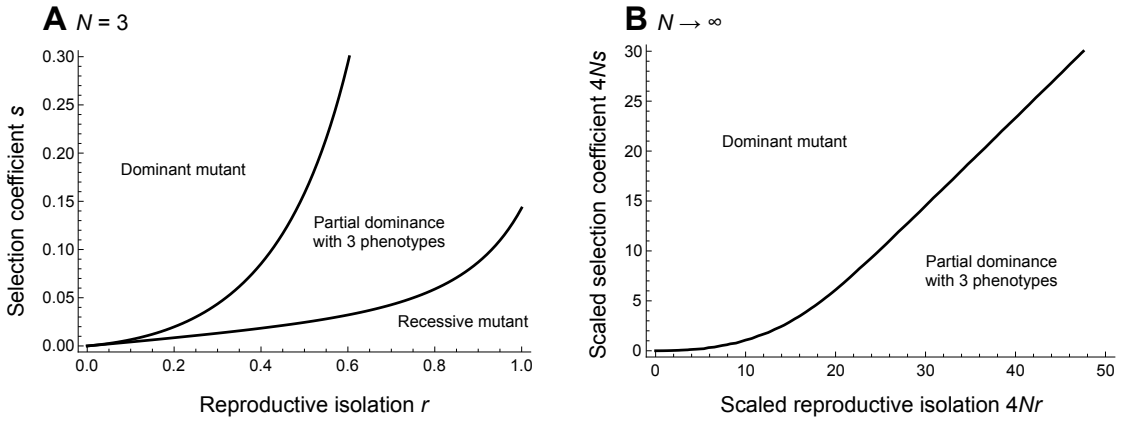

Figure 3.S5: The alleles with the highest fixation probabilities in the diploid model without delayed inheritance given certain strength of reproductive isolation and viability selection. A: $N = 3$ (the first step analysis), B: $N \rightarrow \infty$ (diffusion approximation).

3.7 Acknowledgements

We thank Dr. Masaki Hoso for discussion and valuable comments on our earlier manuscript. We also thank Prof. Stepehn P. Ellner, Prof. Hisashi Ohtsuki, Whit Hairston, and Joseph L. Simonis for their helpful comments. M. Y. was supported by a Research Fellowship of the Japan Society for the Promotion of Science (JSPS) for Young Scientist (21-7611). A. S. is supported by MEXT/JSPS KAKENHI, and the Graduate University for Advanced Studies (Sokendai).

Chapter 4. Concluding Remarks and Perspectives

Essentially, all models are wrong, but some are useful. (Box and Draper 1987)

4.1 Concluding remarks

Contrary to traditional ecology, recent studies are newly introducing evolutionary dynamics as an additional variable to explain ecological dynamics. Experimental and theoretical studies have shown that evolution affect ecological dynamics, so predictive power would increase in future ecological studies. What we need next is to evaluate statistically the effect size of evolution on ecological dynamics (Hairston et al. 2005).

Before that, we need to be cautious because sometimes evolution and plasticity are confounding. In addition, plasticity itself (i.e., reaction norm) can evolve rapidly. Recent papers have indicated the importance of phenotypic plasticity in eco-evolutionary studies (Cortez 2011, Ellner et al. 2011, Yamamichi et al. 2011). I theoretically found that: (1) plasticity can stabilize population dynamics. (2) A plastic genotype has higher fitness in fluctuating environments than stable environments. Combining these aspects of plasticity, eco-evolutionary dynamics of phenotypic plasticity cause intermittent cycles. I proposed to call this as 'eco-evolutionary bursting' from neurobiology.

Single-gene speciation has been an enigma in evolutionary biology, but this can be resolved by adding a perspective from eco-evolutionary feedbacks (Hoso et al. 2010). I revealed that pleiotropy of the speciation gene for anti-predatory defense can promote single-gene speciation. Further studies will be needed to investigate number of genes and conditions required for ecological and non-ecological speciation.

Through several studies on eco-evolutionary dynamics in predator-prey systems, I can contribute to new understanding of the interplay between ecology and evolution. Combining the two studies, I describe unifying picture of this thesis in figure 1. At first, environments are temporally or spatially varying and organisms evolve to adapt the changing environments (e.g., predation pressure). This selection pressure can promote specialization or generalization. The outcome depends on selection pressure and trade-off: When environmental change is intense, one form of generalization, phenotypic plasticity, can evolve (chapter 2). When predation pressure varies spatially and adaptation occurs pleiotropically with evolution of reproductive isolation, it results

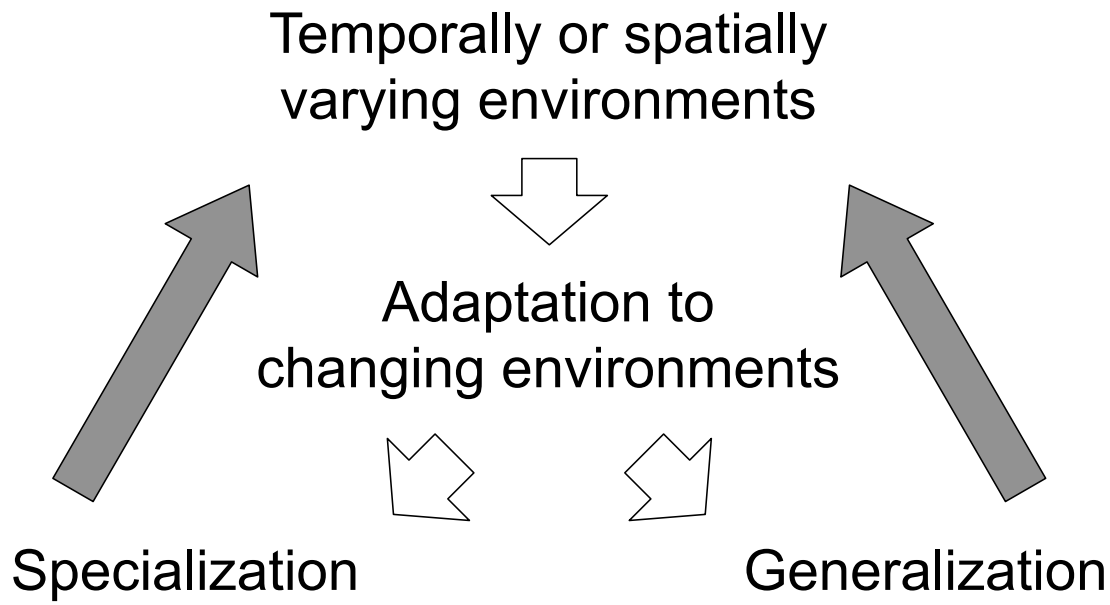

Figure 4.1: Unifying picture of this thesis. Temporally or spatially varying environments (e.g., predation pressure) cause adaptive evolution of specialization (e.g., speciation) or generalization (e.g., phenotypic plasticity), depending on environmental conditions and trade-off (white arrows). Adaptive evolution then gives feedback to environments (gray arrows).

in speciation (chapter 3). Generally, specialization is more probable when environments are stable whereas generalization is pervasive in unstable environments. Adaptive evolution in turn affects environments and selection pressure (gray arrows in fig. 1). In case of plasticity, evolution of plasticity can stabilize temporal oscillations (negative feedback). Then this causes specialization of prey, destabilization of predator-prey cycles, and again, generalization of prey (eco-evolutionary bursting). In case of ecological speciation via pleiotropy, consequence of speciation is not fully investigated: it may cause evolution of 'left-handed' predator, inter-patch movement of predators, or even local extinction of predators. These phenomena will change selection pressure and eco-evolutionary feedbacks will be realized.

Although I concentrated on actual organisms (plankton and snails) to examine my theory empirically in future, further studies are still needed to fully understand the eco-evolutionary feedbacks shown in figure 1. With a general theory to specify the condition of specialization and generalization, more sophisticated statistical methods will be essential to connect current theoretical modeling and empirical data.

4.2 Perspectives

4.2.1 Space and time

Here I did not consider spatial scale of community. Metacommunity are increasingly recognized as an important topic in community ecology (Holyoak et al. 2005) as migration between local communities can change community dynamics significantly. Eco-evolutionary dynamics can potentially alter metacommunity dynamics. Highly complex studies about evolving metacommunity are still rare, but the topic will attract research focus near future (Urban et al. 2008). This kind of study will be possible by connecting two chemostats, for example (Suzuki and Yoshida 2012). By changing migration rate of different trophic levels, it is possible to see how synchrony and evolutionary cycles are affected by the spatial structure.

For longer timescale, there must be balancing selection to maintain genetic polymorphisms in local populations for eco-evolutionary dynamics. For example, studies called as 'community genetics' (Whitham et al. 2006) usually show that when there are more genetic polymorphisms in plant community, arthropod's community is also more diverse. However, as the chemostat study, feedback from arthropod's community to select for more diverse plant community should be considered to understand the mechanisms of genotypic diversity maintenance. In the same way, it will be interesting to investigate the existence of balancing selection in the wild for the defensive trait of *Chlorella* that was observed in chemostats by population genomics (see 4.2.3).

4.2.2 Combining theoretical and empirical approaches

Comparing to population genetics, the divide between theoretical and empirical studies in ecology are still deeper. The most popular model in ecology is deterministic ordinary differential equations, so it is not straightforward to compare empirical data and models statistically. Although stochastic neutral models have been getting popular in ecology (Hubbell 2001), it is still rare to test theoretical prediction in likelihood scheme.

In that sense, one of my favorite studies is Shertzer et al. (2002), in which authors constructed several theoretical models based on hypotheses to explain the strange phenomenon (i.e., anti-phase predator-prey cycles), and estimated parameters by the genetic algorithm (Shertzer et al. 2002). Then the most probable model (rapid evolution of prey species) can actually explained the data well, and this hypothesis was

later examined experimentally (Yoshida et al. 2003). With recent development of hierarchical Bayesian modeling, state-space modeling, efficient sampling methods (e.g., Markov chain Monte Carlo or particle filter) and increasing computational power, it is now becoming possible to analyze data with mechanistic models. Such theoretical – empirical feedback would be ideal, and should be the standard approach in ecology.

4.2.3 Genomics and eco-evolutionary dynamics studies

In this post-genomic era, it will be possible to understand eco-evolutionary dynamics from genomic scale to ecological scale. Genomic studies focusing on non-model species are sometimes called as 'Evolutionary and Ecological Function Genomics' (EEFG) (Feder and Mitchell-Olds 2003). While those studies revealed past demography and adaptation processes in non-model wild organisms (e.g., Colosimo et al. 2005, Hoekstra et al. 2006), direct connections between genomic studies and eco-evolutionary studies are still rare.

For example, by sequencing whole genome of *Chlorella vulgaris*, it would be possible to detect genetic basis of the defensive trait and track its allele frequency dynamics through predator-prey cycles (as Meyer et al. 2006, although they used neutral markers). If the defensive trait were universal one, it would be easy to exam 'the defensiveness' of wild *Chlorella* populations by metagenomics approaches. Although some researchers tried to examine gene expression changes in predator-prey cycles of *Chlamydomonas* by using microarray (Becks et al. 2012), such challenge is still rare. In the same way, if we can obtain genome sequences of snails with dextral and sinistral handedness that have been putatively maintained by balancing selection for long time (as *Amphidromus*) (Schilthuizen et al. 2007, Sutcharit et al. 2007), it would be possible to know the genetic basis of polarity. Then my theoretical prediction about allele dominance with or without right-handed snakes will be examined empirically.

Therefore, future researches are needed to connect evolution in the genomic level and ecological dynamics such as population dynamics, community structures, and ecosystem functions. In this regard, it will be very important to analyze data with coalescent theory of population genetics (Kingman 1982, Hudson 1983, Tajima 1983) to infer past demography (e.g., Yamamichi et al. 2012) or adaptive process (e.g., Linnen et al. 2009). By doing so, it will be possible to understand the ecological meaning of the four letters (ATGC) in genome sequences.

4.2.4 Eco-evolutionary conservation and management

As evolution affect ecological dynamics significantly, it is important to incorporate a perspective of eco-evolutionary feedbacks for conservation and management (Ashley et al. 2003, Stockwell et al. 2003, Kinnison and Hairston 2007, Kinnison et al. 2007). One example is 'evolutionary rescue', in which adaptive evolution to new environments can prevent extinction of populations (Gomulkiewicz and Holt 1995). Bell and Gonzalez (2009) experimentally showed that adaptive evolution of yeast to a new environment (in this case, normally lethal concentrations of salt) can prevent extinction, but the success of rescue depends on initial population size (Bell and Gonzalez 2009). Another example is 'fisheries-induced evolution' (Kuparinen and Merilä 2007). Because of intense selection pressure of fisheries by humans, fish tend to evolve smaller size and early maturation age. Indeed, Olsen et al. (2004) found rapid evolutionary change of the life history traits in northern cod populations before the collapse (Olsen et al. 2004).

Although increasing number of studies have shown the importance of evolution on conservation and management theoretically and experimentally, field survey and statistical method to detect warning signals of evolutionary changes and evolutionary effects on ecological dynamics are still lacking. Future studies need to figure out how to detect, manage, and conserve rapidly evolving wild populations combining above methods.

References

Abrams, P. A. 2000. The evolution of predator-prey interactions: Theory and evidence. Annual Review of Ecology and Systematics **31**:79-105.

Abrams, P. A. 2001. Modelling the adaptive dynamics of traits involved in inter- and intraspecific interactions: An assessment of three methods. Ecology Letters **4**:166-175.

Abrams, P. A. 2005. 'Adaptive Dynamics' vs. 'adaptive dynamics'. Journal of Evolutionary Biology **18**:1162-1165.

Abrams, P. A. and H. Matsuda. 1997. Prey adaptation as a cause of predator-prey cycles. Evolution **51**:1742-1750.

Abrams, P. A., H. Matsuda, and Y. Harada. 1993. Evolutionarily unstable fitness maxima and stable fitness minima of continuous traits. Evolutionary Ecology **7**:465-487.

Agashe, D. 2009. The stabilizing effect of intraspecific genetic variation on population dynamics in novel and ancestral habitats. American Naturalist **174**:255-267.

Agrawal, A. A. 2001. Phenotypic plasticity in the interactions and evolution of species. Science **294**:321-326.

Agrawal, A. A., D. D. Ackerly, F. Adler, A. E. Arnold, C. Cáceres, D. F. Doak, E. Post, P. J. Hudson, J. Maron, K. A. Mooney, M. Power, D. Schemske, J. Stachowicz, S. Strauss, M. G. Turner, and E. Werner. 2007. Filling key gaps in population and community ecology. Frontiers in Ecology and the Environment **5**:145-152.

Agrawal, A. A., C. Laforsch, and R. Tollrian. 1999. Transgenerational induction of defences in animals and plants. Nature **401**:60-63.

Aoki, S. and A. Hino. 1996. Nitrogen flow in a chemostat culture of the rotifer *Brachionus plicatilis*. Fisheries Science **62**:8-14.

Arnaud, J. F. and G. Laval. 2004. Stability of genetic structure and effective population size inferred from temporal changes of microsatellite DNA polymorphisms in the land snail *Helix aspersa* (Gastropoda : Helicidae). Biological Journal of the Linnean Society **82**:89-102.

Asami, T., R. H. Cowie, and K. Ohbayashi. 1998. Evolution of mirror images by sexually asymmetric mating behavior in hermaphroditic snails. American Naturalist **152**:225-236.

Ashley, M. V., M. F. Willson, O. R. W. Pergams, D. J. O'Dowd, S. M. Gende, and J. S. Brown. 2003. Evolutionarily enlightened management. Biological Conservation **111**:115-123.

Barbosa, P. and I. Castellanos. 2005. Ecology of Predator-Prey Interactions. Oxford University Press, Oxford.

Barrett, R. D. H. and D. Schluter. 2008. Adaptation from standing genetic variation. Trends in Ecology & Evolution **23**:38-44.

Barton, N. H. 2010. What role does natural selection play in speciation? Philosophical Transactions of the Royal Society B-Biological Sciences **365**:1825-1840.

Bassar, R. D., M. C. Marshall, A. Lopez-Sepulcre, E. Zandona, S. K. Auer, J. Travis, C. M. Pringle, A. S. Flecker, S. A. Thomas, D. F. Fraser, and D. N. Reznick. 2010. Local adaptation in Trinidadian guppies alters ecosystem processes. Proceedings of the National Academy of Sciences of the United States of America **107**:3616-3621.

Bateson, W. 1909. Heredity and variation in modern lights. Pages 85-101 *in* A. C. Seward, editor. Darwin and Modern Science. Cambridge University Press, Cambridge.

Becks, L., S. P. Ellner, L. E. Jones, and N. G. Hairston. 2012. The functional genomics of an eco-evolutionary feedback loop: linking gene expression, trait evolution, and community dynamics. Ecology Letters **15**:492-501.

Becks, L., S. P. Ellner, L. E. Jones, and N. G. Hairston, Jr. 2010. Reduction of adaptive genetic diversity radically alters eco-evolutionary community dynamics. Ecology Letters **13**:989-997.

Begon, M., C. R. Townsend, and J. L. Harper. 2006. Ecology: From Individuals to Ecosystems. 4th edition. Blackwell Publishing, Oxford.

Bell, G. and A. Gonzalez. 2009. Evolutionary rescue can prevent extinction following environmental change. Ecology Letters **12**:942-948.

Bolker, B., M. Holyoak, V. Křivan, L. Rowe, and O. Schmitz. 2003. Connecting theoretical and empirical studies of trait-mediated interactions. Ecology **84**:1101-1114.

Bolnick, D. I., R. Svanbäck, J. A. Fordyce, L. H. Yang, J. M. Davis, C. D. Hulsey, and M. L. Forister. 2003. The ecology of individuals: Incidence and implications of individual specialization. American Naturalist **161**:1-28.

Box, G. E. P. and N. R. Draper. 1987. Empirical Model-Building and Response Surfaces. John Wiley & Sons, New York.

Boycott, A. E., C. Diver, S. L. Garstang, and F. M. Turner. 1930. The inheritance of sinistrality in *Limnaea peregra* (Mollusca, Pulmonata). Philosophical Transactions of the Royal Society B **219**:51-131.

Bradshaw, H. D. and D. W. Schemske. 2003. Allele substitution at a flower colour locus produces a pollinator shift in monkeyflowers. Nature **426**:176-178.

Carroll, S. P., A. P. Hendry, D. N. Reznick, and C. W. Fox. 2007. Evolution on ecological time-scales. Functional Ecology **21**:387-393.

Charmantier, A., R. H. McCleery, L. R. Cole, C. Perrins, L. E. B. Kruuk, and B. C. Sheldon. 2008. Adaptive phenotypic plasticity in response to climate change in a wild bird population. Science **320**:800-803.

Colosimo, P. F., K. E. Hosemann, S. Balabhadra, G. Villarreal, M. Dickson, J. Grimwood, J. Schmutz, R. M. Myers, D. Schluter, and D. M. Kingsley. 2005. Widespread parallel evolution in sticklebacks by repeated fixation of ectodysplasin alleles. Science **307**:1928-1933.

Coombes, S. and P. C. Bressloff. 2005. Bursting: The Genesis of Rhythm in the Nervous System. World Scientific Publishing Co. Pte. Ltd., Toh Tuck Link, Singapore.

Cortez, M. H. 2011. Comparing the qualitatively different effects rapidly evolving and rapidly induced defences have on predator-prey interactions. Ecology Letters **14**:202-209.

Cortez, M. H. and S. P. Ellner. 2010. Understanding rapid evolution in predator-prey interactions using the theory of fast-slow dynamical systems. American Naturalist **176**:E109-E127.

Coyne, J. A. and H. A. Orr. 2004. Speciation. Sinauer Associates, Inc., Sunderland.

Cressman, R. and V. Křivan. 2010. The ideal free distribution as an evolutionarily stable state in density-dependent population games. Oikos **119**:1231-1242.

Crow, J. F. and M. Kimura. 1970. An Introduction to Population Genetics Theory. Harper & Row Publishers.

Cunningham, C. W. 1999. Some limitations of ancestral character-state reconstruction when testing evolutionary hypotheses. Systematic Biology **48**:665-674.

Darwin, C. 1859. On the Origin of Species by Means of Natural Selection, or the

Preservation of Favoured Races in the Struggle for Life. John Murray, London.

Davison, A., S. Chiba, N. H. Barton, and B. Clarke. 2005. Speciation and gene flow between snails of opposite chirality. Plos Biology **3**:e282.

de Jong, G. 1995. Phenotypic plasticity as a product of selection in a variable environment. American Naturalist **145**:493-512.

DeAngelis, D. L., M. Vos, W. M. Mooij, and P. A. Abrams. 2007. Feedback effects between the food chain and induced defense strategies. Pages 213-236 *in* N. Rooney, K. S. McCann, and D. L. G. Noakes, editors. From Energetics to Ecosystems: The Dynamics and Structure of Ecological Systems. Springer, Dordrecht.

Degner, E. 1952. Der Erbgang der Inversion bei *Laciniaria biplicata* Mtg. Mitteilungen Hamburgisches Zoologisches Museum und Institut **51**:3-61.

DeWitt, T. J., A. Sih, and D. S. Wilson. 1998. Costs and limits of phenotypic plasticity. Trends in Ecology & Evolution **13**:77-81.

Dietl, G. P. and J. R. Hendricks. 2006. Crab scars reveal survival advantage of left-handed snails. Biology Letters **2**:439-442.

Dobzhansky, T. 1936. Studies on hybrid sterility. II. Localization of sterility factors in *Drosophila pseudoobscura* hybrids. Genetics **21**:113-135.

Doebeli, M. 2011. Adaptive Diversification. Princeton University Press, Princeton.

Doebeli, M. and G. de Jong. 1999. Genetic variability in sensitivity to population density affects the dynamics of simple ecological models. Theoretical Population Biology **55**:37-52.

Duffy, M. A. and L. Sivars-Becker. 2007. Rapid evolution and ecological host-parasite dynamics. Ecology Letters **10**:44-53.

Edelstein-Keshet, L. and M. D. Rausher. 1989. The effects of inducible plant defenses on herbivore populations. I. Mobile herbivores in continuous time. American Naturalist **133**:787-810.

Ellner, S. P., M. A. Geber, and N. G. Hairston, Jr. 2011. Does rapid evolution matter? Measuring the rate of contemporary evolution and its impacts on ecological dynamics. Ecology Letters.

Feder, M. E. and T. Mitchell-Olds. 2003. Evolutionary and ecological functional genomics. Nature Reviews Genetics **4**:651-657.

Felsenstein, J. 1981. Skepticism towards Santa Rosalia, or why are there so few kinds of

animals? Evolution **35**:124-138.

Fisher, R. A. 1930. The Genetical Theory of Natural Selection. Clarendon, Oxford.

Fox, J. W. and D. A. Vasseur. 2008. Character convergence under competition for nutritionally essential resources. American Naturalist **172**:667-680.

Freeman, G. and J. W. Lundelius. 1982. The developmental genetics of dextrality and sinistrality in the gastropod *Lymnaea peregra*. Wilhelm Roux's Archives of Developmental Biology **191**:69-83.

Fussmann, G. F., S. P. Ellner, K. W. Shertzer, and N. G. Hairston, Jr. 2000. Crossing the Hopf bifurcation in a live predator-prey system. Science **290**:1358-1360.

Fussmann, G. F., M. Loreau, and P. A. Abrams. 2007. Eco-evolutionary dynamics of communities and ecosystems. Functional Ecology **21**:465-477.

Futuyma, D. J. 2005. Evolution. Sinauer Associates, Inc., Sunderland.

Gause, G. F. 1934. The Struggle for Existence. Williams & Wilkins, Baltimore.

Gavrilets, S. 2004. Fitness Landscape and the Origin of Species. Princeton University Press, Princeton.

Geritz, S. A. H., É. Kisdi, G. Meszéna, and J. A. J. Metz. 1998. Evolutionarily singular strategies and the adaptive growth and branching of the evolutionary tree. Evolutionary Ecology **12**:35-57.

Gingerich, P. D. 1993. Quantification and comparison of evolutionary rates. American Journal of Science **293A**:453-478.

Gittenberger, E. 1988. Sympatric speciation in snails: a largely neglected model. Evolution **42**:826-828.

Gittenberger, E., T. D. Hamann, and T. Asami. 2012. Chiral speciation in terrestrial pulmonate snails. PloS one **7**:e34005.

Gomulkiewicz, R. and R. D. Holt. 1995. When does evolution by natural selection prevent extinction? Evolution **49**:201-207.

Grande, C. and N. H. Patel. 2009. Nodal signalling is involved in left-right asymmetry in snails. Nature **457**:1007-1011.

Gregorius, H. R. 1992. A single-locus model of speciation. Acta Biotheoretica **40**:313-319.

Guckenheimer, J. and P. Holmes. 1983. Nonlinear Oscillations, Dynamical Systems, and Bifurcations of Vector Fields. Springer, New York.

Hairston, N. G., Jr., S. P. Ellner, M. A. Geber, T. Yoshida, and J. A. Fox. 2005. Rapid

evolution and the convergence of ecological and evolutionary time. Ecology Letters **8**:1114-1127.

Hairston, N. G., Sr., F. E. Smith, and L. B. Slobodkin. 1960. Community structure, population control, and competition. American Naturalist **94**:421-425.

Halbach, U. and G. Halbach-Keup. 1974. Quantitative relations between phytoplankton and population dynamics of the rotifer *Brachionus calyciflorus* Pallas. Results of laboratory experiments and field studies. Archiv Fur Hydrobiologie **73**:273-309.

Hendry, A. P. and M. T. Kinnison. 1999. Perspective: The pace of modern life: Measuring rates of contemporary microevolution. Evolution **53**:1637-1653.

Hendry, A. P., P. Nosil, and L. H. Rieseberg. 2007. The speed of ecological speciation. Functional Ecology **21**:455-464.

Hessen, D. O. and E. van Donk. 1993. Morphological changes in *Scenedesmus* induced by substances released from *Daphnia*. Archiv Fur Hydrobiologie **127**:129-140.

Hoekstra, H. E., R. J. Hirschmann, R. A. Bundey, P. A. Insel, and J. P. Crossland. 2006. A single amino acid mutation contributes to adaptive beach mouse color pattern. Science **313**:101-104.

Hoekstra, H. E., J. M. Hoekstra, D. Berrigan, S. N. Vignieri, A. Hoang, C. E. Hill, P. Beerli, and J. G. Kingsolver. 2001. Strength and tempo of directional selection in the wild. Proceedings of the National Academy of Sciences of the United States of America **98**:9157-9160.

Holyoak, M., M. A. Leibold, and R. D. Holt. 2005. Metacommunities: Spatial Dynamics and Ecological Communities. University of Chicago Press, Chicago.

Hoso, M. 2012. Non-adaptive speciation of snails by left-right reversal is facilitated on oceanic islands. Contributions to Zoology **81**:79-85.

Hoso, M., T. Asami, and M. Hori. 2007. Right-handed snakes: convergent evolution of asymmetry for functional specialization. Biology Letters **3**:169-172.

Hoso, M., Y. Kameda, S. P. Wu, T. Asami, M. Kato, and M. Hori. 2010. A speciation gene for left-right reversal in snails results in anti-predator adaptation. Nature Communications **1**:133.

Hubbell, S. P. 2001. The Unified Neutral Theory of Biodiversity and Biogeography. Princeton University Press, Princeton.

Hudson, R. R. 1983. Properties of a neutral allele model with intragenic recombination. Theoretical Population Biology **23**:183-201.

Huffaker, C. B. 1958. Experimental studies on predation: Dispersion factors and predator-prey oscillations. Hilgardia **27**:343-383.

Hughes, A. R., B. D. Inouye, M. T. J. Johnson, N. Underwood, and M. Vellend. 2008. Ecological consequences of genetic diversity. Ecology Letters **11**:609-623.

Hutchinson, G. E. 1965. The Ecological Theater and the Evolutionary Play. Yale University Press, New Haven.

Inoda, T., Y. Hirata, and S. Kamimura. 2003. Asymmetric mandibles of water-scavenger larvae improve feeding effectiveness on right-handed snails. American Naturalist **162**:811-814.

Ives, A. R. and A. P. Dobson. 1987. Antipredator behavior and the population dynamics of simple predator-prey systems. American Naturalist **130**:431-447.

Johnson, M. S. 1982. Polymorphism for direction of coil in *Partula suturalis*: behavioural isolation and positive frequency dependent selection. Heredity **49**:145-151.

Johnson, M. T. J. and A. A. Agrawal. 2003. The ecological play of predator-prey dynamics in an evolutionary theatre. Trends in Ecology & Evolution **18**:549-551.

Johnson, M. T. J. and J. R. Stinchcombe. 2007. An emerging synthesis between community ecology and evolutionary biology. Trends in Ecology & Evolution **22**:250-257.

Johnson, M. T. J., M. Vellend, and J. R. Stinchcombe. 2009. Evolution in plant populations as a driver of ecological changes in arthropod communities. Philosophical Transactions of the Royal Society B-Biological Sciences **364**:1593-1605.

Jones, L. E., L. Becks, S. P. Ellner, N. G. Hairston, Jr., T. Yoshida, and G. F. Fussmann. 2009. Rapid contemporary evolution and clonal food web dynamics. Philosophical Transactions of the Royal Society B-Biological Sciences **364**:1579-1591.

Jones, L. E. and S. P. Ellner. 2004. Evolutionary tradeoff and equilibrium in an aquatic predator-prey system. Bulletin of Mathematical Biology **66**:1547-1573.

Jones, L. E. and S. P. Ellner. 2007. Effects of rapid prey evolution on predator-prey cycles. Journal of Mathematical Biology **55**:541-573.

Jordan, C. Y. and S. P. Otto. 2012. Functional pleiotropy and mating system evolution

in plants: frequency-independent mating. Evolution **66**:957-972.

Kendall, B. E., J. Prendergast, and O. N. Bjørnstad. 1998. The macroecology of population dynamics: taxonomic and biogeographic patterns in population cycles. Ecology Letters **1**:160-164.

Kettlewell, H. B. D. 1958. A survey of the frequencies of *Biston betularia* (L.) (LEP.) and its melanic forms in Great Britain. Heredity **12**:51-72.

Kimura, M. 1962. On the probability of fixation of mutant genes in a population. Genetics **47**:713-719.

Kingman, J. F. C. 1982. The coalescent. Stochastic Processes and their Applications **13**:235-248.

Kinnison, M. T. and N. G. Hairston, Jr. 2007. Eco-evolutionary conservation biology: contemporary evolution and the dynamics of persistence. Functional Ecology **21**:444-454.

Kinnison, M. T. and A. P. Hendry. 2001. The pace of modern life II: from rates of contemporary microevolution to pattern and process. Genetica **112**:145-164.

Kinnison, M. T., A. P. Hendry, and C. A. Stockwell. 2007. Contemporary evolution meets conservation biology II: Impediments to integration and application. Ecological Research **22**:947-954.

Kirkpatrick, M. and V. Ravigné. 2002. Speciation by natural and sexual selection: Models and experiments. American Naturalist **159**:S22-S35.

Kishida, O., G. C. Trussell, A. Mougi, and K. Nishimura. 2010. Evolutionary ecology of inducible morphological plasticity in predator-prey interaction: toward the practical links with population ecology. Population Ecology **52**:37-46.

Kokko, H. and A. López-Sepulcre. 2007. The ecogenetic link between demography and evolution: can we bridge the gap between theory and data? Ecology Letters **10**:773-782.

Kondoh, M. 2003. Foraging adaptation and the relationship between food-web complexity and stability. Science **299**:1388-1391.

Kondoh, M. 2007. Anti-predator defence and the complexity-stability relationship of food webs. Proceedings of the Royal Society B-Biological Sciences **274**:1617-1624.

Kopp, M. and W. Gabriel. 2006. The dynamic effects of an inducible defense in the Nicholson-Bailey model. Theoretical Population Biology **70**:43-55.

Kot, M. 2001. Elements of Mathematical Ecology. Cambridge University Press, Cambridge, U.K.

Křivan, V. 2003. Competitive co-existence caused by adaptive predators. Evolutionary Ecology Research **5**:1163-1182.

Křivan, V. 2007. The Lotka-Volterra predator-prey model with foraging-predation risk trade-offs. American Naturalist **170**:771-782.

Křivan, V. and R. Cressman. 2009. On evolutionary stability in predator-prey models with fast behavioural dynamics. Evolutionary Ecology Research **11**:227-251.

Kuparinen, A. and J. Merilä. 2007. Detecting and managing fisheries-induced evolution. Trends in Ecology & Evolution **22**:652-659.

Kuroda, R., B. Endo, M. Abe, and M. Shimizu. 2009. Chiral blastomere arrangement dictates zygotic left-right asymmetry pathway in snails. Nature **462**:790-794.

Leimar, O. 2005. The evolution of phenotypic polymorphism: Randomized strategies versus evolutionary branching. American Naturalist **165**:669-681.

Lima, S. L. 1998. Nonlethal effects in the ecology of predator-prey interactions: What are the ecological effects of anti-predator decision-making? Bioscience **48**:25-34.

Linnen, C. R., E. P. Kingsley, J. D. Jensen, and H. E. Hoekstra. 2009. On the origin and spread of an adaptive allele in deer mice. Science **325**:1095-1098.

Loreau, M. 2010. From Populations to Ecosystems: Theoretical Foundations for a New Ecological Synthesis. Princeton University Press, Princeton.

Lotka, A. J. 1925. Elements of Physical Biology. Williams and Wilkins, Baltimore.

Lürling, M. and E. van Donk. 2000. Grazer-induced colony formation in *Scenedesmus*: are there costs to being colonial? Oikos **88**:111-118.

Matthews, B., A. Narwani, S. Hausch, E. Nonaka, H. Peter, M. Yamamichi, K. E. Sullam, K. C. Bird, M. K. Thomas, T. C. Hanley, and C. B. Turner. 2011. Toward an integration of evolutionary biology and ecosystem science. Ecology Letters **14**:690-701.

Meyer, J. R., S. P. Ellner, N. G. Hairston, Jr., L. E. Jones, and T. Yoshida. 2006. Prey evolution on the time scale of predator-prey dynamics revealed by allele-specific quantitative PCR. Proceedings of the National Academy of Sciences of the United States of America **103**:10690-10695.

Miner, B. G., S. E. Sultan, S. G. Morgan, D. K. Padilla, and R. A. Relyea. 2005.

Ecological consequences of phenotypic plasticity. Trends in Ecology & Evolution **20**:685-692.

Mittelbach, G. C., C. W. Osenberg, and P. C. Wainwright. 1999. Variation in feeding morphology between pumpkinseed populations: Phenotypic plasticity or evolution? Evolutionary Ecology Research **1**:111-128.

Moore, W. S. 1979. A single locus mass-action model of assortative mating, with comments on the process of speciation. Heredity **42**:173-186.

Moore, W. S. 1981. Assortative mating genes selected along a gradient. Heredity **46**:191-195.

Mougi, A. and O. Kishida. 2009. Reciprocal phenotypic plasticity can lead to stable predator-prey interaction. Journal of Animal Ecology **78**:1172-1181.

Mougi, A. and K. Nishimura. 2008. The paradox of enrichment in an adaptive world. Proceedings of the Royal Society B-Biological Sciences **275**:2563-2568.

Muller, H. J. 1942. Isolating mechanisms, evolution, and temperature. Biological Symposia **6**:71-125.

Murray, J. and B. Clarke. 1966. The inheritance of polymorphic shell characters in *Partula* (Gastropoda). Genetics **54**:1261-1277.

Ng, P. K. L. and L. W. H. Tan. 1985. 'Right handedness' in heterochelous calappoid and xanthoid crabs: suggestion for a functional advantage. Crustaceana **49**:98-100.

Nosil, P. and B. J. Crespi. 2006. Experimental evidence that predation promotes divergence in adaptive radiation. Proceedings of the National Academy of Sciences of the United States of America **103**:9090-9095.

Nowak, M. A., A. Sasaki, C. Taylor, and D. Fudenberg. 2004. Emergence of cooperation and evolutionary stability in finite populations. Nature **428**:646-650.

Ohgushi, T. 2005. Indirect interaction webs: herbivore-induced effects through trait change in plants. Annual Review of Ecology, Evolution, and Systematics **36**:81-105.

Okumura, T., H. Utsuno, J. Kuroda, E. Gittenberger, T. Asami, and K. Matsuno. 2008. The development and evolution of left-right asymmetry in invertebrates: lessons from Drosophila and snails. Developmental Dynamics **237**:3497-3515.

Olsen, E. M., M. Heino, G. R. Lilly, M. J. Morgan, J. Brattey, B. Ernande, and U. Dieckmann. 2004. Maturation trends indicative of rapid evolution preceded the collapse of northern cod. Nature **428**:932-935.

Orr, H. A. 1991. Is single-gene speciation possible? Evolution **45**:764-769.

Orr, H. A. 1996. Dobzhansky, Bateson, and the genetics of speciation. Genetics **144**:1331-1335.

Paine, R. T. 1966. Food web complexity and species diversity. American Naturalist **100**:65-75.

Palumbi, S. R. 2002. The Evolution Explosion: How Humans Cause Rapid Evolutionary Change. W. W. Norton & Company, New York.

Peckarsky, B. L., P. A. Abrams, D. I. Bolnick, L. M. Dill, J. H. Grabowski, B. Luttbeg, J. L. Orrock, S. D. Peacor, E. L. Preisser, O. J. Schmitz, and G. C. Trussell. 2008. Revisiting the classics: Considering nonconsumptive effects in textbook examples of predator-prey interactions. Ecology **89**:2416-2425.

Pelletier, F., D. Garant, and A. P. Hendry. 2009. Eco-evolutionary dynamics. Philosophical Transactions of the Royal Society B-Biological Sciences **364**:1483-1489.

Pinsky, M. A. and S. Karlin. 2010. An Introduction to Stochastic Modeling. 4th edition edition. Academic Press, Burlington, MA.

Post, D. M. and E. P. Palkovacs. 2009. Eco-evolutionary feedbacks in community and ecosystem ecology: interactions between the ecological theatre and the evolutionary play. Philosophical Transactions of the Royal Society B-Biological Sciences **364**:1629-1640.

Price, G. R. 1970. Selection and covariance. Nature **227**:520-521.

Ramos-Jiliberto, R. 2003. Population dynamics of prey exhibiting inducible defenses: the role of associated costs and density-dependence. Theoretical Population Biology **64**:221-231.

Rosenblum, E. B., H. Rompler, T. Schoneberg, and H. E. Hoekstra. 2010. Molecular and functional basis of phenotypic convergence in white lizards at White Sands. Proceedings of the National Academy of Sciences of the United States of America **107**:2113-2117.

Rosenzweig, M. L. 1971. Paradox of enrichment: destabilization of exploitation ecosystems in ecological time. Science **171**:385-387.

Rosenzweig, M. L. and R. H. MacArthur. 1963. Graphical representation and stability conditions of predator-prey interactions. American Naturalist **97**:209-223.

Rundle, H. D. and P. Nosil. 2005. Ecological speciation. Ecology Letters **8**:336-352.

Sasaki, A. and U. Dieckmann. 2011. Oligomorphic dynamics for analyzing the quantitative genetics of adaptive speciation. Journal of Mathematical Biology **63**:601-635.

Scheiner, S. M. 1993. Genetics and evolution of phenotypic plasticity. Annual Review of Ecology and Systematics **24**:35-68.

Schilthuizen, M., P. G. Craze, A. S. Cabanban, A. Davison, J. Stone, E. Gittenberger, and B. J. Scott. 2007. Sexual selection maintains whole-body chiral dimorphism in snails. Journal of Evolutionary Biology **20**:1941-1949.

Schilthuizen, M. and A. Davison. 2005. The convoluted evolution of snail chirality. Naturwissenschaften **92**:504-515.

Schluter, D. 2000. The Ecology of Adaptive Radiation. Oxford University Press, Oxford.

Schluter, D., T. Price, A. O. Mooers, and D. Ludwig. 1997. Likelihood of ancestor states in adaptive radiation. Evolution **51**:1699-1711.

Schmitz, O. J., J. H. Grabowski, B. L. Peckarsky, E. L. Preisser, G. C. Trussell, and J. R. Vonesh. 2008. From individuals to ecosystem function: Toward an integration of evolutionary and ecosystem ecology. Ecology **89**:2436-2445.

Schoener, T. W. 2011. The newest synthesis: understanding the interplay of evolutionary and ecological dynamics. Science **331**:426-429.

Serizawa, H., T. Amemiya, T. Enomoto, A. G. Rossberg, and K. Itoh. 2008. Mathematical modeling of colony formation in algal blooms: phenotypic plasticity in cyanobacteria. Ecological Research **23**:841-850.

Servedio, M. R., G. S. V. Doorn, M. Kopp, A. M. Frame, and P. Nosil. 2011. Magic traits in speciation: 'magic' but not rare? Trends in ecology & evolution **26**:389-397.

Shertzer, K. W., S. P. Ellner, G. F. Fussmann, and N. G. Hairston, Jr. 2002. Predator-prey cycles in an aquatic microcosm: testing hypotheses of mechanism. Journal of Animal Ecology **71**:802-815.

Shimada, M., Y. Ishii, and H. Shibao. 2010. Rapid adaptation: a new dimension for evolutionary perspectives in ecology. Population Ecology **52**:5-14.

Shoup, J. B. 1968. Shell opening by crabs of genus *Calappa*. Science **160**:887-888.

Sinervo, B., E. Svensson, and T. Comendant. 2000. Density cycles and an offspring quantity and quality game driven by natural selection. Nature **406**:985-988.

Slatkin, M. 1982. Pleiotropy and parapatric speciation. Evolution **36**:263-270.

Slobodkin, L. B. 1961. Growth and Regulation of Animal Populations. Holt, Rinehart and Winston, New York.

Stockwell, C. A., A. P. Hendry, and M. T. Kinnison. 2003. Contemporary evolution meets conservation biology. Trends in Ecology & Evolution **18**:94-101.

Stomp, M., M. A. van Dijk, H. M. J. van Overzee, M. T. Wortel, C. A. M. Sigon, M. Egas, H. Hoogveld, H. J. Gons, and J. Huisman. 2008. The timescale of phenotypic plasticity and its impact on competition in fluctuating environments. American Naturalist **172**:E169-E185.

Stone, J. and M. Björklund. 2002. Delayed prezygotic isolating mechanisms: evolution with a twist. Proceedings of the Royal Society of London Series B-Biological Sciences **269**:861-865.

Sutcharit, C., T. Asami, and S. Panha. 2007. Evolution of whole-body enantiomorphy in the tree snail genus *Amphidromus*. Journal of Evolutionary Biology **20**:661-672.

Suzuki, K. and T. Yoshida. 2012. Non-random spatial coupling induces desynchronization, chaos and multistability in a predator-prey-resource system. Journal of Theoretical Biology **300**:81-90.

Svanbäck, R., M. Pineda-Krch, and M. Doebeli. 2009. Fluctuating population dynamics promotes the evolution of phenotypic plasticity. American Naturalist **174**:176-189.

Tajima, F. 1983. Evolutionary relationship of DNA sequences in finite populations. Genetics **105**:437-460.

Tauber, E., H. Roe, R. Costa, J. M. Hennessy, and C. P. Kyriacou. 2003. Temporal mating isolation driven a behavioral gene in *Drosophila*. Current Biology **13**:140-145.

Taylor, P. and T. Day. 1997. Evolutionary stability under the replicator and the gradient dynamics. Evolutionary Ecology **11**:579-590.

Terborgh, J. and J. A. Estes. 2010. Trophic Cascades: Predators, Prey, and the Changing Dynamics of Nature. Island Press, Washington DC.

Thompson, J. N. 1998. Rapid evolution as an ecological process. Trends in Ecology & Evolution **13**:329-332.

Tischner, R. and H. Lorenzen. 1979. Nitrate uptake and nitrate reduction in synchronous *Chlorella*. Planta **146**:287-292.

Tollrian, R. and C. D. Harvell. 1999. The Ecology and Evolution of Inducible Defenses. Princeton University Press, Princeton, U.S.A.

Ueshima, R. and T. Asami. 2003. Single-gene speciation by left-right reversal - A land-snail species of polyphyletic origin results from chirality constraints on mating. Nature **425**:679-679.

Underwood, N. 1999. The influence of plant and herbivore characteristics on the interaction between induced resistance and herbivore population dynamics. American Naturalist **153**:282-294.

Urban, M. C., M. A. Leibold, P. Amarasekare, L. De Meester, R. Gomulkiewicz, M. E. Hochberg, C. A. Klausmeier, N. Loeuille, C. de Mazancourt, J. Norberg, J. H. Pantel, S. Y. Strauss, M. Vellend, and M. J. Wade. 2008. The evolutionary ecology of metacommunities. Trends in Ecology & Evolution **23**:311-317.

Utida, S. 1957. Cyclic fluctuations of population density intrinsic to the host-parasite system. Ecology **38**:442-449.

Utsuno, H. and T. Asami. 2010. Maternal inheritance of racemism in the terrestrial snail *Bradybaena similaris*. Journal of Heredity **101**:11-19.

Utsuno, H., T. Asami, T. J. M. Van Dooren, and E. Gittenberger. 2011. Internal selection against the evolution of left-right reversal. Evolution **65**:2399-2411.

van Batenburg, F. H. D. and E. Gittenberger. 1996. Ease of fixation of a change in coiling: Computer experiments on chirality in snails. Heredity **76**:278-286.

van der Stap, I., M. Vos, B. W. Kooi, B. T. M. Mulling, E. van Donk, and W. M. Mooij. 2009. Algal defenses, population stability, and the risk of herbivore extinctions: a chemostat model and experiment. Ecological Research **24**:1145-1153.

van der Stap, I., M. Vos, A. M. Verschoor, N. R. Helmsing, and W. M. Mooij. 2007. Induced defenses in herbivores and plants differentially modulate a trophic cascade. Ecology **88**:2474-2481.

Vermeij, G. J. 1975. Evolution and distribution of left-handed and planispiral coiling in snails. Nature **254**:419-420.

Verschoor, A. M., I. van der Stap, N. R. Helmsing, M. Lürling, and E. van Donk. 2004a. Inducible colony formation within the Scenedesmaceae: Adaptive responses to infochemicals from two different herbivore taxa. Journal of Phycology **40**:808-814.

Verschoor, A. M., M. Vos, and I. van der Stap. 2004b. Inducible defences prevent

strong population fluctuations in bi- and tritrophic food chains. Ecology Letters **7**:1143-1148.

Vincent, T. L. and J. S. Brown. 2005. Evolutionary Game Theory, Natural Selection, and Darwinian Dynamics. Cambridge University Press, Cambridge.

Volterra, V. 1926. Variazioni e fluttuazioni del numero d'individui in specie animali conviventi. Memorie della R. Accademia Nazionale dei Lincei **6**:30-113.

Vos, M., B. W. Kooi, D. L. DeAngelis, and W. M. Mooij. 2004a. Inducible defences and the paradox of enrichment. Oikos **105**:471-480.

Vos, M., A. M. Verschoor, B. W. Kooi, F. L. Wäckers, D. L. DeAngelis, and W. M. Mooij. 2004b. Inducible defenses and trophic structure. Ecology **85**:2783-2794.

Werner, E. E. and S. D. Peacor. 2003. A review of trait-mediated indirect interactions in ecological communities. Ecology **84**:1083-1100.

Whitham, T. G., J. K. Bailey, J. A. Schweitzer, S. M. Shuster, R. K. Bangert, C. J. LeRoy, E. V. Lonsdorf, G. J. Allan, S. P. DiFazio, B. M. Potts, D. G. Fischer, C. A. Gehring, R. L. Lindroth, J. C. Marks, S. C. Hart, G. M. Wimp, and S. C. Wooley. 2006. A framework for community and ecosystem genetics: from genes to ecosystems. Nature Reviews Genetics **7**:510-523.

Wright, S. 1931. Evolution in Mendelian populations. Genetics **16**:97-159.

Yamamichi, M., J. Gojobori, and H. Innan. 2012. An autosomal analysis gives no genetic evidence for complex speciation of humans and chimpanzees Molecular Biology and Evolution **29**:145-156.

Yamamichi, M., T. Yoshida, and A. Sasaki. 2011. Comparing the effects of rapid evolution and phenotypic plasticity on predator-prey dynamics. American Naturalist **178**:287-304.

Yamauchi, A. and N. Yamamura. 2005. Effects of defense evolution and diet choice on population dynamics in a one-predator-two-prey system. Ecology **86**:2513-2524.

Yoshida, T., S. P. Ellner, L. E. Jones, B. J. M. Bohannan, R. E. Lenski, and N. G. Hairston, Jr. 2007. Cryptic population dynamics: Rapid evolution masks trophic interactions. Plos Biology **5**:1868-1879.

Yoshida, T., N. G. Hairston, Jr., and S. P. Ellner. 2004. Evolutionary trade-off between defence against grazing and competitive ability in a simple unicellular alga, *Chlorella vulgaris*. Proceedings of the Royal Society of London Series B-Biological Sciences **271**:1947-1953.

Yoshida, T., L. E. Jones, S. P. Ellner, G. F. Fussmann, and N. G. Hairston, Jr. 2003. Rapid evolution drives ecological dynamics in a predator-prey system. Nature **424**:303-306.